Universidade de Aveiro Departamento de Química
2017

Daniel João Pires de Mendonça Silva

Estratégias de entrecruzamento para melhoria das propriedades de membranas proteicas nanofibrosas

Crosslinking strategies to improve properties of protein-based nanofibrous membranes

Daniel   João Pires
de Mendonça Silva

Estratégias de entrecruzamento para melhoria das propriedades de membranas proteicas nanofibrosas

Crosslinking strategies to improve properties of protein-based nanofibrous membranes

"Vem por aqui" — dizem-me alguns com os olhos doces

Estendendo-me os braços, e seguros

De que seria bom que eu os ouvisse

Quando me dizem: "vem por aqui!"

Eu olho-os com olhos lassos,

(Há, nos olhos meus, ironias e cansaços)

E cruzo os braços,

E nunca vou por ali...

A minha glória é esta:

Criar desumanidades!

Não acompanhar ninguém.

— Que eu vivo com o mesmo sem-vontade

Com que rasguei o ventre à minha mãe

Não, não vou por aí! Só vou por onde

Me levam meus próprios passos...

Se ao que busco saber nenhum de vós responde

Por que me repetis: "vem por aqui!"?

José Régio, Cântico Negro

o júri

presidente

Prof.ª Doutora Luísa Alexandra Seuanes Serafim Martins Leal
Professora Auxiliar do Departamento de Química da Universidade de Aveiro

Prof. Doutor José António Teixeira Lopes da Silva
Professor Auxiliar Departamento de Química da Universidade de Aveiro

Doutora Paula Alexandrina de Aguiar Pereira Marques
Equiparada a Investigadora Principal do Centro de Tecnologia Mecânica e Automação (TEMA) da Universidade de Aveiro

Agradecimentos

Venho em primeiro lugar agradecer ao meu orientador Professor José António Lopes da Silva por esta jornada de descoberta e criação, e por toda a paciência, atenção e consideração.

Agradeço também àqueles que colaboraram comigo para a realização de processos técnicos ao longo do trabalho, nomeadamente: Dra. Manuela Marques, Departamento de Química, pela realização da Análise Elementar; Tiago Silva, Departamento de Engenharia de Materiais e Cerâmica, pela a análise SEM; Dr. Igor Bdikin, Departamento de Mecânica, pela a análise AFM.

Por último e igualmente importante, agradeço a toda a rapaziada e familiares que foram estando presentes.

palavras-chave   Nanofibras, electrofiação, gliadina, biopolímeros, ligações-cruzadas, calor, genipina, ácido cítrico, eco-amigável

resumo   O objetivo deste estudo foi desenvolver uma matriz nanofibrosa e ecológica de gliadina de trigo para ser submetida e testada a agentes de reticulação alternativos, calor, genipina, ácido cítrico e o convencional e tóxico glutaraldeído, de modo a que as conhecidas limitações estruturais e de resistência mecânica de fibras proteicas pudessem ser ultrapassadas, nomeadamente quando utilizadas em ambiente aquoso. Nanofibras lisas, bem definidas e sem grânulos de gliadina, com um diâmetro médio de 665 nm, foram produzidas por eletrofiação a uma concentração otimizada de 30% de gliadina (m/v), utilizando como solvente uma mistura de ácido acético/etanol. A maioria dos métodos de reticulação testados não conduziu a resultados satisfatórios, no que respeita à obtenção de membranas nanofibrosas de gliadina que preservassem a sua integridade estrutural e porosidade quando em contacto com a água. O procedimento de reticulação por calor não teve um impacto significativo nas propriedades das fibras, as quais continuaram solúveis em água. Em contraste, a capacidade resistência à água das membranas foi aumentada através de genipina, glutaraldeído e ácido cítrico, mas apenas a combinação de genipina e calor, a 120ºC, foi capaz de manter ligeiramente a estrutura porosa e fibrosa da matriz proteica. O tratamento com genipina a uma concentração de 5% (m/m) permitiu obter membranas com propriedades mecânicas melhoradas. O tempo de reação entre genipina e a proteína, assim como o tempo de maturação após eletrofiação, revelaram-se parâmetros importantes para o aumento da tolerância à água e melhoria das propriedades mecânicas. O tratamento a 120ºC tornou as fibras mecanicamente melhores, destacando-se aquelas tratadas com uma concentração de genipina de 5% após um tempo de armazenamento de um mês e aquelas tratadas com uma concentração de genipina de 10%. O tratamento tradicional com vapor de glutaraldeído resultou em fibras com uma capacidade de alongamento significativamente maior e com um aumento de força à rutura, embora o aumento do tempo de reação leve também a um significativo encolhimento da membrana e aumento da sua rigidez.

abstract   The aim of this study was to develop an eco-friendly gliadin electrospun nanofibrous matrix and its appropriate crosslinking to improve mechanical properties and water resistance. Smooth, well-defined and beadless gliadin nanofibers, with an average diameter of 665 nm, were produced by electrospinning at an optimized concentration of 30% gliadin (w/v), using a mixture of acetic acid/ethanol as the solvent. Different crosslinking methods have been tested, such as heat, genipin, citric acid, and the conventional and toxic glutaraldehyde. Most of the crosslinking methods tested did not lead to satisfactory results in obtaining gliadin nanofibrous membranes that preserved their structural integrity and porosity when in contact with water. The heat-crosslinking procedure did not have a significant impact on the properties of the fibers, which remained soluble in water. In contrast, the water-resistance ability of the membranes was increased through the treatments with genipin, glutaraldehyde and citric acid, but only the combination of genipin and heat treatment at 120 °C was able to slightly maintain the porous and fibrous structure of the protein matrix. Treatment with genipin at a concentration of 5% (w/w) allowed obtaining membranes with improved mechanical properties. The reaction time between genipin and the protein, as well as the time of maturation after electrospinning, were important parameters for water tolerance increase and improvement of the mechanical properties. The treatment at 120 °C increased the fibers mechanical resistance, especially those treated with a concentration of 5% genipin after a storage time of one month and those treated with 10% genipin. The traditional treatment with glutaraldehyde vapor resulted in fibers having significantly greater elongation and increased strength at break, although the increase in reaction time also lead to significant membrane shrinkage and increased stiffness.

Preface

Dear fellows, friends and respectful people, I present to you, without any more delays: "Crosslinking strategies to improve properties of protein-based nanofibrous membranes". The result of an entire academic year, under the academic guidance of Professor António Lopes da Silva.

The objective of this present work lies in the development of a protein-based fibrous membrane and consequent comparative study of crosslinking approaches, that aim to enhance their mechanical, structural and water stability properties, so that a better and sustainable substitute fibrous matrix can be produced to compete with those non eco-friendly. Fibrous gliadin mats, were obtained through the electrospinning technique, with a previous extraction of gliadin protein from wheat gluten. The subsequent crosslinking treatments are based on the use of genipin, heat, citric acid and the traditional glutaraldehyde.

Written in chapters this thesis is divided into five main parts: the first, the introduction, will provide a bibliographic review on the electrospinning world, meaning the theoretical know-how and the latest developments, innovations, and applicability, focusing on a sustainable and ecological policy, namely biopolymers and eco-friendly processes. It follows by second part, "Materials and Methods", with a description of all laboratory methods progressively employed, in order to achieve the proposed global objective. A third and fourth part, will contemplate the obtained results, with an analysis and discussion, as well as the achieved conclusions, respectively. The chapter "Future Objectives" closes the approached and explored theme in this thesis, with future considerations and opportunities.

Making a personal contextualization to the dear reader, about the unfolding of this work, in the early beginning of the academic year a challenge was set. After some minor deviations and change of objectives, the challenge was set. Yet, other changes came along the way. But for someone with the eagerness to create something from the start, "change" was something to be expected of, as part of the process. Once, during my lab time, my esteemed thesis advisor confirmed it. Because not only the scientific battle against the unknown is sometimes a difficult one to win, but in fact, this is how science is produced. As my Professor said to me that time, "Results might not appear as we would wish or expect, because it is part of the deal". Back then, what I concluded was that, putting aside the frustration, readaptation through the change would be a necessary tool to successfully reach the end. For you, dear reader, to concretely contextualize you, my Master's thesis theme changed from "Nanofibrous membranes for lactose removal from milk and whey" to "Crosslinking strategies to improve properties of protein-based nanofibrous membranes". This change was a premeditated and weighted choice, reflecting the need to invest and explore more about the obtained protein fibers, knowing their limitations. Consequently, with the objective to solidify the knowledge in this matter, to pave future successful developments, an attempt has been made to overcome various technical and scientific challenges, about protein-based electrospun fibers, maintaining in the best interests an ecological mentality.

Equally important, for me, during all research process, was to be aware and respect my timeline, and therefore I would have only a year. Thus, despite my great personal satisfaction, the full potential of the project or what could still be explored or optimized, this year would pass, and would pass quickly. And that was it. Fidel Castro reminds me exactly that, when on his last know known speech, at the VII Cuban Communist Party Congress, in Havana, he realizes "Soon I will be 90. It was not the fruit of any effort, it was the whim of fate. Soon I will be like all the rest. Everybody's turn comes".

It remains for me to thank all those, without excluding anyone, that gave me somehow any kind of contribution and made this process more dynamic, exciting and bearable. A great thank you to all of you! To the reader I wish you an excellent curiosity journey. Be aware that patience, enthusiasm, self-criticism is advised to continue reading forward, because in the end it aims to confirm answers, incite questions and even raise doubts.

Contents

List of Figures

List of Tables

Notation

List of Abbreviations

β-Gal	β-Galactosidase
AFM	Atomic Force Microscopy
CA	Citric Acid
DMAc	N,N-dimethylacetamide
DMF	N,N-dimethylformamide
DMSO	Dimethylsulfoxide
EC	Enzyme Commission
EDC	1-Ethyl-3-(dimethylaminopropyl)-carbodiimide
EDS	Energy Dispersive Spectroscopy
FDA	Food and Drugs Administration
GLU	Glutaraldehyde
Gal	Galactose
GEN	Genipin
GOS	Galacto-oligosaccharide
GRAS	Generally Recognized as Safe
MW	Molecular Weight
NHS	N-hydroxysulfosuccinimide
NMP	N-methyl-2-pyrrolidone
OM	Optical microscope
PCL	Poly(ε-caprolactone)
PEI	Polyethylenimine
PEO	Poly(ethylene oxide)
PGA	Polyglycolide
PLA	Polylactic acid
PVA	Poly(vinyl alcohol)
PVP	Poly(vinyl polypyrrolidone)
SEM	Scanning Electron Microscope
SDS	Sodium Dodecyl Sulfate
TGase	Transglutaminase

1. Bibliographic Review

1.1. Electrospinning

1.1.1. Historic and Current Background

Fibers have been surrounding humans since the birth of the mankind. Natural fibers like cotton, silk, animal fibers - Figure 1 - or human hairs are examples of these, although the ways they are produced are different form the ones obtain artificially, as they come from a much more complex process. Our natural fibers serve expected functions, and humans have learned to use these in its favor for all sorts of applications [1].

Figure 1 – Fibers in a spider web [1].

Nowadays, there is a huge interest in fibers created artificially, mainly in nanotechnology, because of their enormous potential in a diversity of industries like aerospace, infrastructure, military, marine, consumer commodities, electronics, medical and food. For that matter, electrospinning technique started gaining great attention, because of its versatility and inexpensive way to produce nanofibers – Figure 2 – with primary applications in tissue engineering, drug delivery, fiber-based sensors, medicine, photovoltaic, filtration membranes, advanced photonic applications, wound healing, and composite materials [2]. In fact, this method is becoming the ideal to produce optimized functionalized fibers, capable of having diameters ranging from nanometers to few micrometers, from a variety of materials such as

polymers (synthetic or natural), composite materials, metals in solution or melted, ceramics and glass, with the ability of controlling the morphology, chemical and mechanical properties of the fibers, according to their purpose and research field [1,3].
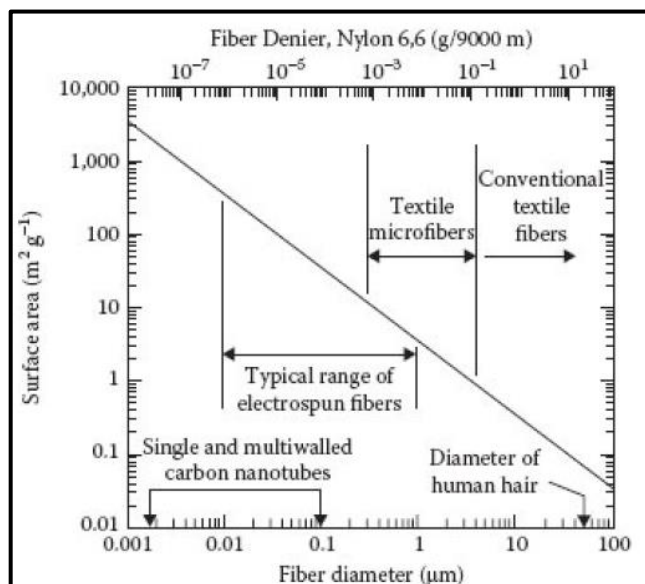
Figure 2 – Characterization of fibers according its diameter [2].

The first experiments regarding electrospinning date back the late sixteenth century, by W. Gilbert who observed that charged amber would eject small droplets from a tip of a cone shape formed, when near a droplet of water. Later, in 1745 G. Bose applied electrical charges on the surface of droplets originating aerosols, and then in 1882, L. Rayleigh, studied the relation and stability of liquid jets in an electric field. The first three patents were filled in 1900 and 1902, about dispersing fluids using electrical charges, by J. Cooley and W. Morton, separately. Another advanced apparatus patent happened in July 1934, by A. Formhals, with the production of spun fibers of cellulose acetate, and in 1939, he patented a second apparatus that allowed multiples needles from the same solution, optimizing the distance between the spinning site and the collector plate [2,4]. In 60's, Sir Geoffrey Taylor published a series of important studies, where he developed a mathematical model that helped to understand the behavior of jets produced under a given electric field: first in 1964, he studied the disintegration of drops in strong electric fields [5]; later, in 1966, Taylor reported his experiments about the force that a strong electric field exert on a conducting fluid, producing a fine jet [6]; and then in 1969, he studied the fluids projected from the vertices of a conducting

tube, where an electric force was applied [7]. In 1971, P. Baumgarten produced electrospun fiber with less than 1 μm, from acrylic polymers, and studied the effects of solution viscosity, surrounding gas, flow rate, voltage, and apparatus geometry on fiber diameter and jet length [8]. Later, in 1981, L. Larrondo and R. Manley produced continuous filaments from melted polymers, such as polyethylene and polypropylene, applying an electric field [9-11]. Between 1986 and 1987, Hayati et al. published a series of studies reporting the process and movement of pendant drops and liquid stable jets, once projected, observing the effects of changing the electric field, environment and solution conductivity [12-14].

In the middle of the 90's, an important work was presented by J. Doshi and D. Reneker, describing the production of fibers of poly(ethylene oxide) (PEO) ranging from 0.05 to 5 micron, in which they listed a number of possible commercial uses of this kind of fibers, like wound dressing materials, reinforcing materials and others; they ultimately coined this process as Electrospinning [15]. From the following years, this and others reports contributed for the increase of knowledge and the elucidation on the potential applications of electrospun nanofibers, that lead to an exponential interest in the electrospinning process by the scientific community, since 2000, as can be seen in Figure 3A [16-21]. Since then, a great number of studies, were published, mainly in China and United States – Figure 3B - for diverse subject areas – Figure 4 - testing different set-ups and models, conditions and controlling parameters, as well as using different materials or mixtures, with a particular recent interest for biopolymers and the use of green solvents [21-24].
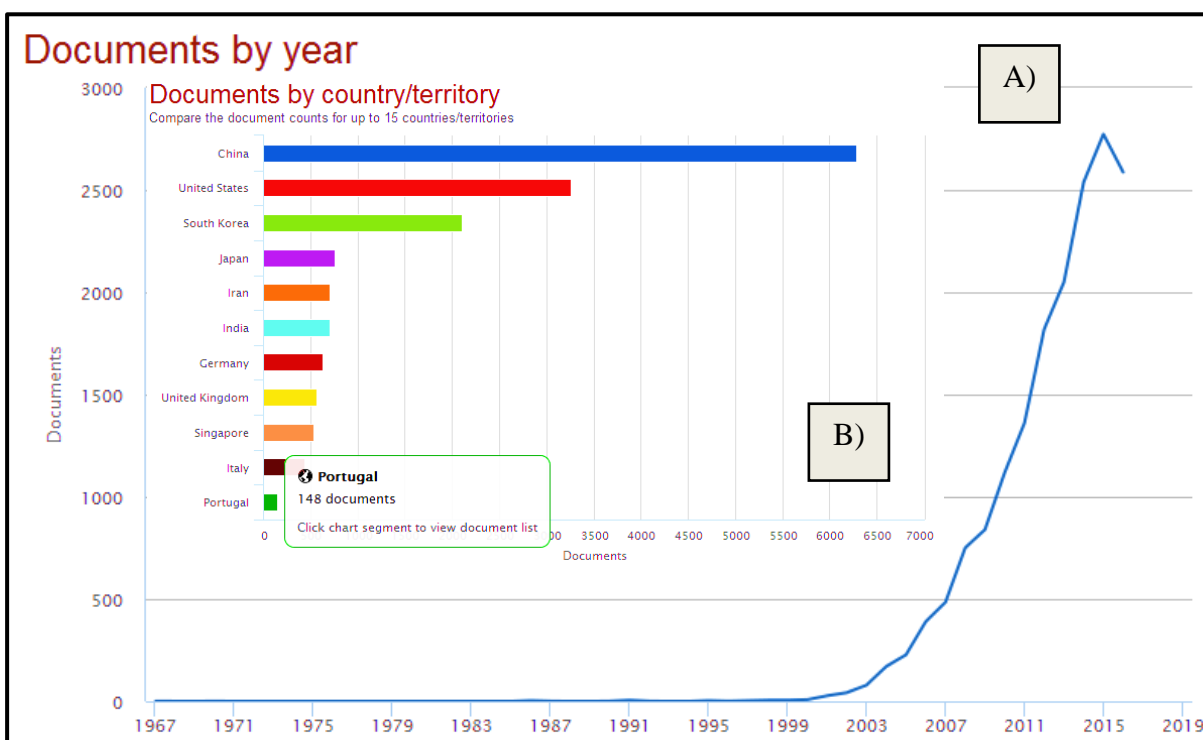
Figure 3 - Scopus keyword search "electrospinning", for articles, until 2017. **A)** Published articles by year - approximately after 2000 there was an exponential increase in publications; there was a slight decrease from 2015 to 2016. **B)** Published articles by country/territory – China is the leader in publishing articles on electrospinning, followed by United States; Portugal published so far 148 articles [21].
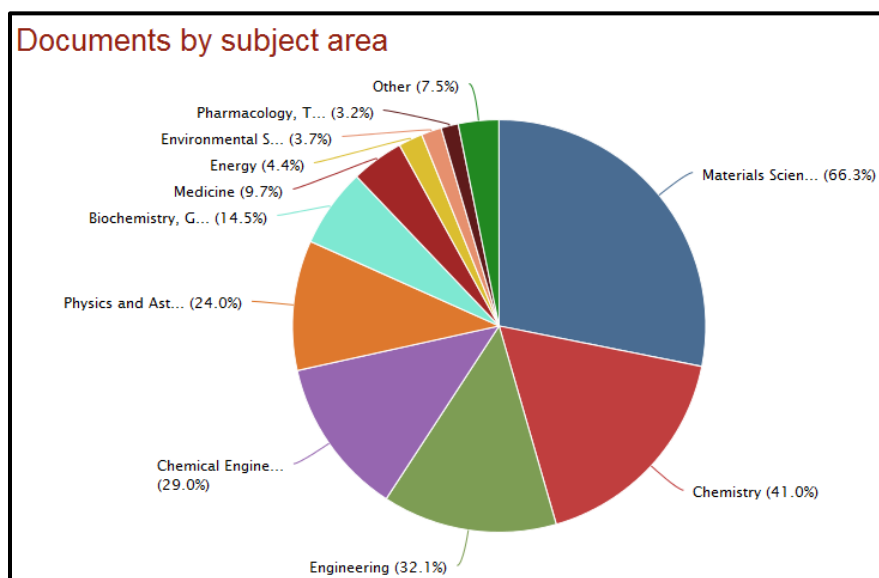
Figure 4 - Scopus keyword search "electrospinning", for articles, until 2017. Published articles by subject area – The leading subject area of publishing on electrospinning is Materials Science, followed by Chemistry, and then Engineering [21].

1.1.2. Theoretical Principles

Electrospinning technique, because of its simple and versatile way of producing nanofibers, is the ideal approach to produce desirable 1D/3D nanostructures, in a continuous process, with a high-volume production. The generated fibers are a result of a unique, rapidly bending thread, that passes through a process of self-assembly induced by electric charges, caused by an external electric source, responsible for the repulsive Coulomb interactions between charged elements on the fluid to be spun [25,26]. However, long before fully understanding this method and the formation of the thin and defined fibers, the process was not enough controlled, and instead small particles or droplets were obtained– a process called electrospraying. The difference is related with the capacity of the produced fiber-jet being continuously stretched, under an electrified charge, but when this does not happen the result

will be the jet atomization originating electrospraying, often due to a low viscosity of the solution [2,25].

Electrostatic spinning of a polymeric solution starts after the fluid is pumped through a syringe, where in its needle is applied a certain electric charge [27]. The formation and the projection of an electrospun fiber are described according experimental and theoretical observations of the process. Firstly, a droplet forms at the tip of the syringe needle, where the electric field plays a crucial function, interacting with the charged fluid and modifying the droplet shape attached to a tip, which means that it allows the droplet (assuming a prolate shape) to become increasingly longer, as the electric field increases, forming a characteristic conical shape (Taylor cone) with a stable jet – Figure 5 A) [1,28-30]. Development of a rectilinear stable jet comes next, for a limited length - Figure 5 B), - which diameter is known to decrease as the distance from the tip increases, mostly due to solvents evaporation, but also because of the longitudinal elongation of the induced jet, identified as longitudinal force [26,30]. In the end of the straight segment, bending deformations are observed with spiraling and looping trajectories, because the jet can no longer maintain a rectilinear direction towards the collector, due to insignificantly longitudinal force, giving rise to those bending instabilities. Consequently, as the loop diameter increases, the jet becomes more stretched and narrowed, looping in itself [1,31,32]. Eventually, the solidified fiber or the projected jet reaches and deposits on a collector, corresponding to the final step of electrospinning. The final diameter obtained is derived from both the thinning and elongation during the straight jet phase and the looping phase, but also from the solvent evaporation during those same steps. Moreover, deposition of fibers happens regardless the time of the fiber formation or even the boiling point of the solvent, however it could reflect on the morphology and characteristics of the fiber network [26,27]. Besides, under some experimental conditions, it is possible to observe a jet branching with multiple trajectories, during jet motion and on the fibers deposition, being this originated from electric effects [33]. Finally, it's also important to note that gravitational force has no significant role in electrospinning [27].
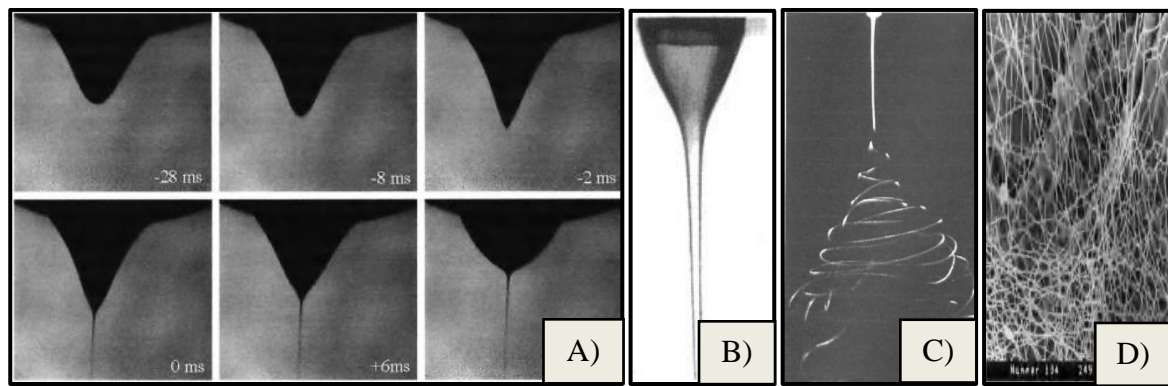
Figure 5 - Observational experiments of electrospun fiber formation process. **A)** Deformation of a pending droplet by electric fields. **B)** Cone-shaped droplet and rectilinear jet region, at elevated electric fields. **C)** Looping trajectory of the jet. **D)** Deposition of the fiber in a collector (Adapted) [1].

1.1.3. Mechanical Setup

The design of electrospinning mechanical setups has been changing through the years, according with the experimental needs and objectives. The necessary equipment for a successful electrospinning process, on a laboratory scale, consists in a simple setup composed by a high voltage power supply, a syringe pump, a spinneret and a collector, as can be seen on Figure 6 [34].

It is known that the electrostatic force field is crucial on the spinning process, and thus one of the major components is a high-voltage external power supply, as referred, usually a direct current power supply, that provides an electrostatic field, ranging from a few thousands of volts to a hundred thousand of volts [22,25]. Besides that, for the process to occur a glass or plastic syringe, with a certain polymeric solution, is copulated to a flow pump system that defines a constant and controllable feed rate of the spinning fluid [25]; this arrangement can be different with for example the use of an apparatus that uses a constant pressure header tank [34]. A spinneret, normally a metallic needle, attached to the syringe, where the solution flows through, possesses different arrangements depending on the desired fiber conformation: a normal single spinneret, coaxial, or side by side spinneret; or multi-spinnerets, varying the axis alignment or the number of spinnerets, often used to increase the volume production [35-38]. The collector itself, a grounded conductor, can also have a variable design, which could be a plate, or simply a sheet of aluminum foil, or even a rotating drum that is more suitable for obtaining aligned fibers, rather than randomly orientated [24,39,40].
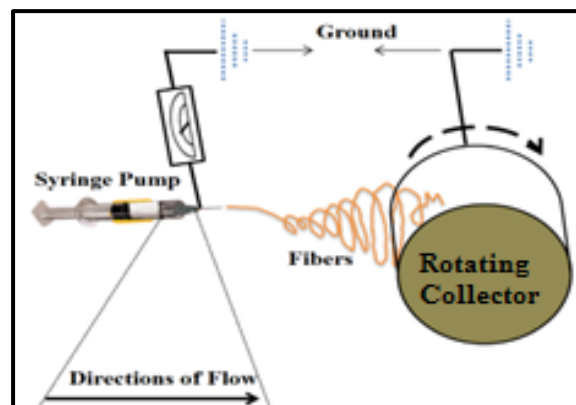
Figure 6 – Illustration showing electrospinning mechanical setup and process (Adapted) [22].

1.1.4. Controlling Parameters

The ability to achieve desirable fibers depends hugely on the experimental parameters and on the properties of the polymers and solvents intended to produce electrospun mats. In fact, process optimization is typically a multivariate problem where several interacting variables must be taken into consideration; these controlling parameters are generally divided on solution parameters, processing parameters, and ambient parameters, and they are known to greatly influence final fiber characteristics, including their morphologies and diameters [41].

1.1.4.1. Solution Parameters

Concentration

Testing the proper concentration of a polymer solution is a crucial step, knowing that for limiting concentrations, from excessively low to too high, electrospinning process may not happen. When the concentration is low, electrospraying occurs, instead of electrospinning, given the low viscosity and high surface tension of the solution; increasing it a little further it is possible to obtain some fibers, although with beads on them, with different sizes. Using appropriated concentration smooth and fine fibers are observed; above the suitable

concentration, fibers lose definition and their diameter increase, so helix-shaped micro-ribbons fibers are usually produced [22,42,43,44].

Molecular Weight

It is possible to have the same polymer and solution concentration, under the same experimental conditions, and still obtain different fibers morphologies. That is due to molecular weight (MW) effect, which reflects in the solution viscosity; for a given concentration it is expected that the solution viscosity decreases as the polymer MW decreases; lowering the MW can result in the formation of fibers with beads, a similar effect as having a low concentration, as described above; however, increasing the MW smooth fibers are possibly obtained, and increasing it further micro-ribbon fibers are likely formed [41,45,46].

Viscosity

It is known that there is a relationship between viscosity and concentration, or even MW, which means that increasing concentration, reflects on a higher viscosity, and the same could happen with MW. Indeed, viscosity is an important factor for polymeric spinning solution, because with a very low viscosity it is not possible to observe continuous beads-free fibers, but increasing the solution viscosity usually leads to beadless and smoother fibers – Figure 7; above a certain critical viscosity, it may become impossible to perform the electrospinning process, since the fluid becomes too viscous and the applied electrostatic forces are no longer able to promote the jet formation [45-48].
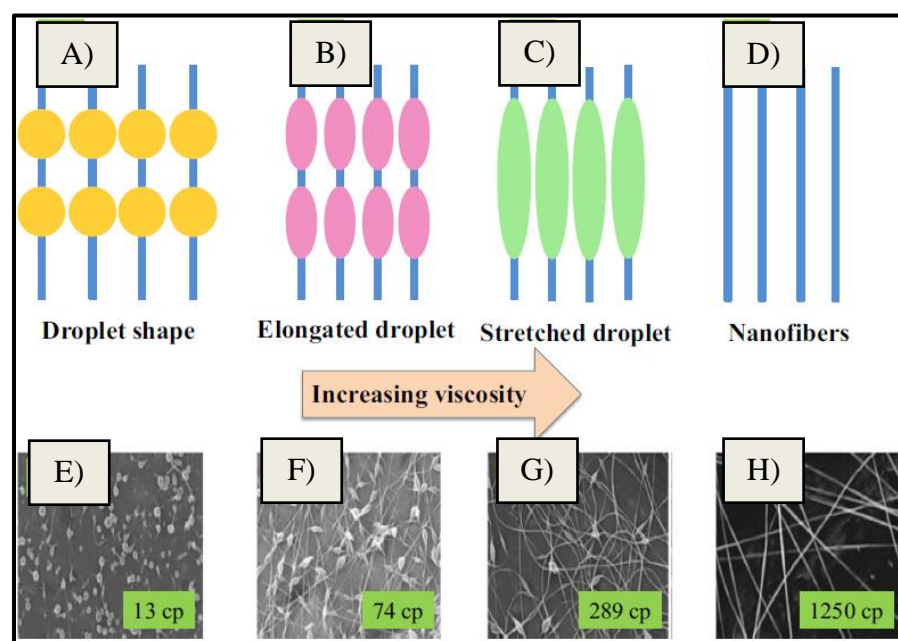
Figure 7 – Process of increasing viscosity to obtain fine and beadless fibers: A-D) Illustrations; **E–H)** Scanning Electron Microscope (SEM) micrographs, showing the increasing viscosity values [22].

Surface Tension

Surface tension is also a recognized important factor, attributed to solvents in the spinning solution, with a significant effect on the morphology of the electrospun fibers. It becomes the dominant factor, when the viscosity remains low and the surface tension of a solution decreases, producing then beaded fibers or just beads. Consequently, its increase may assist in the production of larger fiber. It's essential to notice that surface tension is a variable characteristic of each solvent and that reducing it smooth fibers are likely to be obtained instead of beaded fibers [41,42,44].

Conductivity

The solution conductivity also affects the electrospinning process due to the importance of charge repulsion to stretch the polymer solution. Choosing a polymer, a solvent or salt to produce the spinning solution determine mostly of solution conductivity, because of the electronic charges of their natures, so it affects the Taylor cone formation and fiber diameter. Considering a situation where the solution charge density is not enough for the formation of the Taylor cone, under a certain electric field, increasing the solution conductivity will increase the charge on the surface of the droplet and thinner fibers may be produced [22,49,50].

1.1.4.2. Processing Parameters

Applied Voltage

The presence of a certain applied voltage, supplied by an external power supply is a major factor on electrospinning, as stated before (§ 1.1.3). It defines not only the jetting start or change process from Taylor cone, when the applied voltage is above the threshold voltage – Figure 8 - but also the final morphology of spun fibers. However, the relation between the electric field and final fiber morphology and diameter is still poor understood and discordant results have been reported; increasing voltage can increase, diminish or maintain the final fiber diameter, depending on other variables, although it is clearly a process parameter that exerts a

crucial influence on the final fibers' characteristics [22,29,30,51-56].
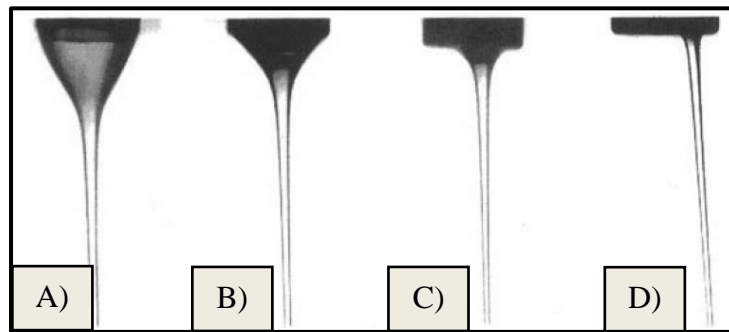
Figure 8 – Increasing the electric field can lead to a cone deformation: **A)** ideal cone shape; **B–D)** strong deviations on the cone shape, resulted of a higher voltage [30].

Feed Rate

The feed rate, or flow rate, determines the volume solution within the syringe that passes through the needle to the outside, during a period of time. Normally, a higher feed rate could create unspun droplets, on the tip of needle, and also form bead fibers with larger diameters; so generally, testing with a low feed rate smooth and thin fibers are produced, which means that a balance is required between the amount of solution that leaves the tip of the needle and is ejected and the rate of replacement of the solution on the tip of the needle [22,41,57].

Distance between the Tip of the Syringe and Collector

There's a proven effect relation between the needle-to-collector distance and the final fibers' diameters and morphologies. Solvent volatility is one reason for this relation, because solvent needs to evaporate so that the fibers can solidify and become thinner before depositing. On short distance, there will not be enough time for drying, and the fibers become thicker, although it all depends on the solvent volatility; moreover, for longer distances, beaded or thinner fibers can be observed [43,50,55,56,58,59]. This distance not only affects the flight time but also the electric field strength. The electric field increases as the distance decreases, which leads to an increase in jet acceleration, also contributing to hinder the solvent evaporation and to originate bead fibers and/or fusion of fibers [27,34,59].

Needle Diameter

Needle diameter can affect the final diameter of fibers, because as the orifice size is reduzed, less volume of the spinning solution is gathered at the tip, so thinner fibers are obtained and with less beads. However, a larger needle diameter can lead to formation of large droplets at the tip; or in the presence of too small orificie the solution may not be pumped through [59,60].

1.1.4.3. Ambiental Parameters

Temperature

Given that temperature has an inverse relationship with the solution viscosity: smaller fiber diameters were observed as the temperature increases. Also, higher temperatures are expected to result in an increase of solvent evaporation rate, which at the end leads to a decrease of fiber diameter [59,61,62].

Humidity

Relative humidity influences the fiber morphology mainly due to the effect on the solvent evaporation rate. Low humidity levels can rapidly increase solvent evaporation and thus contribute to a decrease of fiber's diameter, whereas high humidity can induce a thicker diameter fiber; however this depends on the chemical nature of the polymer and other parameters discussed above [62-65].

1.2. Biodegradable Polymers and its Applications in Electrospinning

As electrospinning technology continues to grow, a lot of attention is reserved for its potential role in helping to solve environmental and energy issues worldwide. For that reason, attempts have been made to answer those concerns by designing and creating functionalized and optimized nanofibers capable of compete on global industry, to make a better and sustainable substitute for those non eco-friendly. Electrospinning has proven to be a technique with a great potential in energy fields such as on organic and hybrid solar cells, carbon dioxide capture, hydrogen storage, thermal storage, and dye-sensitized solar cells; besides that, a great initiative is being successfully made using nanofibers, in environmental fields, for liquid and air filtration, sensors, adsorbents and photocatalytic applications [66]. In addition, biomedical and food engineering are other two major fields where extensive and promising research is being done, having in consideration an ecological side: the first one, because of biological similarity of some polymers to regulate and support cellular activities of the human tissues and organs, and for that and more being used in cosmetics, tissue engineering, drug delivery and biosensors applications; the second one, due to the fact that nanofibers might improve some food processing methods and at the same time reducing the toxicity risk of material surrounding the food or used in the food industry, with applications such as separation operations, encapsulation of food bioactive compounds or microorganisms and food sensors [67,68].

Having this in consideration it is important to remember that the primary effort is in fact to produce electrospun fibers in a greener way, hence using biodegradable polymers, characterized for being naturally degradable, nonabrasive, nontoxic, low-cost, renewable, and eco-friendly solvents, which will be discussed below. Biodegradable polymers can be divided into two families: natural polymer (biopolymers) or synthetic polymers, according to Figure 9 [23].
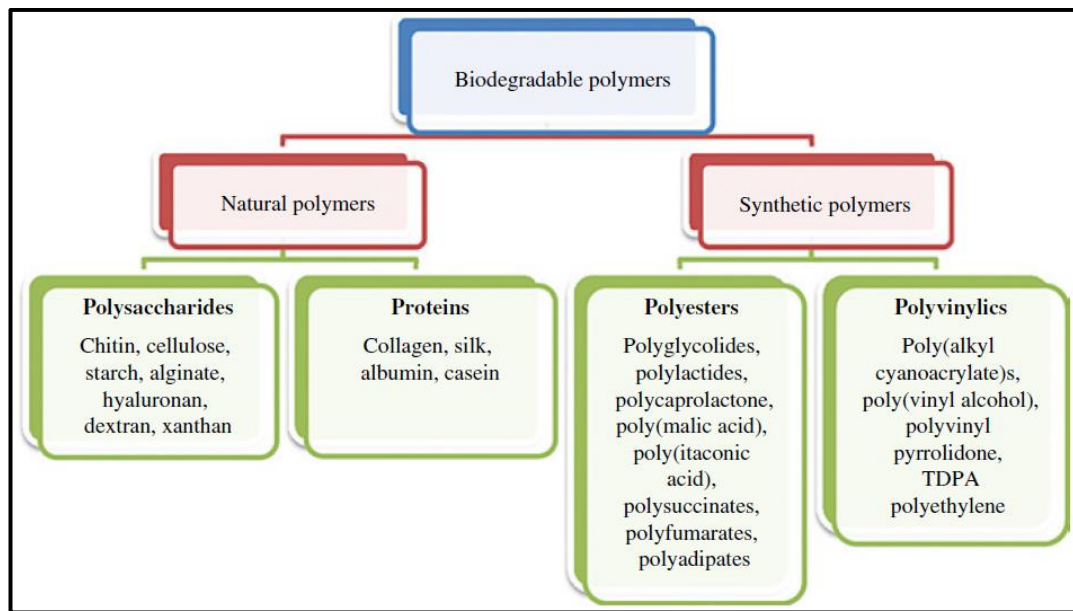
Figure 9 – Categorization of biodegradable polymers into two families (natural polymers and synthetic polymers), each one of those divided into two groups [23].

1.2.1. Synthetic Polymers

In general, biodegradable synthetic polymer are divided into two groups, according to their main functional group: polyesters, such as poly(ε-caprolactone) (PCL), polyglycolide (PGA) and polylactic acid (PLA) and its copolymers; and the polyvinylics, such as the largely used poly(vinyl alcohol) (PVA) and poly(vinyl polypyrrolidone) (PVP) [23]. Because of their characteristic nature some of them, such as PVA or PCL, have been approved by Food and Drugs Administration (FDA) for clinical or food use [68-71]. Equally important to mention, it is that that even though they are biodegradables, some synthetic polymers, PCL, polybutylene succinate and polyester amide, are petroleum- derived [23].

Electrospun polyester polymers are vastly used for medical applications, particularly for wound dressings and tissue engineering, because they have a great capacity to simulate the extracellular matrix, originating synthetic scaffolds (for example, skin tissue and nerve regeneration, and engineered tendons) that exhibit high wettability among cells, nontoxicity, biodegradability, structural integrity and biocompatibility [2,72-75]. Moreover, these polymers can also be employed in many other areas such as food engineering, for enzyme immobilization or for air particles filtration [76-78].

Electrospun fibers of polyvinylic polymers have a wide range of applications, which allow a great versatility in various research fields. PVA fibers, whose polymer is water-

soluble, for instance, when combined with metal, metal oxide or a mixture of other polymers, exhibit photonic functions by emitting strong light from fibers, magnetic properties and also work as dye-sensitized solar cells. Besides, among others, PVA electrospun fibers demonstrated a good result for enzymes, viruses and bacteria encapsulation, potential for wound dressing and for environmental solutions, as air particle filter [79-86]. PVP, another highly water-soluble polymer, which is frequently blended with other polymers, is used as a polymer-stabilizer of metal nanoparticles, like platinum, rhodium or gold to serve as a catalyst, and has also proven potential applications in water remediation field, wound dressing and due to antimicrobial activity when doped with metals [84,86-90].

1.2.2. Biopolymers

Biopolymeric fibers have been providing an alternative way to contest the use of non eco-friendly polymers, because not only natural polymers (some examples are shown in Figure 10) are obtained from a low-cost, renewable and ecological source, thus distancing themselves also from those petroleum- based biodegradable polymers, but also the electrospun fibers show very high porosity, high surface area per unit mass, adjustable mechanical properties [23,66,91]. Furthermore, they may exhibit better fibers cytocompatibility response than those synthetic, once that they could retain their natural cell-bindings sites [72]. Despite these facts, biopolymers could demonstrate a certain difficulty to be electrospinnable, namely polysaccharides, and spun fibers enzymatic biodegradation and their water solubility can occur naturally [72,91]. This family of polymers can be divided into Polysaccharides and Proteins – Figure 9 [23].
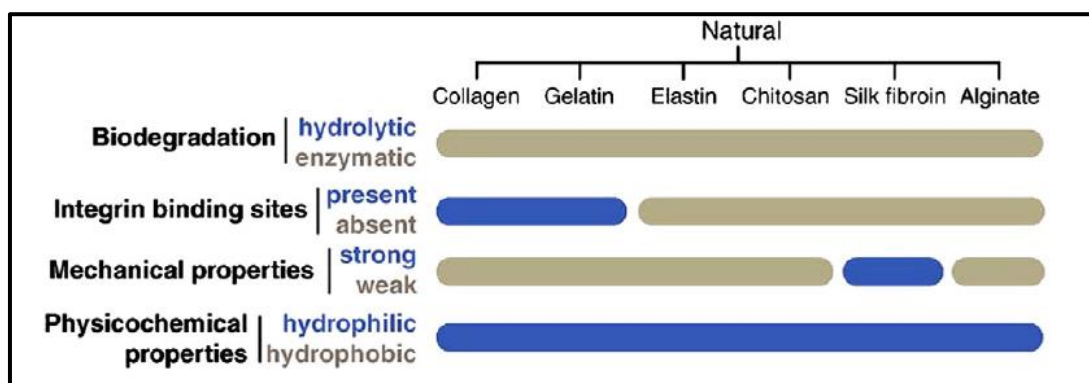
Figure 10 – Example of some biopolymers and their comparative properties [68].

1.2.2.1. Polysaccharides

The list of polysaccharides already electrospun is extensive, alone or combined with other biodegradable polymers, being the biomedical area one of the most representative application areas [91].

Most polysaccharide solutions, above a certain critical concentration, show the typical shear thinning behavior, i.e., the apparent viscosity decreases as the shear rate increases. For fiber formation during electrospinning, a small shear thinning degree is usually desirable, since if there is a too pronounced decrease in viscosity due to the deformation imposed by the electric field, the spinning fluid jet on the tip of the needle breaks easily and there is no fiber formation [92].

Chitosan is a cationic polysaccharide whose application in electrospinning has been largely studied [23]. The spinning solution of chitosan can be prepared using solvents like hydrochloric acid, acetic acid, and trifluoroacetic acid; fiber diameters ranging of 60 to 200nm were obtained with this last solvent, according different polymer MWs and concentrations [91,93]. Synthetic polymers of PVA, PCL and PEO are commonly used to produce blended nanofibers with this chitin-derived polymer. The majority of applications have to do with biomedical reasons, for example for prevention of wound infections and local chemotherapy, tissue engineering of liver, or even for wound dressing and anti-microbial applications [91,94-96].

Another abundant polymer is cellulose, which due to the strong bond interactions makes the solubilization difficult in common solvents, limiting the process, so a better alternative is to use cellulose derivates, for example, hydroxypropyl methyl cellulose, ethyl cellulose and cellulose acetate [66]. Some of the functional properties of these biopolymer electrospun fibers have been applied for tissue engineering of bone, water remediation for removal of heavy metals, anti-microbial and enzymatic immobilization [91,97-99].

Dextran is another natural material where smooth electrospun fiber can be produced ranging hundred nanometers to few micrometers [100]. Various solvents are used in particular water, but mixture of dimethylsulfoxide (DMSO)/N,N-dimethylformamide(DMF) and DMSO/water as well [91]. Blended nanofibers of dextran and antibacterial compounds showed high antimicrobial activity against gram positive and negative bacteria, and exhibited useful applications as wound dressings [101,102].

Starch, alginate, pullulan and cyclodextrin are some of other few polysaccharides that can be used to obtain fine electrospun fibers; nevertheless, the list of polysaccharides for

electrospinning continues to grow, and future developments are expected in this area [91].

1.2.2.2. Proteins

Protein can be used as a natural source to obtain functional biomaterials, and according to the source, they can be categorized as animal proteins, such as whey protein, collagen, gelatin and casein, or plant protein, like soy protein, wheat, or canola [23]. In general, the physical and chemical properties of proteins (namely globular proteins, which are typically soluble in water or in acid/base aqueous solvents, and fibrous proteins, water insoluble) are related with the kind of amino acid residues existing and their position on the polymer chain [103]. Because of their stable 3D structure, due to hydrogen bonding and hydrophobic interactions, or even disulfide bonds, it may be necessary to partially unfold proteins to allow for molecular reorientation and to make them suitable to produce biomaterials [23,103]. Therefore, it may be required to choose proper solvents, might them be aqueous acids or bases, the use of heat or the addition of denaturing agents [91]. In the same way as polysaccharides, protein fibers alone show some problems related with mechanical strength and aqueous media stability, so they are frequently combined with other polymers, mainly biodegradables ones, or there is the need to perform some kind of post-electrospinning treatment, namely cross-linking, as will be discussed in section § 1.2.3.[91].

Prolamins are among the proteins most used so far to obtain electrospun nanofibers, such as zein, hordein, glutenin and kafirin, from maize, barley, wheat and sorghum, respectively [104-107]. Generally and according to their solubility, cereal plant proteins are classified into albumins, globulins, prolamins and glutelins, being the prolamins soluble in aqueous alcohol solutions (70–90%), and characterized by high content of proline and glutamic acid. Depending on the cereal, the prolamin content is variable between 35-50% of all protein content, in wheat, barley, maize, and sorghum [108,109]. Among prolamins, zein has been the most studied to produce electrospun nanofibers, using solvents like ethanol, isopropanol, acetic acid or even DMF. Characteristics as biodegradability and biocompatibility brand this once low-valued material as a versatile electrospinnable polymer capable of providing new resources for biomedical applications, mostly by mixing with other biodegradable polymers, e.g. zein-collagen fibrous membranes for wound healing[111], polyurethane–cellulose acetate–zein antibacterial composite mats[112] and fluorescent nanofibrous scaffolds containing curcumin for soft tissue engineering [113].

Although with fewer research studies published, hordein shows less cytotoxicity than zein, plus nanofibrous membranes from this biopolymer showed attractive characteristics as flexible materials with temperature sensing properties for sensors and electronic devices, and when combined with zein, as useful nonadherent biocompatible materials for controlled drug delivery in wound dressings and other applications [105,114-117].

Wheat (*Triticum spp.*) is one of the most cultivated cereals, since the beginning of human civilization, compose by 60-80% starch and 7-22% storage proteins. Wheat proteins are recognized to be influenced by plant genotype and environmental factors, and are responsible to form the visco-elastic dough. These proteins are known as gluten proteins corresponding to the grain storage protein fraction and comprising around 80-85% of total wheat proteins. Gluten can be divided into two functional groups of proteins: gliadins that contribute to dough cohesiveness, softness and extensibility, therefore conferring viscous behavior; and glutenins responsible for dough hardness and elasticity [108,118]. The first successful study regarding the production of electrospun nanofibers from gluten is dated 2005, but other studies have since appeared using gluten alone or blended with PVA, using solvents such as 1,1,1,3,3,3-hexafluoro-2-propanol, ethanol/2-mercaptoethanol or water/1-propanol. The presence of disulfide bonds in gluten proteins makes wheat gluten not suitable for a direct electrospinning from aqueous dispersions, therefore the use of solvents like 1,1,1,3,3,3-hexafluoro-2-propanol or 2-mercaptoethanol increases wheat gluten solubility, as well as thiolated additives as reducing agents [119-124]. Gluten-based nanofibers have shown interesting properties, for example antimicrobial activity against *Staphylococcus aureus* when blended with PVA and zirconia, and incorporated with nisin, controlled prolonged-release of certain polar compounds such as urea, or as efficient low-cost adsorbents in aqueous environments to remove and recover metal nanoparticles, also when combined with PVA [122-124].

Glutenins, part of the referred wheat gluten protein fraction, are recognized as a heterogeneous protein mixture, whose MW ranges between 80000 and several million Da [108]. This electrospinnable protein has great water stability, due to the extensive inter- and intra-crosslinking by disulfide bonds, due to the elevated presence of cysteine. For this reason, sodium dodecyl sulfate (SDS) is often added to the spun dope to decrease the degree of S-S bonding, thus allowing a better spinning solution to be obtained. Hence, PVA nanofibers have been prepared using glutenin as an additive to improve elasticity. In addition, wheat glutenin was used to produce a promising 3D electrospun nanofibrous structure for adipose tissue engineering [108,125,126].

Gliadins

Gliadins are also wheat gluten prolamins, whose MWs are defined between 30000-80000 Da, and represents circa of 40-50% of the total storage proteins. As well as glutenins, however differently, gliadins contain disulfide bonds, in particular intra-molecular on α-, β-, and γ –gliadins, but no S-S bonds at all on ω-gliadins. The different macromolecular organization and intra- and intermolecular interactions are responsible for different solubility, and contrarily to glutenins, gliadins are soluble in aqueous alcohols. Gliadins are also rich in proline and glutamine, and when solubilized in 70% aqueous they adopt a globular shape [127].

The first fruitfully attempt for obtaining electrospinnable fibers made from gliadin used an acetic acid extracted protein fraction from commercial wheat gluten. Fibers obtained ranged from 100 nm to 5 μm. However, fine and smooth fibers were not obtained (Figure 11), probably due to the too low polymer concentration and/or because the protein extract was rich mainly in low MW gliadins [119].

Gliadin nanofibers were also successful produced using hybrid organic–inorganic molecules (polyhedral oligomeric silsesquioxane) as nanofillers to improve fiber properties. Comparing gliadin with gluten fibers, the first showed better, smother and thinner fibers (average diameter 222±12 nm) than gluten (diameter around 460 nm). Thinner fibers, although presenting some beads, but also higher jet instabilities were obtained due to the presence of the fillers [128].
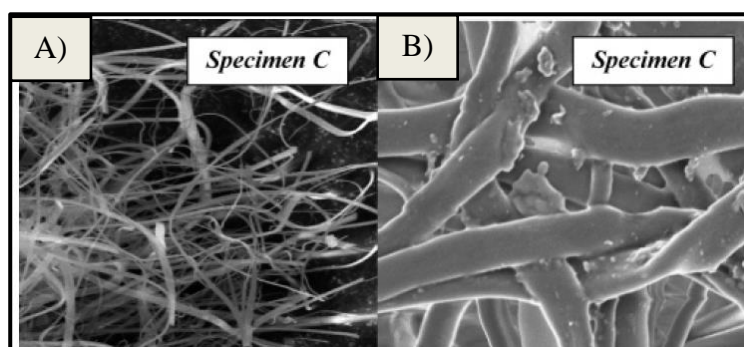
Figure 11 - SEM micrograph of electrospun fibers of wheat gluten low MW fraction. **A)** Fibers obtained were not uniform or smooth. **B)** Fibers without fine definition at a higher magnification [119].

A major study was made to compare three prolamins for electrospinning: zein, hordein and gliadin. Acetic acid or a mixture of water and acetic acid were used to solubilize the three

proteins, which were all alcohol-extracted. Analyses showed that hordein and gliadin have similar amino acid content, but the second one showed a higher content in cysteine of all three, and thus a higher probability to form disulfide bonds. Higher protein concentration and the increase of the amount of acetic acid in the mixed solvent led to an increase of solution viscosity, with hordein exhibiting the most viscous solution and zein the least. It was proposed that the optimized concentration, using acetic acid 100% as the solvent, would be 200 mg/mL for gliadin. All prolamin proteins displayed similar fiber diameters, about 200 nm, at their optimized concentrations, however morphology changed between them, as can be compared in Figure 12. It is possible to observe more uniform nanofibers using gliadin, although with some bead formations (Figure 12 B). Comparing mechanical properties, gliadin nanofibrous mats showed a higher tensile strength of all three, probably due to smaller changes in the protein secondary structures and interactions during the electro-spinning process. In terms of biocompatibility, hordein fibers exhibited much lower cytotoxicity than gliadin and zein fibers, showing gliadin fibers the highest [114].
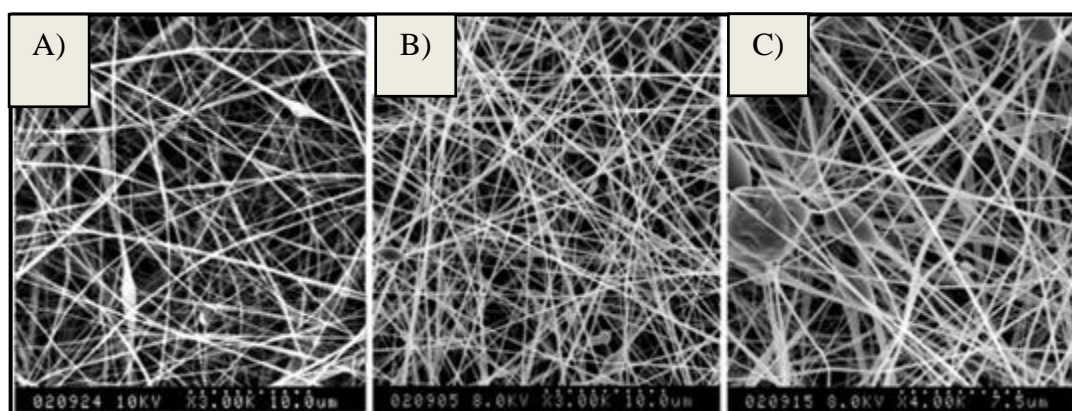
Figure 12 - SEM micrograph of prolamins electrospun fibers at their optimized concentrations. **A)** Hordein nanofibers (150 mg/mL). **B)** Gliadin nanofibers (200 mg/mL). **C)** Zein nanofibers (300 mg/mL) [114].

1.2.3. Crosslinking of Electrospun Fibers

Electrospun biopolymeric materials have been potentiating biomedical and food research, due to their ecological side and versatile properties. In the last two decades, a great emphasis has been placed on the fabrication of biomaterials based on proteins such as silk, albumin, gelatin, or cereal proteins in general. Scaffolds with ability to mimic extra cellular matrices, related to the protein cytocompatibility and biodegradability, and mats with capability of loading nanoparticles, drugs or nutraceuticals to induce their sustained released, or as nano structured supports to immobilize enzymes, are some examples [103,129].

Although protein spun fibers present themselves as a sustainable and good alternative to synthetic polymers and even other biopolymers, they typically demonstrate insufficient mechanical properties and poor stability in aqueous media or under high relative humidity conditions, often losing their fibrous and porous structure, or even dissolve or disintegrate. Figure 13 shows an example of the observed morphological and structural changes for zein electrospun fibers when in contact with aqueous medium [130]. To overcome these challenges, one way is to produce blends: mixtures of different polymeric materials provide the final blended product improved physical and structural properties, as was already shown, for example, for polyurethane/cellulose acetate/zein, amaranth protein isolate/pullulan, soy protein/lignin, or PCL/gelatin, polyurethane/gelatin and PLA/gelatin electrospun fibers [91,112,131, 132,133].
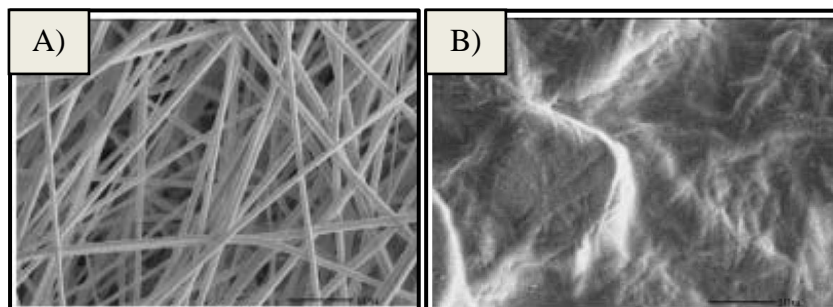
Figure 13 - SEM micrograph of zein electrospun fibers, without any treatment. **A)** Zein fibers at 2000X. **B)** Zein fibers after wetting with water and drying (Adapted) [130].

Crosslinking treatments, summarized on Figure 14, are another alternative popularly used to increase electrospun fibers performance, improving in general their mechanical and

structural functions, which results from the action of crosslinking agents that interconnects polymer molecules [129]. Crosslinking of proteins may result in protein interactions within the same polypeptide chain or between different polypeptide chains from the same protein, or between different proteins [134]. Crosslinking treatments have been used in the majority of all electrospinnable proteins studied so far, such as zein, wheat, soy, whey, gelatin, collagen and fibrinogen confirming the improvement of the characteristics of these fibrous materials that can be obtained by this approach [91,135-138]. For example, noncytotoxic soy protein electrospun fibers with higher fiber strength were obtained after crosslinked using 1-ethyl-3-(dimethylaminopropyl)-carbodiimide(EDC)/N-hydroxysulfosuccinimide (NHS) [139].

Crosslinking can be accomplished by enzymatic, physical or chemical methods [91]. Physical treatments, like heat-induction or UV-irradiation may introduce desired changes on the fibers. Irradiation treatments (UV, γ-irradiation) may cause different modifications on proteins, namely oxidation of amino acids, conformation modifications, formation of protein free radicals or establishment of covalent bonds [103,129,140]. In one report, UV radiation and genipin cross-linking were compared to immobilize collagen on the surface of electrospun poly (methyl methacrylate) nanofibers; even though the amount of collagen immobilized by genipin cross-linking was significantly higher, the UV-irradiated fibers exhibited greater potential for cellular growth and proliferation of respiratory epithelial cells [141]. Heat is another method to induced crosslinking reactions, first through protein denaturation, then promoting interactions between peptides chains such as covalent bonds [103,136]. Heat-induced covalent crosslinking was investigated in PEO blended nanofibers, with whey proteins, specifically whey protein isolate and β-lactoglobulin, by submitting the produced fibers to temperatures above the gelation temperature of whey proteins. After one-hour treatment at 80ºC, fibers kept their fibrous structure as well as the fiber diameter, and even increasing thermal stability for the β-lactoglobulin/PEO fibers. To water insolubility impact was evaluate by immersing electrospun mats after a procedure at 100ºC for 24 to 44h, in which they prove to be water-resistant, even after days in water, thus it could be suggested the existence of a protein crosslinking caused by the β-lactoglobulin unfolding and the formation of disulfide bonds; moreover, the insolubility effect was dependent of the treatment time and sample thickness [136].

For protein-based materials, enzymatic crosslinkings can be achieved using the microbial enzyme transglutaminase (TGase), obtained commercially from *Streptoverticillium mobaraense*. Also known as protein-glutamine γ-glutamyltransferase (EC 2.3.2.13), this enzyme catalyzes the establishment of inter- and intramolecular covalent bonds between

amino acids residues of glutamine and lysine. Nowadays, it has a vast application in food industry, mainly to change and improve the techno-functional properties of proteins, and consequently the appearance and texture of food systems [142]. Through the enzymatic crosslinking with transglutaminase, fish gelatin spun fibers loaded with nanodiamond particles were successfully obtained, with the objective of developing extracellular matrix analogues [143].

For last, chemical methods are the most commonly used to ensure crosslinks among proteins in different types of materials. Different compounds have already been used as crosslinkers, such as aldehydes (glutaraldehyde (GLU), formaldehyde), carbodiimides or sodium metaphosphate [129]. Nevertheless, glutaraldehyde remains the most practical and chosen crosslinking agent, not only due to limitations of the others, related mostly with their efficiency, but also because GLU is a low cost and versatile crosslinker, that can guarantee chemically and thermally stable crosslinks between both proteins and polysaccharides, under short reaction times [129,144,145]. GLU, a 5-carbon dialdehyde, is a clear liquid, soluble in water and in several alcohols and other organic solvents. This non-specific reagent can react with several amino acids, like cysteine, proline, lysine, tyrosine, phenylalanine, serine, tryptophan and arginine, histidine, and glycine, by interacting with different functional groups such as phenol, amine, imidazole, and thiol [144]. In general, using a large excess of this reagent, inter- and intramolecular crosslinkings can occur between proteins, through the ε-amino group of lysyl residues, present in most proteins, involving reactions such as aldol condensations. There are diverse mechanisms responsible for the crosslinking reactions, which depend on the medium conditions[134,146]. In terms of applications, improved spun fibers made from zein were crosslinked using 8% glutaraldehyde (w/v), becoming relatively water-insoluble, especially after heating treatment[130]. Moreover, gelatin crosslinked scaffolds acquired aqueous stability and improved tensile properties, after treated with GLU[147]. Also, GLU crosslinking treatment was done on PVA/Gluten nanofibers, producing mats to act as adsorbents, to remove nanoparticles from water [110].
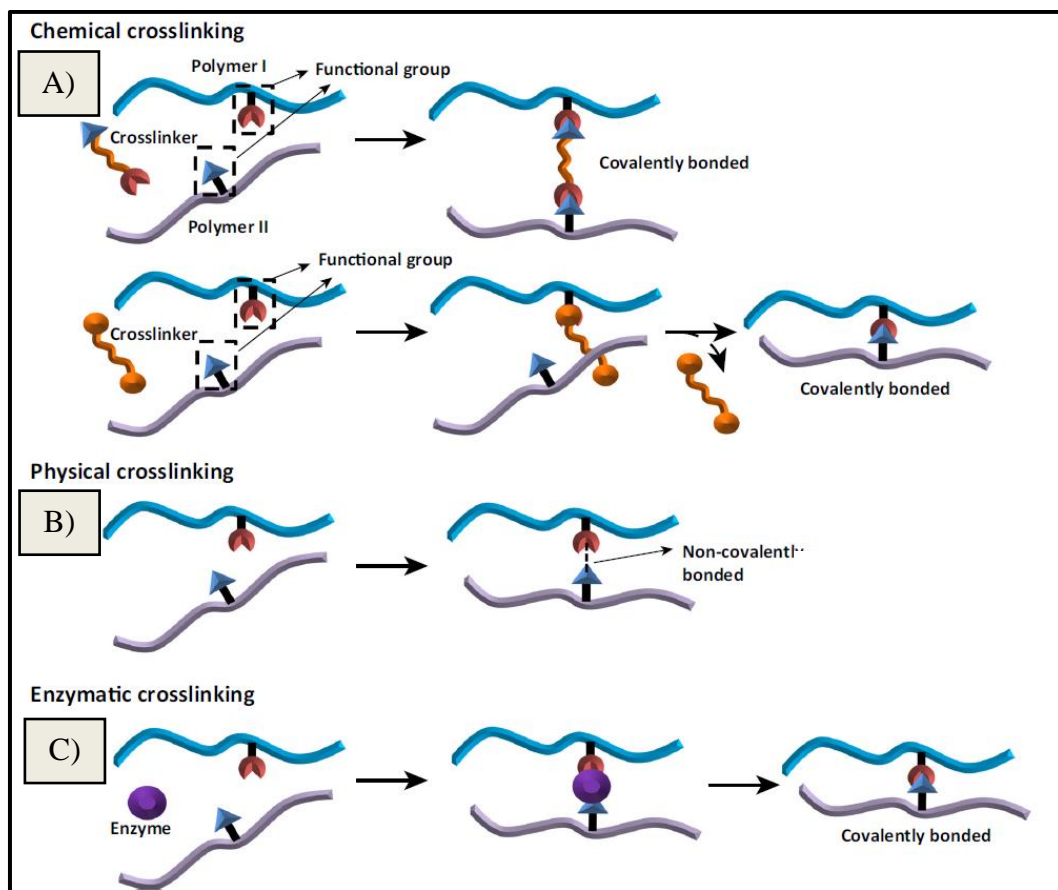
Figure 14 – Illustration of crosslinking methods applied in biopolymers electrospun fibers. **A)** Chemical crosslinking. **B)** Physical Crosslinking. **C)** Enzymatic crosslinking [129].

While remaining a widespread tool for crosslinking of biopolymer scaffolds in biomedical applications and enzyme immobilization, treatments with GLU also present several drawbacks [91,129,146]. First, the maneuvering of GLU might get complicated, because of its low vapor pressure and strong odor [129]. In addition, it is responsible for adverse health effects, related with the handling, such as irritation of skin, respiratory tract, eyes, allergic contact dermatitis and genotoxicity, among others [145]. Finally, GLU-crosslinked biomedical materials might exhibit some evidences of cytotoxicity, which limits its use [129,145]. On one report, while comparing different crosslinking agents, glyceraldehyde and genipin (GEN) were shown to be more reliable and with lower toxicity in electrospun gelatin fibers than GLU, that at a higher concentration showed toxic effects for cell proliferation and viability [148]. Fabricated gelatin electrospun fibers were crosslinked using GEN, procyanidine and GLU. In contrast with GEN and procyanidine, GLU was shown to have a higher cytotoxicity effect on the proliferation of fibroblasts on the matrix [149].

The variety of crosslinking agents is vast, and its choice depends on the polymer or blends to be used, solvents, applications field of the electrospun fibers and ecological

considerations. In addition, undesired consequences might be expected from the use of the crosslinkers on the fibers, besides the potential cytotoxicity of the materials, namely the decrease of available functional groups and the increase in degradability of the materials[91,129].

1.2.3.1. Ecological approaches for Protein-based mats

The search for the ideal crosslinker may not be easy, given that a set of conditions must be considered. While it is important to guarantee biomaterial functionality and reliability, it is also of interest to maintain the process of production reproducible and sustainable. Furthermore, it is imperative assuring that not only during the production of biomaterials, as well during their application, the risk of inducing harmful effects is minimized, while ecological options are maximized, essentially in fields related directly with the human heath, like biomedical fields and food areas. For that reason, green alternative approaches for crosslinking are being explored and some of them have already exhibited similar advantages, of even higher, as those commonly applied [91,129,145].

Among these greener crosslinking methods which include the use of EDC, TGase, and polycarboxylic acids, it is worth noting the use of GEN and citric acid [129,148,150,151]. Comparing the performance of TGase and EDC-NHS approaches, both strategies have shown similar effectiveness in crosslinking of collagen electrospun fibers, resulting in water-resistant fibers capable of supporting cellular growth [150]. Testing gelatin crosslinking agents, such as GLU, EDC, and microbial TGase, on electrospun blended fibers of gelatin and synthetic biodegradable polymers, indicated microbial TGase as a better crosslinking agent, because it increased fibers' mechanical strength and allowed for a better membrane performance when it was included in the spinning solution [151].

Genipin

Genipin is a natural phytochemical obtained from plants belonging to the Rubiaceae family, in particular *Genipina americana L.* and *Gardenia jasminoides*, constituting 1-3% and 0.17% of the plant, respectively. This iridoid compound can be extracted directly from genipap, *Genipina americana L.* fruit, whose native origins come from the Central America, or can be extracted indirectly from gardenia, *Gardenia jasminoides* fruit. The latter, or Zhizhi

fruit as the plant is known in China, where it is popularly cultivated, contains up to 10.9% of a major bioactive product, geniniposide, that can be hydrolyzed by enzyme β-glucosidase to obtain GEN. Because of its complex and high cost extraction and purification, GEN is a high value compound, even though it has multiples applications mainly on food industry and medicine. In medical applications, positive *in vivo* effects have been reported such as hepatoprotective, inhibition of gastric lesions, antithrombotic, antidiabetic, although its use may show genotoxicity, causing DNA damage [152,153].

Naturally, this ecological crosslinking agent is water and ethanol soluble and reacts spontaneously to form blue pigments. When in contact with primary amine groups of amino acids, peptides or proteins, a crosslinking reaction takes place (Figure 15), occurring a bimolecular substitution by the referred amine group, following a nucleophilic substitution to form a secondary amide link with the polymer [152].
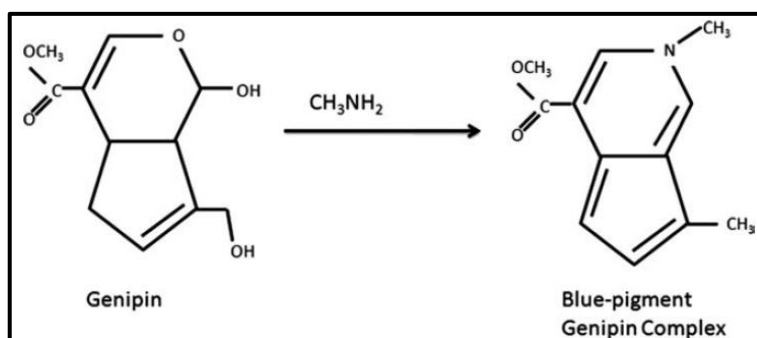
Figure 15 – Crosslinking reaction mechanism of genipin with primary amine groups to form the genipin blue-pigment [155].

Its exponential interest and application on biomaterials started when it was first reported its huge potential as an effective crosslinker due to its capacity to increase mechanical strength and enzymatic degradation resistance of crosslinked materials and its ability to significantly reduce the cytotoxicity compared with GLU or an epoxy compounds [154]. Through the years, several other studies demonstrated GEN low cytotoxicity comparing with chemical crosslinking agents, being even 5000-10000 less cytotoxic than GLU; despite this, some contradictory evidences report cytocompatibility issues under some GEN doses applied in tissue engineering [152,155]. Nevertheless, GEN is a great alternative agent, mostly employed in electrospun fibers for biomedical applications, made from a limited range of biopolymers such as collagen, fibrinogen and frequently gelatin, chitosan or its blends [148,151,156-158].

Mechanical properties and water resistance of silk fibroin/hydroxybutyl chitosan or gelatin nanofibrous crosslinked scaffolds, were enhanced by genipin (Figure 16) [158,159]. Besides, it was demonstrated *in vivo* and *in vitro* by cell viability and wound-healing tests that electrospun crosslinked scaffolds could mimic natural extracellular matrix, being GEN a better crosslinker than GLU and ethanol [158]. In another study, biocompatibility analysis confirmed genipin treated gelatin scaffolds as a cytocompatible platform to act as a rat decellularized brain extracellular matrix for nervous tissue regeneration [160]. On the opposite side, the referred GEN toxicity could also exhibit a negative impact on cell growing, migration and viability, in biopolymeric electrospun fibers [156,161,162]. While comparing the effects of two crosslinking methods, UV and GEN, in gelatin nanofibers, cell viability was described to be dose dependent of GEN, as stated before, with biocompatibility decreasing as the GEN concentration increased from 0.5% (w/v) to 2% (w/v)[155,162]. Additionally, higher crosslinker content increased nanofibers diameters and also had a positive influence preventing their swelling in water [162].
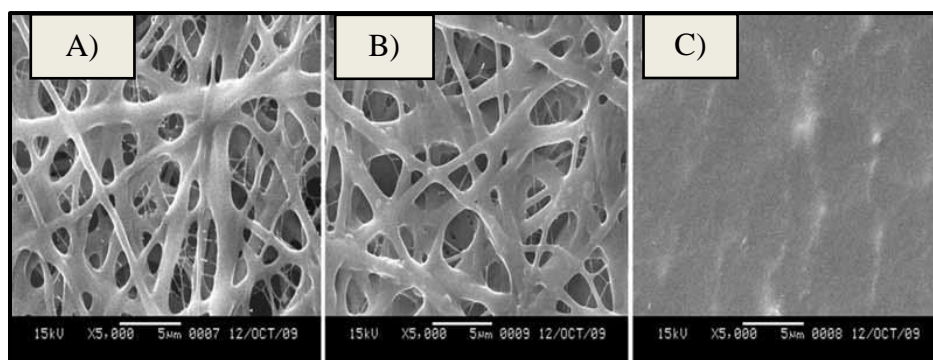
Figure 16 – SEM micrographs of crosslinked silk fibroin/hydroxybutyl chitosan after wetting with water. **A)** Genipin treated fibers for 48h. **B)** Glutaraldehyde treated fibers for 24h. **C)** Ethanol treated fibers for 24h (Adapted) [158].

Citric Acid

Citric Acid (CA), or 2-hydroxy-1,2,3-propanetricarboxylic acid, is an polycarboxylic acid compound found in citrus fruits, like limes and lemons and it is an important intermediary on Krebs metabolic cycle. This natural and inexpensive substance, whose molecular formula is $C_6H_8O_7$, exists commercially in monohydrate and anhydrous forms, as white powder or a colorless crystalline solid, both odorless with a strong acid taste and highly soluble in water

[163,164]. CA plays several roles as preservative flavorant, emulsifier, acidulant, among others, in a diversity of industries (cosmetic, beverage, food, pharmaceutical). When associated with the food industry as an additive, CA has a Generally Recognized as Safe (GRAS) status, which is a FDA designation, and in European Union it has the food ingredient code E330 [163]. Generally, this compound is of safe use to humans and environments, nevertheless a few precautions need to be attended with the handling to prevented skin and eye irritation, and obviously to avoid direct oral intake [164]. In the past few years, some emerging uses for CA must be highlighted, for example, application for environmental remediation, to clean industrial and nuclear residues, because of CA metal chelating properties, as a powerful disinfectant, including virus, and as an extracting agent, for example, in the extraction of compounds of industrial value like pectins [163].

CA used as the main crosslinking monomer has already originated a new class polyesters (poly(diol citrates)) with widespread use as biomaterials in tissue and regenerative engineering, owing to improved and tunable functionalities, such as mechanical, antimicrobial and antioxidant properties [165].

Recently, the use of CA as a polymer crosslinker has gained strength [129]. In fact, ceramic composites, biofilms, and electrospun fibers were already successfully treated by CA, which resulted in biomaterials with enhanced stability and mechanical properties [129,163]. Concerning the use of CA in electrospun polymer fibers, cellulose acetate/benzoxazine nanofibers were produced with high mechanical and thermal properties, demonstrating potential as an adsorbent for water treatment [166]. Similarly, functionalized mats made of ethylene-vinyl alcohol demonstrated high adsorption capacity for proteins [167]. In terms of biocompatibility, using the water-soluble polymer PVA, non-toxic and water stable nanofibers were achieved, with good durability in aqueous media [168]. Regarding protein spun fibers, one of the first attempts to use CA as a crosslinker was tested for zein[169]. Sodium hypophosphite monohydrate was used as a catalyst to assist the crosslinking reaction, and the resulting fibers showed higher strength (Figure 17A) and improved water stability (Figure 17B), when compared with the non-treated fibers[169]. Following studies confirmed the efficiency of CA as a crosslinking agent for zein fibers, allowing the integrity of the fibers in aqueous medium to be maintained, and the preparation of useful biocompatible materials for grow of fibroblasts, making possible their use for biomedical engineering [170], or materials for controlled drug-delivery [171].

CA was also tested as a crosslinker for other proteins, such as collagen and keratin electrospun fibers [172,173]. In the first case, a comparison of crosslinking methods using CA

(5% and 11% w/w), GA and EDC revealed the better performance of CA in terms of cytocompatibility and aqueous structural maintenance[172]. Combination of CA and heat treatments may improve the crosslinking results under certain circumstances, namely increasing the number of crosslinkings and, consequently, the mechanical properties and structural integrity of the resulting fibrous mats[169-173].

The crosslinking reaction between plant proteins, as gliadins, and carboxylic acids, for example CA, has already been tested to synthesize crosslinked films [174-176]. Usually, alkaline conditions are more favorable for the crosslinking reaction[174,175], and under this pH conditions the amine groups from proteins, rather than hydroxyl groups, react with carboxyl groups in citric acid, to form amide linkages (Figure 18). Nevertheless, the mechanism itself, as well the reaction, requires further understanding [176].
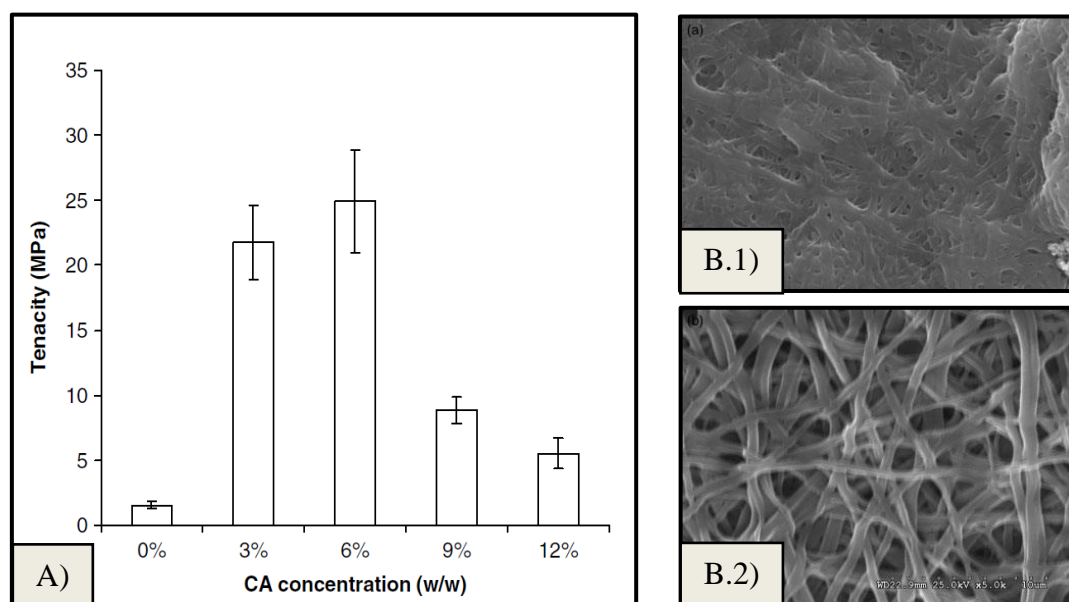
Figure 17 – Crosslinking effect of CA on zein spun fibers, 26% (w/w) zein. **A)** Effect of CA concentration on the tenacity. **B.1)** Non-crosslinked after washing and drying; **B.2)** Crosslinked after washing and drying; 6% (w/w) CA and 3.3% (w/w) sodium hypophosphite monohydrate (Adapted) [169].
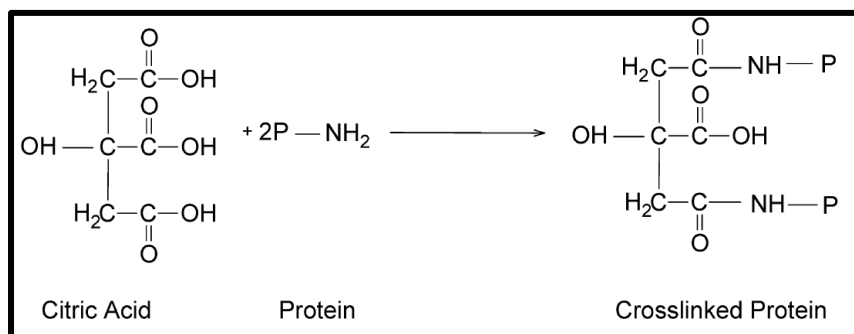
Figure 18 – Crosslinking interactions between proteins amine groups reacting with citric acid carboxyl groups, to form amide linkages [175].

1.2.4. Use of Green Solvents

Replacing more commonly used toxic solvents for other ones, more harmless and eco-friendly may not be an easy task, given that the spinning process and the final fiber characteristics are strongly dependent on solvent properties (§1.1.4.1). To be considered a "green solvent", the solvent needs to be sustainable, nonflammable, low-cost, with reduced reactivity and low toxicity [177]. Hazardous solvents such as DMF, N,N-dimethylacetamide (DMAc), toluene, N-methyl-2-pyrrolidone (NMP) and chloroform are being used, since the beginning of electrospinning, even though they represent a dangerous for human life and for the global environment [44,45,47,178-183]. However, due to global green awareness, others eco-friendly solvents are being increasingly considered or other polymers that allow the use of those green solvents. Some examples are ionic liquids, ethyl acetate, water, ethanol, 1-butanol and acid acetic [38,64,121,178,181-184].

Nevertheless, it is essential to understand that the existence of several solvent selection guides difficult the consensus about solvents, due to different categorization metrics, even though they employ an identical definition of "green solvent". Moreover, due to new knowledge, solvent selection guides are in constant updating, which may also influence the sustainable status of a certain solvent [178].

1.2.5. Global Opportunities in the Food Industry: A Strategy for Lactose Removal

There are many useful areas of application for electrospun fibrous materials, due to the capability of designing and developing innovative functional materials, in part related with the versatility of the available polymers and their properties [26]. Focusing in the food area, there is an overall interest and potential for separation processes, enzyme immobilization, delivery system to encapsulate and release bioactive molecules among others, where such fibrous matrices can assume an important role in the industry, in order to help optimize or create new processes [67]. Here we shortly discussed one of them related to the immobilization of β-Galactosidase enzyme, that could serve as an industrial strategy for lactose removal.

The consume of milk has been dated from over thousands of years and nowadays milk and its dairy products, such as cheese, yogurt, butter, milk beverages, ice cream, represent a huge part of food industry [185]. In Europe Union, 96.8% of all 168.2 million tonnes of milk produced, in 2015, came from cow's milk production, being mostly of the produced reserved to diary food manufactures [186]. Milk is a colloidal fluid with a complex constitution, that consists in a continuous phase of an aqueous solution containing predominantly lactose, whey proteins, vitamins and salts, and a dispersed phase composed by small globules of lipids and large agglomerates of casein proteins [187]. Lactose is the main carbohydrate in milk. Responsible for its breakdown, there is the hydrolase enzyme β-Galactosidase (β-Gal) (EC 3.2.1.23) that promotes the hydrolytic cleavage of the β1-4 glycosidic bond between the two monosaccharides, galactose and glucose [188].

The availability of effective methods of removing lactose from milk and other dairy products is becoming increasingly important for the food industry, due to: (1) human health issues, related with the high percentage of world population affected by intolerance to lactose; (2) the increasing of organic waste resulting from dairy industry manufacturing, in particular whey, that increases the environmental hazards; and (3) food processing associated problems cause by lactose crystallization, sweetness, solubility or its changes induced by heat [187-189].

Effective removal and/or hydrolysis of lactose generates new market possibilities such as the manufacture of glucose-galactose syrups, the production of prospective prebiotics, such as galacto-oligosaccharide (GOS), for human health benefit, and, mainly, production of lactose-free dairy products for the food industry [187,190]. Nowadays, overall strategies focus mainly on the employment of the enzymes responsible for lactose hydrolysis, in a free or

immobilized state, to produce lactose-free products or for whey lactose treatment [189]. Industrially, the use of free enzymes in solution is technically simpler, but immobilized enzymes enable reutilization, better and easier product recovery, less product contamination, a better control of the catalyzed reaction and the setup of continuous operation, with many advantages from an economic point of view[191].

Electrospun ultrafine fibers have already demonstrated high potential to be used as support materials for enzymatic immobilization because of their maneuverable, high porosity and interconnectivity of the fiber arrays combined with the large surface area per mass unit, and their chemical and physical versatility, thus allowing for high enzyme loads, adequate substrate accessibility, improved mass-transfer rates and the possibility of large scale productions and continuous processes [67,192].

Satisfactory results have been already obtained for the immobilization of different enzymes in/on electrospun polymeric fibers, including lipases, hydrolases or catalases, although only few reports are available about β–Gal [193-196]. Various benefits are being highlighted from enzymatic confinements on spun fibers such as the improvement of operational temperature and pH stability, higher catalytic activity and increased storage stability[193].

Different strategies can be used to immobilize enzymes using electrospun fibers as nanostructured supports[193]. In one of the first published reports regarding β–Gal immobilization, a multi-phase electrospun fiber was synthesized by a co-polymer of methyl methacrylate and acrylonitrile, and polyethylenimine (PEI) was used as a spacer-arm, allowing the presence of free amino groups on the surface of the spun fibers; Further, GA was used to promote the covalent attachment of the enzyme (Figure 19). The results showed an enzyme activity retention of 68%, with stability improvement, such as higher optimum catalytic temperature and higher pH range tolerance, in comparison with the free enzyme [194].

A different approach was also reported for *A. oryzae* β–Gal immobilization onto PEO and the polypropylene oxide block copolymer, Pluronic F-127, electrospun fibers, using a one-step immobilization process. The polymers were dissolved in water, with subsequent addition of the free enzyme directly into the spinning solution. The result confirms an efficient distribution and immobilization of the β–galactosidase, above 68%, in the smooth and beadles produced nanofibers, with the ability to be stored for 4 weeks, in dry and humid conditions; no significant changes on fiber morphology were observed during the different storage conditions (Figure 20) [195].
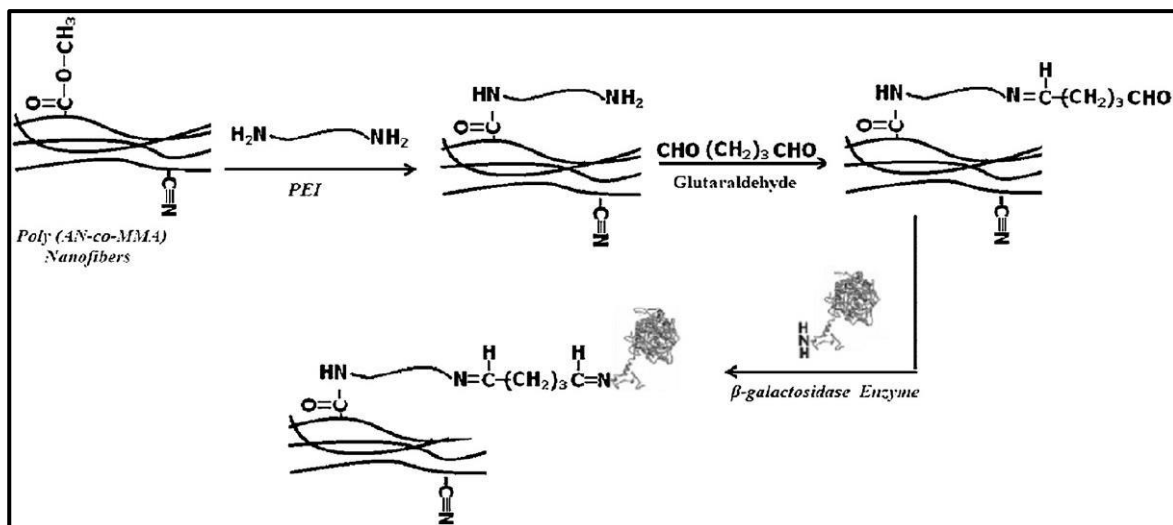
Figure 19 – Illustration of the process treatment of electrospun fibers. Modification of the matrix surface with addition of spacer-arms (PEI), with posterior treatment with glutaraldehyde to introduce functional groups for covalent bounding of the enzyme β–galactosidase [194].
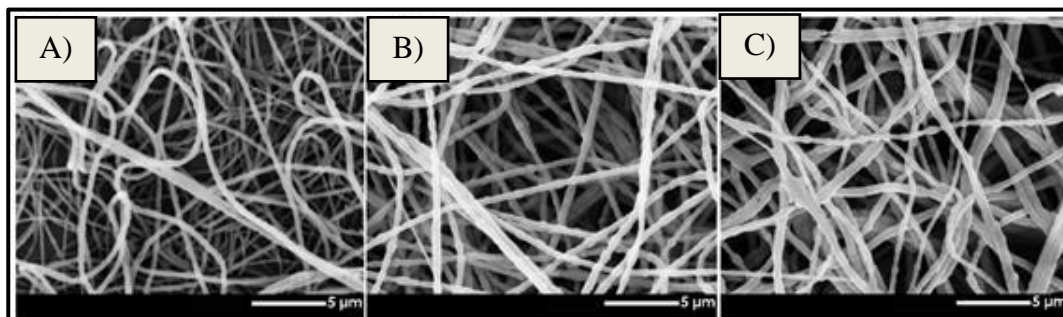
Figure 20 – SEM micrographs, at 5000X magnification, of electrospun nanofibers immobilized with β–galactosidase: **A)** Normal immobilized spun fibers. **B)** Immobilized spun fibers, stored at 4ºC, 15% relative humidity, for 4 weeks. **C)** Immobilized spun fibers, stored at 4◦C, 70% relative humidity, for 4 weeks [195].

2. Materials and Methods

2.1. Materials

Wheat Gluten (WG) (CAS 8002-80-0), glutaraldehyde (50 wt.% in H_2O) (CAS 111-30-8), citric acid (CAS 77-92-9) were purchased from Sigma-Aldrich (St. Louis, MO, USA). According to the commercial supplier, wheat gluten protein content was higher than 80% of the dry weight. Ethanol (absolute) (CAS 64-17-5), acetic acid (glacial) (CAS 64-19-7) and acetone (CAS 67-64-1) were commercially obtained from Scharlab S.L. (Barcelona, Spain) Sodium hydroxide (CAS 1310-73-2) was acquired from Loba Chemie PVT, Ltd. (Mumbai, India). and genipin (CAS 6902-77-8) was obtained from Challenge Bioproducts Co. (Taiwan R.O.C.). All chemicals were used without any additional treatment.

2.2. Extraction of Gliadin from wheat gluten

Gliadin extraction from wheat gluten was based on previously reported methods[196,197]. Wheat gluten was dispersed in aqueous ethanol (70%, v/v), in a 1:10 (w/v) ratio. A sieve was used to increase the dispersion of the powder gluten. The dispersion was kept under magnetic stirring at 300 rpm, for 2 hours, at room temperature, and then centrifuged at 10000 rpm, for 15 min, at 20°C. The sediment was discarded and the supernatant proceed to rotary evaporation (Buchi Rotavapor R-114; Buchi Waterbath B-480), at 40°C, until most of the ethanol was evaporated and a phase separation was possible to observe. Then, cooled (- 20 ºC) acetone was added to the viscous gliadin-rich fraction (1:4 (w/v)) acetone and left under slight stirring for 4 hours. Then, the solvent was discarded and the gliadin-rich precipitate was collected and dried at 37ºC, overnight. The dried sample was then ground using a mortar. Figure 21 illustrates the main steps followed to obtain the gliadin fraction starting from the commercial gluten sample.
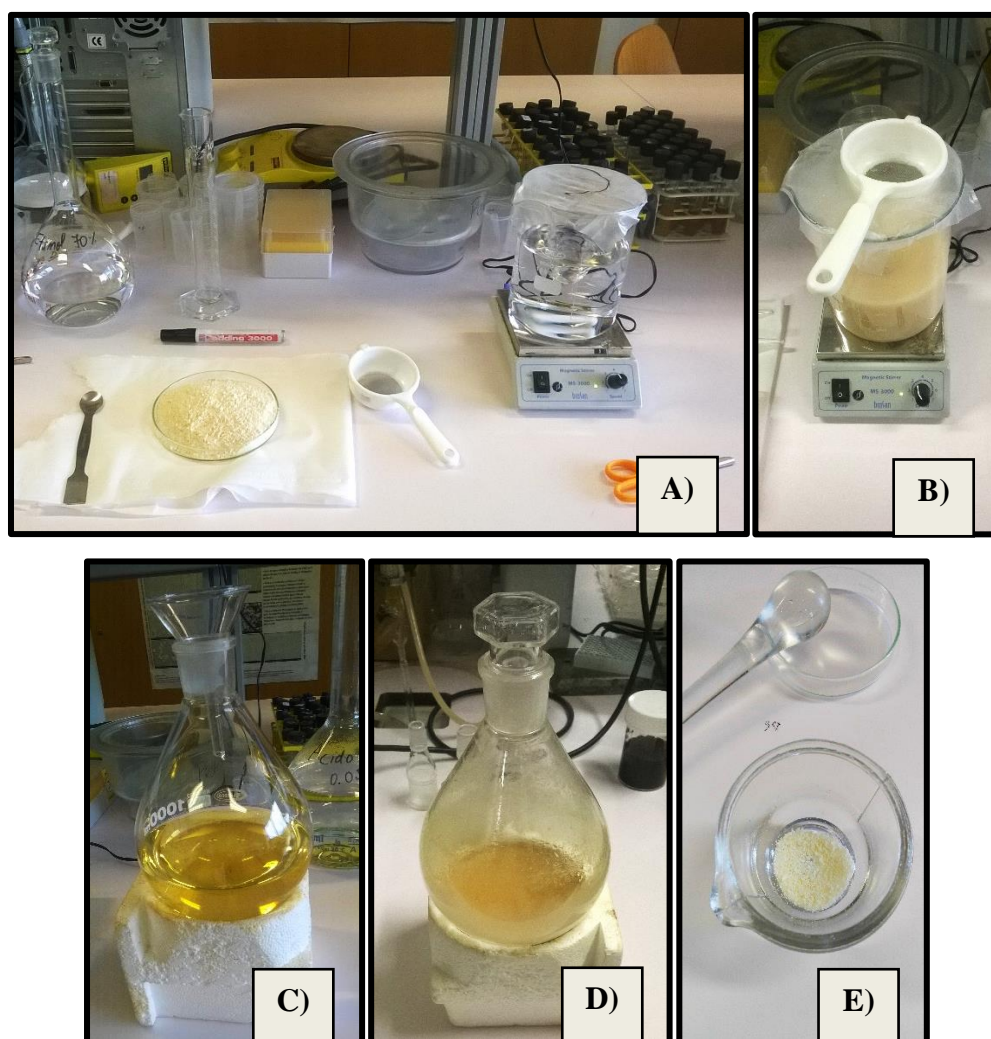
Figure 21 – Gliadin extraction from commercial gluten powder. **A)** Dispersion preparation; **B)** Dispersed gluten in ethanol 70% (v/v); **C)** Yellowish supernatant obtained after centrifugation; **D)** Viscous gliadin-rich fraction after rotary evaporation; **E)** Final dried protein powder.

2.2.1. Elementary Analysis of Gliadin and WG Powder

Collected dry samples of wheat gluten and gliadin fraction were examined through elemental analysis performed with a TruSpec 630-200-200 CNHS Analyser (C, H, N and S) (Leco Corporation, Saint Joseph MI, USA), at a combustion furnace temperature of 1075 ℃. Carbon, hydrogen, and sulfur were detected using infrared absorption, and nitrogen by thermal conductivity. The analysis was performed in triplicate. Protein content was determined from the total nitrogen content using a factor of x 6.25 [114].

2.3. Development and Optimization of Gliadin Electrospun Mats

2.3.1. Electrospinning System Setting

The horizontal electrospinning setup to produce electrospun mats was a previously made laboratorial apparatus, as shown in Figure 22, composed by [42]:

- ◦ A syringe pump, Harvard Apparatus PHD 2000, with a syringe support and an infuse rate control between 0.0006 mL/h and 13249.2 mL/h;
- ◦ A high voltage power supplier, Spellman CZE1000R, with continuously adjustable voltage and current from 0 to 30 kV and 0 to 300 uA, respectively.
- ◦ A grounded rotating aluminum drum (radius of 4.8 cm), connected to a Siemens motor, manually regulating the rotating speed by a Lenze SMD Frequency Inverter equipment.
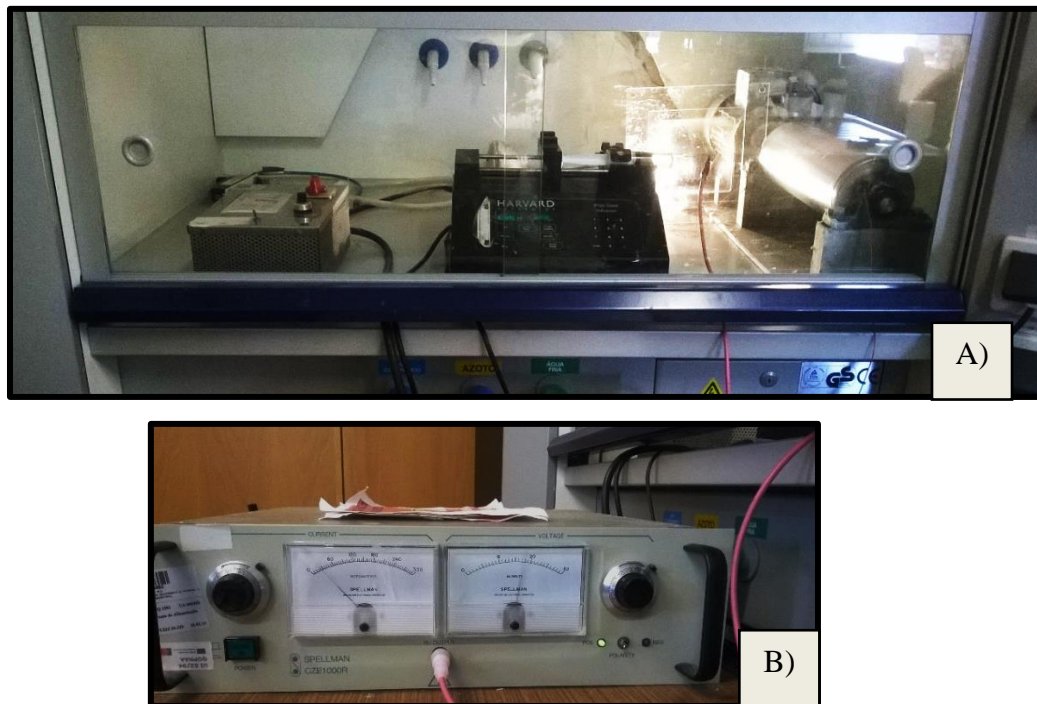
Figure 22 – Working laboratorial electrospinning setup, in the hotte. **A)** Syringe pump (on the center); rotating drum (on the right); rotating speed regulator (on the left). **B)** Voltage power supplier that connects to the tip of the needle syringe and to the rotating drum.

For each experiment, a blunt-ended metallic needle was attached to the 20 mL plastic syringe, containing the spinning solution, and coupled in the support of the syringe pump, while the cylinder collector was lined with aluminum foil (325 x 290 mm) for an easier posterior collection of the fibrous mat. Temperature and relative humidity were measured using a digital thermohygrometer (Cole-Parmer Digital Thermohygrometer).

To prevent the disturbance of external factors, the electrospinning equipment was mounted inside a chemical cabinet (hotte); during electrospinning the hotte window was closed and the venting turned off. Additionally, to assist in the spinning jet visualization, a lamp light was placed inside the cabinet, as noticed on Figure 22 A.

2.3.2. Preparation of gliadin solutions

Solutions of the gliadin-rich extract obtained as previously described (§2.2) were prepared in different solvents and at different protein concentrations, in order to test their performance under the electrospinning process, including the effect on the stability of the electrospinning process and on the final fibers' morphology. The protein was progressively added to the liquid solvent, at room temperature, under constant magnetic stirring of 300 rpm, for 4 h, before electrospinning. Solutions were prepared in glacial acetic acid at a protein concentration from 10 to 60 (w/v). Other solvents (mixtures of acetic acid/ethanol, acetic acid/water and acetic acid/ethanol/water) were also tested, for selected gliadin concentrations (25 to 35 %(w/v)), as shown in Table 1. One of the aims of testing other solvents was to achieve less harsh solubilization conditions in terms of the high acid concentration and the inherent handling and toxicity limitations.

Table 1 – Composition of spinning solutions using different solvents and gliadin concentrations.

	% Gliadin (w/v)	25	25	25	25	25	25	25	25	30	30	35	35
Solvent Mixture	% Acetic Acid (glacial)	50	70	85	50	70	85	50	70	70	85	70	85
	% Ethanol (absolute)	50	30	15	---	---	---	25	15	30	15	30	15
	% Deionized water	---	---	---	50	30	15	25	15	---	---	---	---

2.3.3. Optimization of electrospinning parameters

Electrospinning parameters were defined based on bibliographic references and preliminary tests on electrospun gliadin fibers [114,128]. Pre-tests consisted in a spinning solution of 20% gliadin (w/v) in 100% acetic acid (glacial) prepared at room temperature, with constant magnetic stirring of 300 rpm, for 4 h. The optimized electrospinning operating conditions were thus defined based on the visual inspection of the electrospinning process and on the analysis of the collected fibers by optical microscopy (OM). These conditions, indicated below, were designed to create a stable and continuous electrospun jet and fine, bead-free, homogenous fibers mats, with comparative low diameter, and served as a basis for all the preparations, except when indicated.

Selected electrospinning operating conditions:

- ◦ Applied Voltage: 15 kV
- ◦ Distance needle-to- collector: 10 cm
- ◦ Feed Rate: 1.0 mL/h
- ◦ Needle diameter: 0.6 mm (23G)
- ◦ Collector rotating speed: 6.1 Hz
- ◦ Temperature: $21 \pm 3°C$
- ◦ Relative humidity: 41 ± 5 %

After each electrospinning process, venting was turned on to eliminate residual solvents. All electrospun mats were collected in an aluminum foil (coating the metal cylindrical collector) and were stored in an acrylic desiccator cabinet at room temperature, until further analysis.

2.4. Crosslinking of Gliadin Fibers

Different strategies were employed to crosslink gliadin fibers, namely during or after the electrospinning process, or a combination of both, in order to investigate their potential role to enhance mechanical and structural properties and aqueous stability. The selected methods include treatments with genipin, heat, citric acid, and by the conventional crosslinking with glutaraldehyde vapor, as summarized in Table 2. To understand the

increased water stability crosslinked samples were rinsed in deionized water and then dried, in the oven, at 37ºC for posterior microscopic analysis. Due to water fragility of uncrosslinked fibers, those treated at 60ºC and 120ºC, and GEN mats, 2.5 and 5% GEN (w/w), instead of rinsed, they were dripped with deionized water.

Table 2 – Summary description of crosslinking experimental conditions

Method	Samples	Reacting on	Crosslinking Conditions	
			Before Electrospinning	**After electrospinning**
Heat	T60_O	Electrospun Fibers	--------------	60ºC, overnight
	T120_O			120ºC, overnight
Genipin	G2.5_O	Spinning solution	2.5 % GEN	16 h, 37ºC	--------------
	G5_O		5 % GEN		
	G5_OM		5 % GEN	16h, 37ºC	Stored for 1 month and half
	G5_24		5 % GEN	24h, 37ºC	
	G7.5_O		7.5 % GEN	16h, 37ºC	--------------
	G10_O		10 % GEN		
Genipin and Heat	G2.5_O120	Spinning solution and fibers	2.5 % GEN	16 h, 37ºC	120ºC, overnight
	G5_O120		5 % GEN		
	G5_OM120		5 % GEN		120ºC, overnight (after 1 month and half of storage)
	G7.5_O120		7.5 % GEN		120ºC, overnight
	G10_O120		10 % GEN		
Citric Acid	CA5	Spinning solution and fibers	5% CA	in 70% Ethanol, at pH 4.9, adding 50% gliadin, 48h, room temperature	150ºC, 2.5h
	CA9		9% CA		
	CA13		13% CA		
Glutaraldehyde Vapor	Glu2	Fibers	--------------		2h, at room temperature
	Glu4		--------------		4h, at room temperature
	Glu24		--------------		24h, at room temperature

Note: T60_O – Temperature 60ºC, overnight; T120_O – Temperature 120ºC, overnight; G2.5_O – 2.5% Genipin, reacting overnight; G5_O – 5% Genipin, reacting overnight; G7.5_O – 7.5% Genipin, reacting overnight; G10_O – 10% Genipin, reacting overnight; G5_O – 5% Genipin, reacting 24 h; G5_O – 5% Genipin, reacting overnight, storage a month and a half; G2.5_O120 – 2.5% Genipin, reacting overnight, post-treatment at 120ºC; G5_O120 – 5% Genipin, reacting overnight, post-treatment at 120ºC; G7.5_O120 – 7.5% Genipin, reacting overnight, post-treatment at 120ºC; G10_O120 – 10% Genipin, reacting overnight, post-treatment at 120ºC; G5_O – 5% Genipin, reacting overnight, storage a month and

a half, following a post-treatment at 120ºC; CA5 – 5% citric acid; CA9 – 9% citric acid; CA13 – 13% citric acid; Glu2 - Glutaraldehyde vapor, treatment time of 2 h; Glu4 - Glutaraldehyde Vapor, treatment time of 4 h; Glu24 - Glutaraldehyde vapor, treatment time of 24 h;

2.4.1 Crosslinking with genipin

Genipin crosslinking approaches were based on previous studies on protein electrospun fibers [161,162]. Crosslinking with genipin was attempted during the electrospinning process, by adding powder genipin to the previous prepared gliadin solution and dissolution by magnetic stirring at 300 rpm, 37ºC, overnight (~16 h) or for 24 h, in order to have final concentrations of genipin between 2.5 to 10 % ($w_{GEN}/w_{gliadin}$). Preliminary tests indicated that the use of higher temperatures (35-37ºC), rather than room temperature (20-25ºC), would increase the crosslinking reaction, since it was perceptible an increase in solution viscosity and in the intensity of the blue coloration (Figure 23 A). Sometimes it was necessary to clean the tip of the needle, during the electrospinning, in order to prevent solution accumulation and disruption of the continuous jet to the collector. To minimize this and to achieve a more stable jet, a larger diameter needle (0.9 mm inner diameter (20G)) was used for the more viscous spun solutions: 5 % GEN (w/w), reacting 24 hours, and 7.5-10 % GEN (w/w), reacting overnight. After electrospinning, mats were dried overnight, at 37ºC, in the oven.

2.4.2 Crosslinking by thermal treatment

The possible heat-induced crosslinking was also tested [136,200], by placing the electrospun fiber mats inside a ventilated oven at 60ºC or 120ºC, overnight (~16 h) (Figure 23 B).

2.4.3 Crosslinking by genipin and thermal treatment

GEN mats (2.5 to 10 % w/w) were also subjected to thermal treatment, at 120ºC

overnight (~16 h). In one case, 5% GEN fibers were stored at room temperature for a month and half, and then they were subjected to the same thermal treatment. Preliminary tests indicated that better results could be obtained by combining the genipin reaction and thermal treatment, and also that it might be advantageous to prolong the reaction time with genipin prior to heat treatment.

2.4.4 Crosslinking with citric acid

As will be discussed in the Results and Discussion section, preliminary tests have shown that the crosslinking with citric acid was not feasible using the previously optimized gliadin solubilization conditions. Therefore, citric acid crosslinking method was based on previous procedures using zein polymer [170,171]. Citric acid powder was dissolved in a ethanol 70% (v/v) aqueous solution, in order to obtain three different final concentrations, 5, 9, and 13% ($w_{CA}/w_{Gliadin}$), and the pH was adjusted to 4.9 using a 0.2 g/mL NaOH solution. Then, gliadin was dissolved in each pH adjusted CA solution to have a final concentration of 50 % gliadin (w/v), under magnetic stirring, at room temperature, followed by a reaction time of 48 h. CA solutions with higher NaOH additions exhibited a whitish coloration (Figure 23 C) and possibly a phase separation or salt precipitation. After the 48 h ageing, the 50% gliadin solution was diluted to 25 % (w/v) with 70% ethanol. The electrospinning process was carried out using different operating conditions than those previously discussed (§2.3.3): Applied Voltage of 19.5 kV, distance needle-to-collector of 20 cm, feed rate of 2.0 mL/h, and a 0.8 mm inner diameter (21G) needle. To increase of CA crosslinking through esterification reactions, the obtained mats were placed in the oven for 2.5 h, at 150 ºC.

2.4.5 Crosslinking by glutaraldehyde vapor

Crosslinking through glutaraldehyde (GLU) vapor was carried out following essentially the procedures previously reported [123]. A desiccator was set, in the hotte, containing 75mL of an aqueous solution of 50% GLU (w/v), in the bottom, with a metallic net support to elevate the mats (Figure 23 D). Gliadin fibrous mats were placed inside the sealed glass container, during 2, 4 and 24 h (Figure 23 E). To eliminate residual traces of GLU, the membranes were put in the oven, for 24h, at 37ºC.
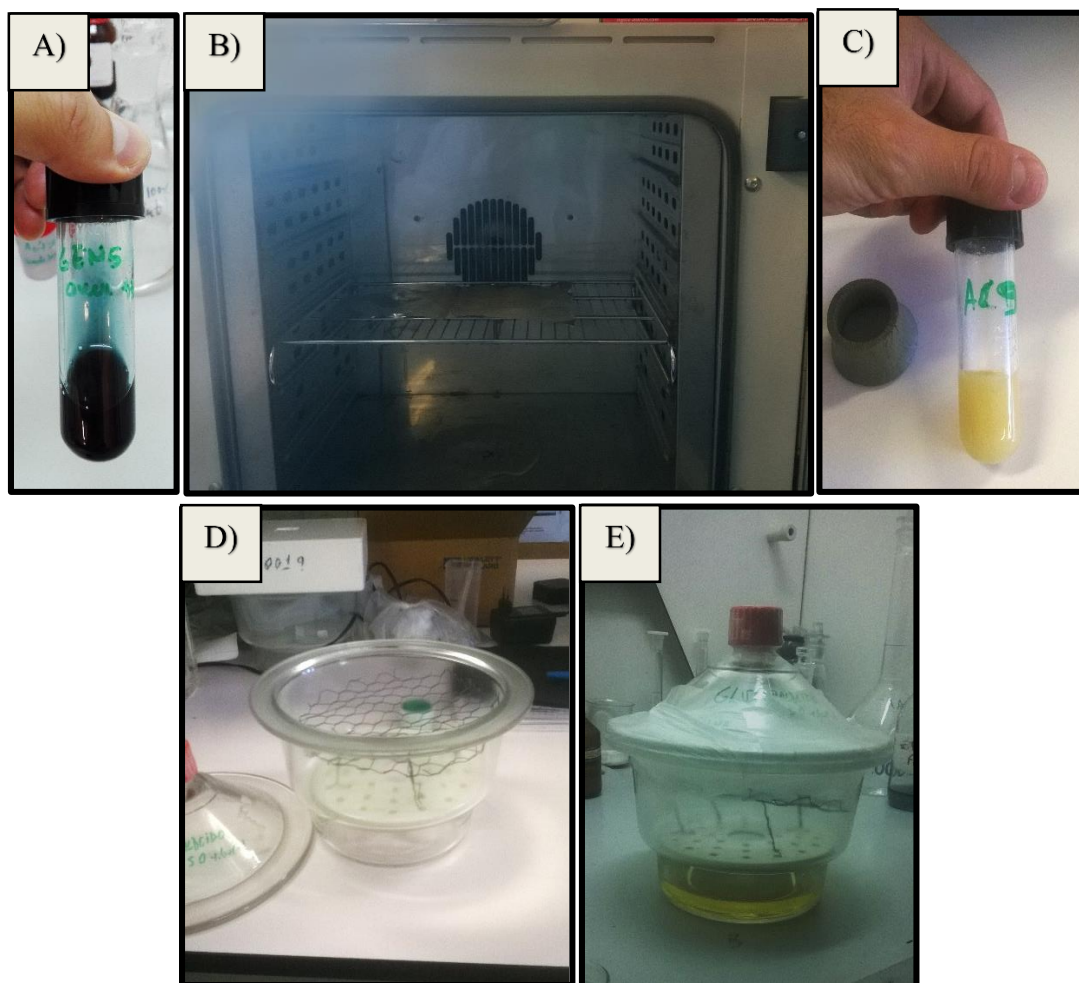
Figure 23 – Crosslinking approaches. **A)** Genipin spinning solution, prepared overnight, with a characteristic blue coloration. **B)** Fibrous membranes placed inside the venting oven. **C)** Yellow whitish 9% CA solution, after a reaction time of 48h. **D)** Preparing desiccator with a metallic net support for fibers. **E)** Sealed desiccator, in the hotte, already containing fibers and the yellowish 50% GLU solution, in the bottom.

2.5. Characterization of the electrospun fibrous mats

2.5.1. Fiber Morphology

General analyzes and comparisons of fibers definition as well as the overall network structure of fibrous mats were carried out, after being collected in a dry state, by optical microscopy using a Carl Zeiss microscope (Axiostar plus Transmitted-Light Microscope). Two dimensional photographs were taken through the microscope eyepiece 10X, using objective magnifications of 5X, 10X, 40X and 100X. Due to tridimensionality of the samples,

occasionally it was difficult to obtain general focused photographed images in some magnifications.

Topographic fiber analysis was done using Atomic force microscopy (AFM; Veeco NanoScope IV SPM Controller). Quadrangular dry samples (10 x 10 mm) were cut from the fibrous mat collected on the aluminum foil, in zones where fibrous density was smaller. Only selected samples were scanned: gliadin uncrosslinked mats and G5_O.

Detailed fiber morphology investigation was conducted using a Scan Electron Microscope (SEM; Hitachi SU–70), at 15kVa and 36 uA, with Schottky emission, followed by analyze of Energy Dispersive Spectroscopy (EDS; model QUANTAX 400, Bruker). Previous preparation of the samples was needed, hence small fibrous mat samples were cut and fixed on a round metallic support, using a double-layer adhesive tape, being after sputter-coated with a thin layer of gold (*Unit E500, Polaron Equipment Limited*), as observed on Figure 24. Only selected samples were scanned: gliadin uncrosslinked mats, G5_O, Glu4 and CA13.

The average fiber diameter was determined from 30 measurements on each sample, through SEM micrographs obtained and an image analysis program (ImageJ 1.51j8, Wayne Rasband, National Institute of Health, USA).

Figure 24 – Sputter-coated fibrous samples with a thin layer of gold.

2.5.2. Swelling Degree

With the objective to determine the swelling degree of crosslinked fibers, dry quadrangular samples (10 x 10 mm) of each obtained mat were cut and rigorously weighted [162]. After, they were immersed in 20 mL of deionized water, in a controlled ambient at 25ºC, under constant smooth agitation (Agitorb 200 ICP) for 24 h (Figure 25). Then the fibers were

removed from water and dried between paper filter and accurately weighted. Tests were done in triplicate. To calculate the swelling degree, it was used the following equation:

$$SD = \frac{(w_f - w_i)}{w_i} \times 100 \qquad (1)$$

Where *SD* represents the swelling degree, w_f defines the final sample weight after swelling and w_i expresses the initial weight of the dry sample.
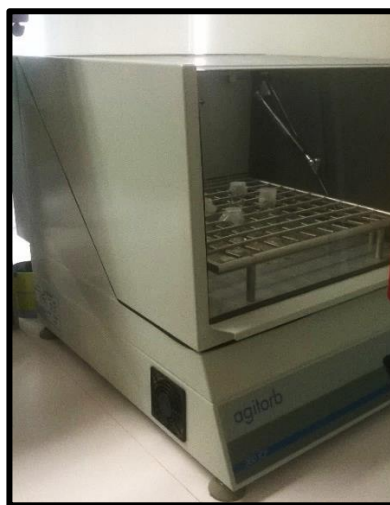

Figure 25 – Controlled ambient, at 25ºC, with constant smooth agitation, where fibrous samples are hydrating for 24h, to determine the swelling degree.

2.5.3. Contact Angle

To evaluate hydrophobicity of un- and crosslinked fibrous mats, water contact angle determinations were carried out in a Dataphysics contact angle system OCA-20 (Figure 26 A). Rectangular dry membrane strips were cut and placed over a cover glass, in the testing plate, while a gastight 500 µL syringe (DS 500/GT, Hamilton) with a metallic needle (0,52 mm), containing liquid deionized water, was loaded on the equipment. By dispensing manually 5 µl water drops (sessile drop), as seen on Figure 26 B), measurements were executed in ten different positions on each sample using ellipse fitting method, at room temperature, as noticed on Figure 26 C). For posterior analysis and determinations, a movie was recorded during measurements, and a photograph was taken from the video frames analyses, immediately after the fallen drop stabilize on the sample surface to proceed to contact angle calculation. Sample

mats from glutaraldehyde vapor, for 24h, were not tested, given that the obtained fibers were too stiff and shrunk to be manipulated.
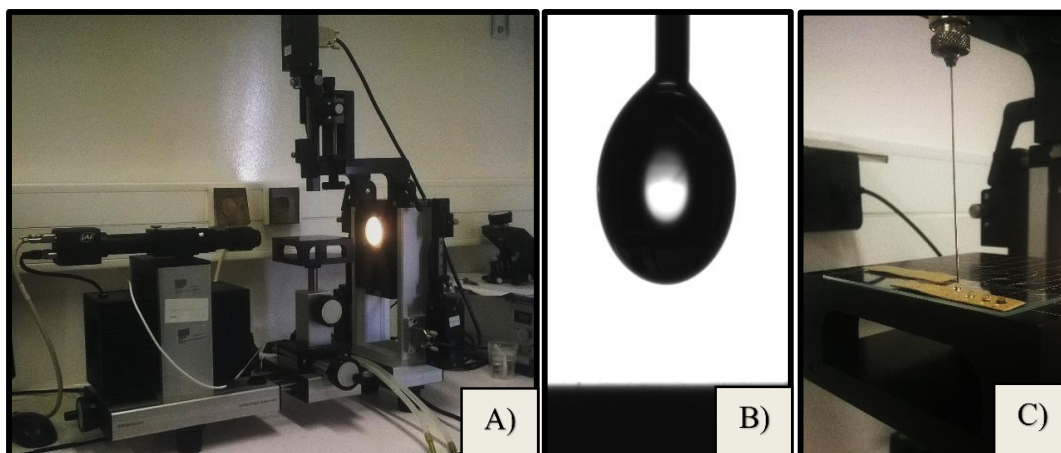

Figure 26 – Contact angle measurements using deionized water. **A)** Contact angle equipment (Dataphysics contact angle system OCA-20). **B)** 5 µl water drops (sessile drop). **C)** Fiber mat sample over a cover glass, in the testing plate, with water drops on the surface, during tests.

2.5.4. Mechanical Properties

Mechanical tests were performed on each electrospun sample to evaluate tensile strength (MPa), elongation-at-break (%) and Young's modulus (E), using a texture analyzer equipment (model TA.Hdi, Stable Micro Systems, England) (Figure 27 A). The texturometer was equipped with two metal tensile grips, aligned vertically and coated with thin rubber in the interior, defining a grip length separation of 50 mm and a crosshead speed of 0.5 mm/s (Figure 27 B).

Rectangular dry membrane strips (10 x 90 mm) were cut and its thickness measure using a digital micrometer (model MDC-25L, Mitutoyo Corp., Tokyo, Japan). The determinations were done in three different places, being the average thickness considered as the final thickness value.

Membrane strips were attached vertically on the grips, from 20 mm on both sides of samples (Figure 27 C). Through the uniaxial tensile tests, a membrane complete break is induced (Figure 27 D), where stress (MPa) vs strain (%) curves were obtained for posterior analyses. All samples were tested ten times, except the case of Glutaraldehyde Vapor, for 24h, given that the obtained mats were too stiff and shrunk to be manipulated.
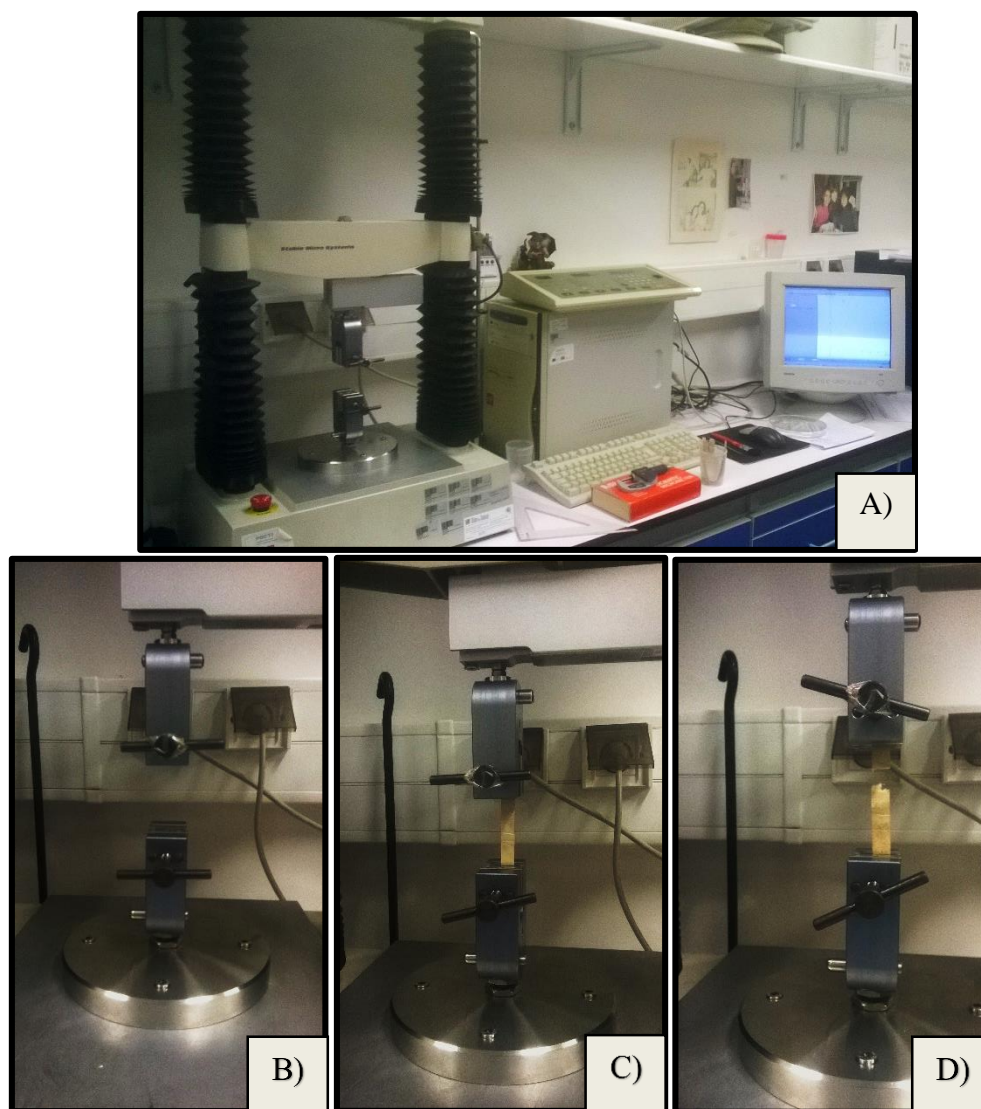
Figure 27 – Mechanical tests of membranes on a texturometer (model TA.Hdi, Stable Micro Systems, England). **A)** Mounted equipment ready to begin tensile trails. **B)** Close image of the two fixed metal grips, aligned vertically, with a grip length separation of 50 mm. **C)** Close image of membrane strip attached vertically under tension. **D)** Close image of sample rapture cause by a uniaxial tensile strength, during the test.

2.5.5. Statistical Data

Graphical depictions of mean data were constructed with Microsoft Excel 2016, with error bars representing standard deviations. Statistical analysis was performed using one-way analysis of variance (ANOVA) with Tukey's pair-wise multiple comparison test to determine significant differences between groups, considering p-values<0.05. Results data labeled with different letters exhibit statistical differences.

3. Results and Discussion

3.1 Development and Optimization of Gliadin Electrospun Mats

3.1.1 Gliadin extracted powder

Commercial wheat gluten and the extracted gliadin sample revealed a similar elementary composition (Table 3), and, more importantly, that we have obtained a gliadin-rich fraction with a high protein content, which reflects an efficient protein extraction process.

Table 3 – Elementary analysis results and protein content for the commercial wheat gluten and the extracted gliadin

Sample	Elements %				% Total Protein Content
	% C	% H	% S	% N	
Wheat Gluten Supplier Information	-----	------	-----	-----	>80
Wheat Gluten	47.4	6.29	0.794	13.6	84.8
Gliadin	49.0	6.46	0.787	15.9	99.5

3.1.2 Preliminary evaluation of the concentration effect in glacial acetic acid

Dissolution of gliadin was first tested in 100% acetic acid, at different protein concentrations, obtaining homogeneous yellowish solutions. Solution color became darker and changed from yellowish white to yellowish brown tones (Figure 28), and the solution viscosity increased, in accordance with previous observations, as the protein concentration increased from 10% to 60% gliadin (w/v) [114]. For concentrations above 45% gliadin, dissolution was more difficult, hence needing more time than 4 h to obtain a complete homogenous solution.
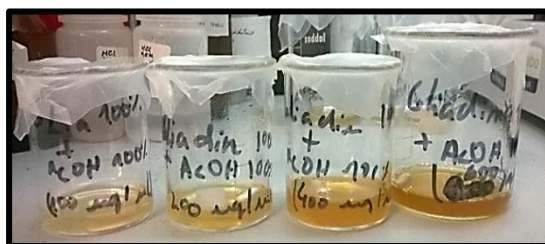

Figure 28 – Gliadin solutions, in 100% acetic acid, with increasing protein content: 10%, 20%, 40%, 60% gliadin (w/v) (from the left to right).

To test the electrospinning fiber formation, all solutions were loaded into the 20 mL syringe and subjected to the electrospinning process accordingly to the conditions previously described (§2.3.3). For gliadin concentrations of 10 and 15% (w/v), the solutions were just electrosprayed and didn't produce any fibers (Figure 29 (B) and (C), respectively). This is justified because gliadin is expected to form compact globular structures in 100% acetic acid, with little tendency to form intermolecular interactions, thus higher protein concentrations are needed to increase those interactions and consequently to produce fibers [114]. Electrospun fibers started to be formed for concentrations equal to or greater than 20 up to 45 % gliadin (w/v) (Figure 29 (D) to (I)), where the spinning jet phase was continuous, thereby obtaining a fibrous homogeneous white membrane as illustrated in Figure 29 (A). For concentrations of 40 and 45% (w/v), the spinning process was not so smooth, often leading to accumulation of solution at the tip of the needle, due to the solution high viscosity. For 60% gliadin, the solution was not electrospinnable, because it was too viscous to pass through the needle, even using needles with a larger inner diameter.

In terms of fibers morphology, it was possible to detect the presence of fiber beads in those samples electrospun from gliadin solutions at 20, 25 and 30% (w/v) (Figure 29 (D), (E) and (F), respectively), more notable at 20% gliadin and less seen at 30% gliadin, which is in accordance with previous observations for similar systems [114]. Increasing the protein concentration lead to the decrease of beads, and so the electrospun fibers obtained for gliadin concentration of 35% or higher were essentially bead-free (Figure 29 (G-I)).

Furthermore, the increase of protein concentration lead to a distinguished increase of the fiber diameter, what can be observed by comparing Figure 29 J), K) and L), in agreement to what was previously reported for other proteins, such as zein and soy protein [105, 139]. For gliadin solutions with concentration above or equal to 30%, fibers start to exhibit some branches that tend to increase as the concentration increases (Figure 29 (I) and (L)). Finally, for concentrations equal to or higher than 40 %, fibers begin to lose their fine and linear definition, as shown in Figure 29 (H).

From the results obtained, we concluded that in 100% acetic acid, gliadin concentrations from 25 to 35 %(w/v) originate fibers with more promising morphological characteristics, namely fine, regular and generally oriented fibers, with few or no beads.
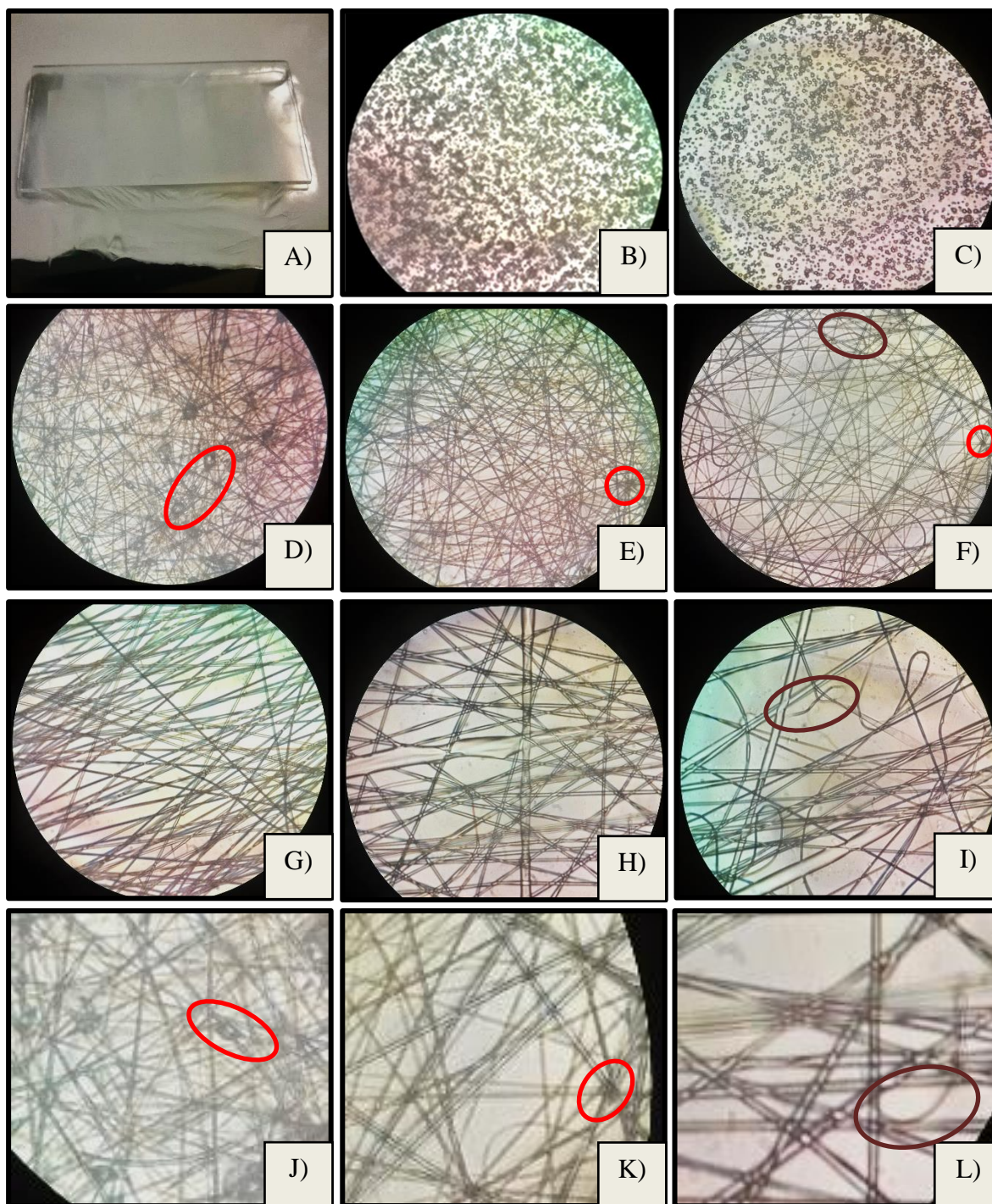
Figure 29 – Photographs taken on the produced fibers from gliadin spinning solution from 10 to 45% (w/v). Images from B) to L) are taken at the OM at 1000X magnification. **A)** Collected spun mat of 20% gliadin in the aluminum foil. **B)** Electrospraying generated from 10% gliadin. **C)** Electrospraying generated from 15% gliadin. **D)** 20% gliadin fibers, where is it possible to observe beads (red circle). **E)** 25% gliadin fibers, where is it also possible to observe beads, although less (red circle). **F)** 30% gliadin fibers, with even fewer beads (red circle). Possible to observe branched fibers (brown circle). **G)** 35% gliadin fibers. **H)** Larger and irregular fibers from 40% gliadin. **I)** Larger and irregular fibers from 45% gliadin, also some visible branched fibers (brown circle). **J)** Close-up image of 20% gliadin fibers. Visible beads (red circle). **K)** Close-up image of 30% gliadin fibers. Visible beads (red circle).

L) Close-up image of 40% gliadin fibers. Visible branched fibers (brown circle).

3.1.3 Solvent effects

According to the previous fiber morphology analysis, concentrations of the gliadin spinning solution from 25 to 35% (w/v) were selected to analyze some solvent composition effects, testing mixtures of acetic acid, ethanol and deionized water (Table 1), although still using acetic acid as the base solvent. Table 4 lists the used solvents and their properties.

Table 4 – Solvents physicochemical properties [199-204]

Solvent	Molecular Formula	Molar Mass (g/mol)	Density (20 ºC) (g/cm³)	Viscosity (20ºC) (mPa/s)	Boiling Point (ºC)	Surface Tension (25ºC) (mN/m)	Vapor Pressure (20 ºC) (hPa)	Dielectric Constant (25 °C)
Acetic Acid	CH_3COOH	60.05	1,05	1.124	117	27.10	15,4	6.19
Ethanol	C_2H_5OH	46.07	0,79	1.074	78.3	21.97	59	24,3
Water	H_2O	18.02	1	0.891	100	0.07	23.3	78.39

Visually, for the 25% gliadin solutions in acetic acid/water, the color changed from yellowish to pale yellow tones (Figure 30 A), and the viscosity decreased, with the increase in water content in the spinning solution. In fact, this induced viscosity decrease is related with the increase of protein hydrophobic interactions, which leads to the formation of large and irregular compact aggregates [114]. Different behavior was found due to the increase in ethanol content for the solutions prepared in acetic acid/ethanol, since there were no considerable color changes (Figure 30 B). The presence of ethanol in the mixed solvent might have a neutral or even a positive impact in prolamins dissolution, considering that usually 70-90% aqueous alcohol solvents are used to solubilize those proteins [104,206]. Moreover, this solvent system alone was successfully employed to obtain zein electrospun fibers [105,205]. The combined use of deionized water and ethanol in the mixed system, at concentrations of 15% and 25% (v/v$_{total}$ $_{solvent}$), both on the same proportion 1:1, revealed solutions with identical appearance, although the solution containing 25% water was lighter and less viscous than the others (Figure 30 C), due to higher water content. Nevertheless, evidences suggest that different solvents induce different interactions and conformational changes for the proteins in solution, and

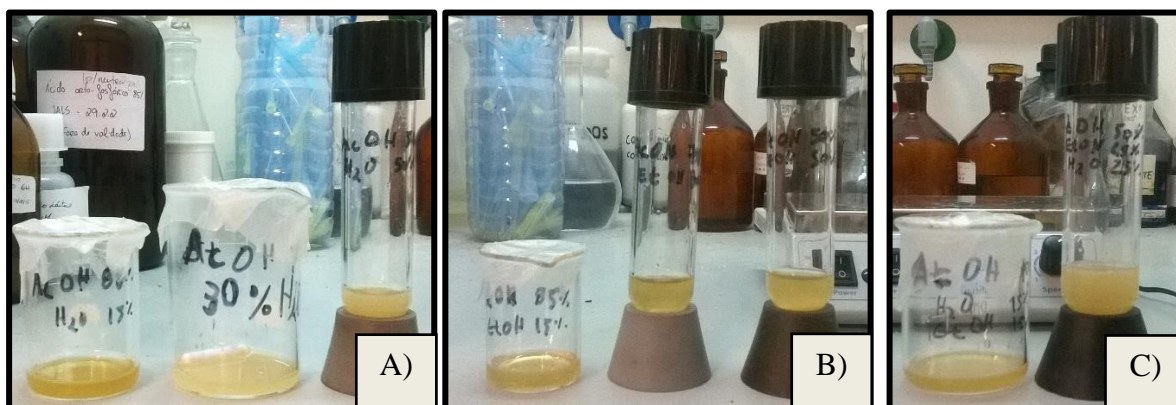consequently, different characteristics for the electrospun fibers [114, 205,206].

Figure 30 – 25% Gliadin spinning solutions. **A**) Gliadin dissolution in acetic acid/deionized water, 85:15, 70:30 and 50:50 (from the left to the right). **B**) Gliadin dissolution in acetic acid/ethanol, 85:15, 70:30 and 50:50 (from the left to the right). **C**) Gliadin dissolution in acetic acid/ethanol/deionized water mixtures, 70:15:15 and 50:25:25 (from the left to the right).

As expected from previous studies, the use of different solvents leads to changes in both the electrospinning process and the characteristics of the obtained fibers obtained [114,205]. Firstly, it was demonstrated that the use of water and the increase of its amount in the mixed solvent worsened the electrospinning process and fiber morphology, in accordance to previous studies using prolamins [114, 205]. At 30% water, the jet phase became more unstable and at 50% water it started to drip towards the collector. Electrospun fibrous network became heterogenous and the collected fibers lost quality, once that at 15 and 30% water beads were substantially present, as seen in Figure 31 (A) and (B), respectively. Different outcomes were obtained for zein, which could not be electrospun using aqueous acetic solutions as solvent, containing 10 to 40% water content [205]. At 50% water the process was an electrospraying, instead of an electrospinning (Figure 31 (C)), and identical results were reported for other prolamins, including gliadin [114].

As for the combined use of acetic acid and ethanol, the increase of this last one, up to 50%, it always guaranteed an electrospinning process, with production of a fibrous homogeneous white film, however the jet phase became a little unstable, for ethanol concentrations equal or higher than 30%. Comparing electrospun fibers, on Figure 31 D), E) and F), for increasing ethanol concentrations in the mixed solvent, they maintained a similar

good morphology between them, exhibiting fine smooth fibers, although they continue presenting beads. Due to jet instability, during electrospinning, it was also possible to observe the presence of some solution drops on the matrix network, for ethanol concentrations equal or higher than30% (Figure 31 (I)). It is suggested that the psychochemical properties of the solvents (Table 4) might be responsible for the spinning stability: acetic acid has the lowest vapor pressure, of 15.4 hPa, as for ethanol the highest, 59 hPa, which means that the increase of ethanol content in the solvent mixture would lead to an increase of solvent evaporation at the tip of the needle, considering also its lower boiling point 78.3ºC. Furthermore, the addition of ethanol would increase the dielectric constant of the solvent and consequentially it could increase the existing longitudinal elongation forces, resulting in a loss of the fiber integrity during the spinning jet phase [205].

Analyzing the results obtained for the solvent system of acetic acid mixed with water and ethanol, showed that the increase to 25% water and 25% ethanol had a negative impact on fibers quality (Figure 31 (H)), even though the solutions were capable of electrospinning. In comparison with 15% water and 15% ethanol (Figure 31 (G)), those fibrous network were more heterogenous and the beads presence was more significative, possible due to the increase of water content, also a certain jet instability, during electrospinning was possible to be seen.
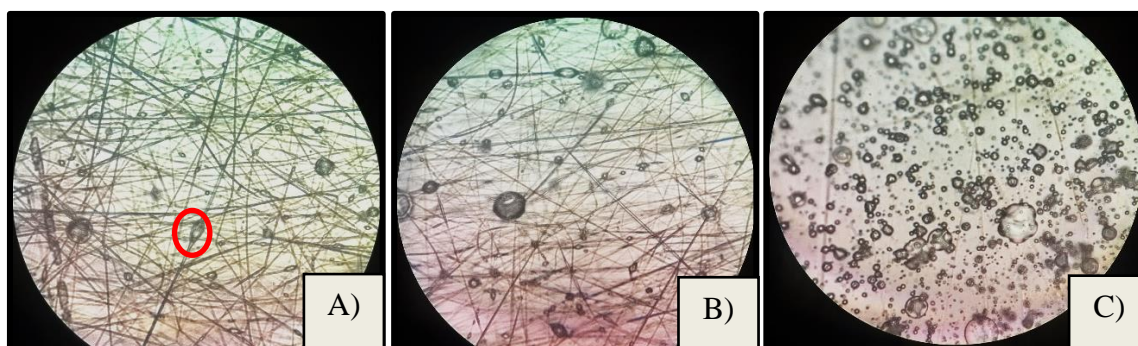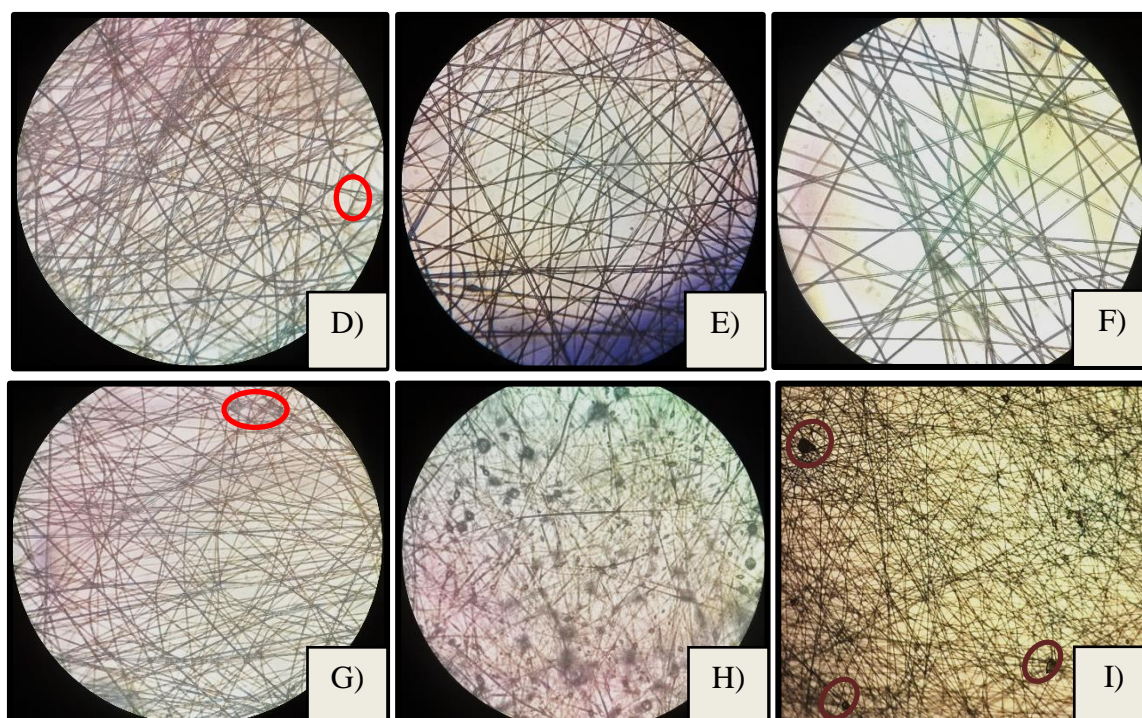
Figure 31 – Photographs taken from optical microscope observations (at 1000X magnification) for electrospun fibers from the 25 % gliadin spinning solution: **A)** Solvent mixture = 85% Acetic Acid and 15% Water. Presence of beads marked in a red circle. **B)** Solvent mixture = 70% Acetic Acid and 30% Water. **C)** Solvent Mixture = 50% Acetic Acid and 50% Water. **D)** Solvent Mixture = 85% Acetic Acid and 15% Ethanol. Presence of beads marked in a red circle. **E)** Solvent Mixture = 70% Acetic Acid and 30% Ethanol. **F)** Solvent Mixture = 50% Acetic Acid and 50% Ethanol. **G)** Solvent Mixture = 70% Acetic Acid, 15% Water and 15% Ethanol. Presence of beads marked in a red circle. **H)** Solvent Mixture = 50% Acetic Acid, 25% Water and 25% Ethanol. **I)** Close-up image of the fibrous network, using 50% Acetic Acid and 50% Ethanol, at 100X magnification. Multiple solution drops visible (brown circle).

These morphology comparisons show that water content has a negative effect as a solvent in fibers morphology and in the process of fiber-making, either combined with acetic acid or with acetic acid and ethanol. Acetic acid/ethanol demonstrated to be the best solvent choice in order to reduce the dependence on acetic acid, while maintaining the gliadin fiber morphology. Acetic acid is considered a reasonable environmental friendly solvent, nevertheless some cautions need to be attended with its use and handling [178,200]. Ethanol concentrations of 15 and 30% were selected for further tests, due to their respective good gliadin fiber morphology, while assuring an efficient electrospinning process.

In an attempt to produce a more homogenous fiber network containing beadless fibers, 30 and 35% gliadin concentrations were also tested, in acetic acid/ethanol mixed

solvent with 15 or 30% ethanol. All prepared spinning solutions revealed similar yellowish aspect, slightly darker as protein concentration increased.As shown in Figure 32, larger spun fibers were obtained, with possible branches but no beads, especially for the higher amount of ethanol.

The fibers dimension increment was a result not only of gliadin concentration increase, as already concluded before and possible to be observed again while comparing Figure 32 A) and C), but also it was due to ethanol increase in the mixed solvent, for the same protein concentration, as seen on Figure 32 A) and B).
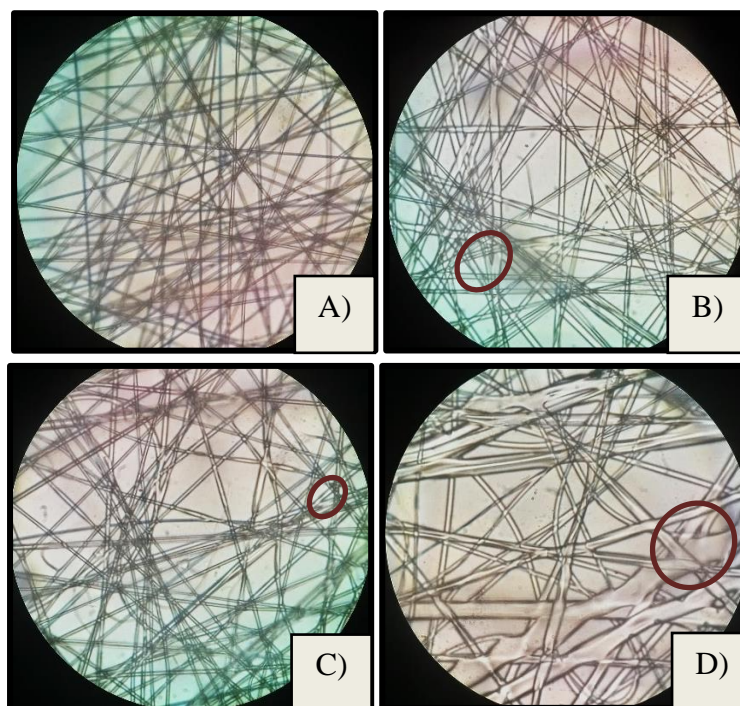
Figure 32 – Photographs of the produced fibers from the gliadin spinning solution, at the OM, at 1000X magnification. **A)** 30% Gliadin. Solvent Mixture = 85% Acetic Acid and 15% Ethanol. **B)** 30% Gliadin. Solvent Mixture = 70% Acetic Acid and 30% Ethanol. Visible branched fibers (brown circle). **C)** 35% Gliadin. Solvent Mixture = 85% Acetic Acid and 15% Ethanol. Visible branched fibers (brown circle). **D)** 35% Gliadin. Solvent Mixture = 70% Acetic Acid and 30% Ethanol. Visible branched fibers (brown circle).

Therefore, after investigating the relevant impact of solvents on fiber morphology and spinning process, 30% gliadin concentration, using a solvent composition of 85% acetic acid and 15% ethanol, was selected as the optimized spinning solution conditions. In fact,

detailed SEM images, Figure 34, confirmed that while reducing the amount of acetic acid used, 100% to 85%, it was possible to create a homogenous gliadin fibrous matrix, containing defined and regular beads-free fibers, with smooth surface, also visible on AFM topography images, as seen on Figure 34; fibers had an average diameter of about 665 ± 170 nm. Comparatively, lower diameter was already observed on gliadin fibers, specifically 192.4 ± 60.6 nm [114]. This difference is probably related to the higher protein concentration used in the present work, 30% gliadin (w/v) instead of 20% gliadin (w/v), but also due to the solvent system used for the spinning solution, 85% acetic acid and 15% ethanol instead of 100% acetic acid; considering that the increase of ethanol content appears to increase the diameter of fiber.
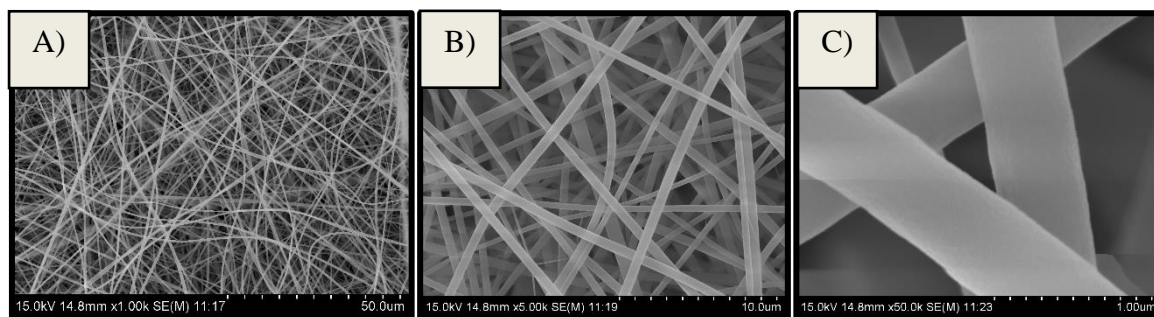
Figure 33 – Micrographs of gliadin fibers at their optimized concentration. **A)** SEM at 1000X magnification. **B)** SEM at 5000X magnification. **C)** SEM at 50000X magnification.
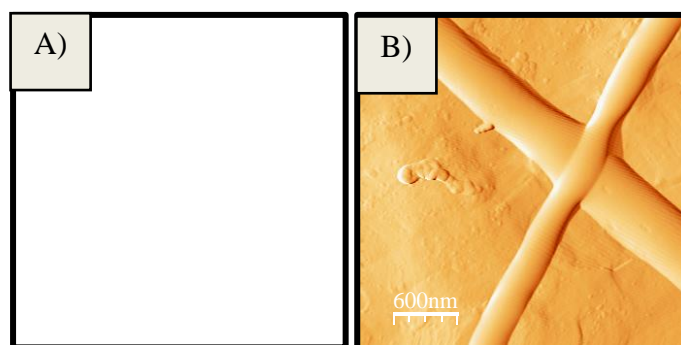
Figure 34 – Topography AFM images of gliadin fibers at their optimized concentration.

3.2. Crosslinking of Gliadin Fibers

3.2.1 Fiber morphology

Most crosslinking strategies, except for the citric acid crosslinking method, were carried out using the previous optimized gliadin solution (30% gliadin in 85% acetic acid/15% ethanol) and electrospinning operational conditions. The treatments were applied directly in the spinning solution, or on the gliadin produced fibers, or even in both cases, as discussed in § 2.4, Table 2.

Collected gliadin fibers were post-treated by heat at two alternative temperatures, 60 and 120ºC. Visually, the resultant fibers appeared externally dried with a wrinkled surface. A closer analysis by OM showed that nanofibers remained similar to those uncrosslinked, as can be compared at Figure 35 A) and B), meaning they could retain their structural morphology, despite the use of two different temperatures. Identical morphological results were obtained, after heating at 80 ºC, for whey protein:PEO electrospun fibrous mats, allowing them to retain their fiber diameter and fibrous structure [136]. Even so, the fiber diameter was not determined, and some changes may have occurred due to the heat treatment, which have already been reported for fibers of other biopolymers, e.g. a higher fiber diameter, as reported for chitosan electrospun fibers [198].
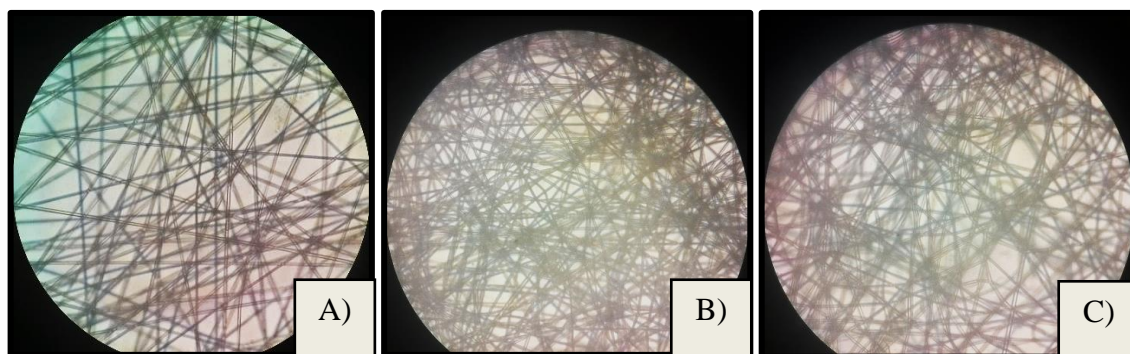
Figure 35 – Photographs of uncrosslinked and heat-induced crosslinked fibers, at the OM, at 1000X magnification. **A)** G30. **B)** T60_O. **C)** T120_O.

Genipin crosslinking was also tested, and at the best of our knowledge is was the first time genipin was used as a crosslinker agent for plant protein electrospun fibers. All solutions exhibited a characteristic blue coloration, which became darker with the increase of GEN amount and with the increase of reaction time, in accordance with previous observations [148,207]. Being so, the change in color and the expected increase in solution viscosity indicate the formation of a secondary amide bond, from the crosslinking reaction taking place within the fibers, between the protein amine groups and the carboxymethyl group of genipin [162]. Similarly, the increase in viscosity was reflected in the behavior of the solution during the spinning process and in the collected mats: accumulation of the solution at the tip of the needle was frequent, resulting in more heterogeneous fibrous networks, with the presence of larger and darker irregular fibers, and darker solution drops, as seen on Figure 36 (A). Besides, due to solution coloration, bluish fibrous mats were produced, passing from a slightly bluish white, 2.5G_O, to a darker bluish white, G10_O, or in the case of G5_24, completely blue. Furthermore, the increase of GEN amount turned and a little more rough and crispy. Storing G5_O during a month and a half, at room temperature led the fibers to become completely greenish blue, probably related to the continued occurrence of the reaction during the storage period. Generally, genipin fibers presented identical morphology, where it was possible to observe regular defined fibers, along with branched and irregular ones. Detailed SEM and AFM images of G5_O samples (Figure 37 and 38) show the existence of smooth well-defined fibers with an average diameter of 1934± 501 nm. Considering the average diameter determined for the non-treated fibers, of about 665 ± 170 nm (Figure 33), crosslinking by genipin clearly induced the increase of fibers diameter, especially when higher GEN amounts were employed, as reported in a number of previous studies [162, 208, 209]. This makes it possible to anticipate that G7.5_O, G10_O and G5_24 fibers would have an even larger diameter, not

only because of the increased GEN amount, but also because a needle with a larger inner diameter was required for electrospinning, due to the high viscosity of the solution.
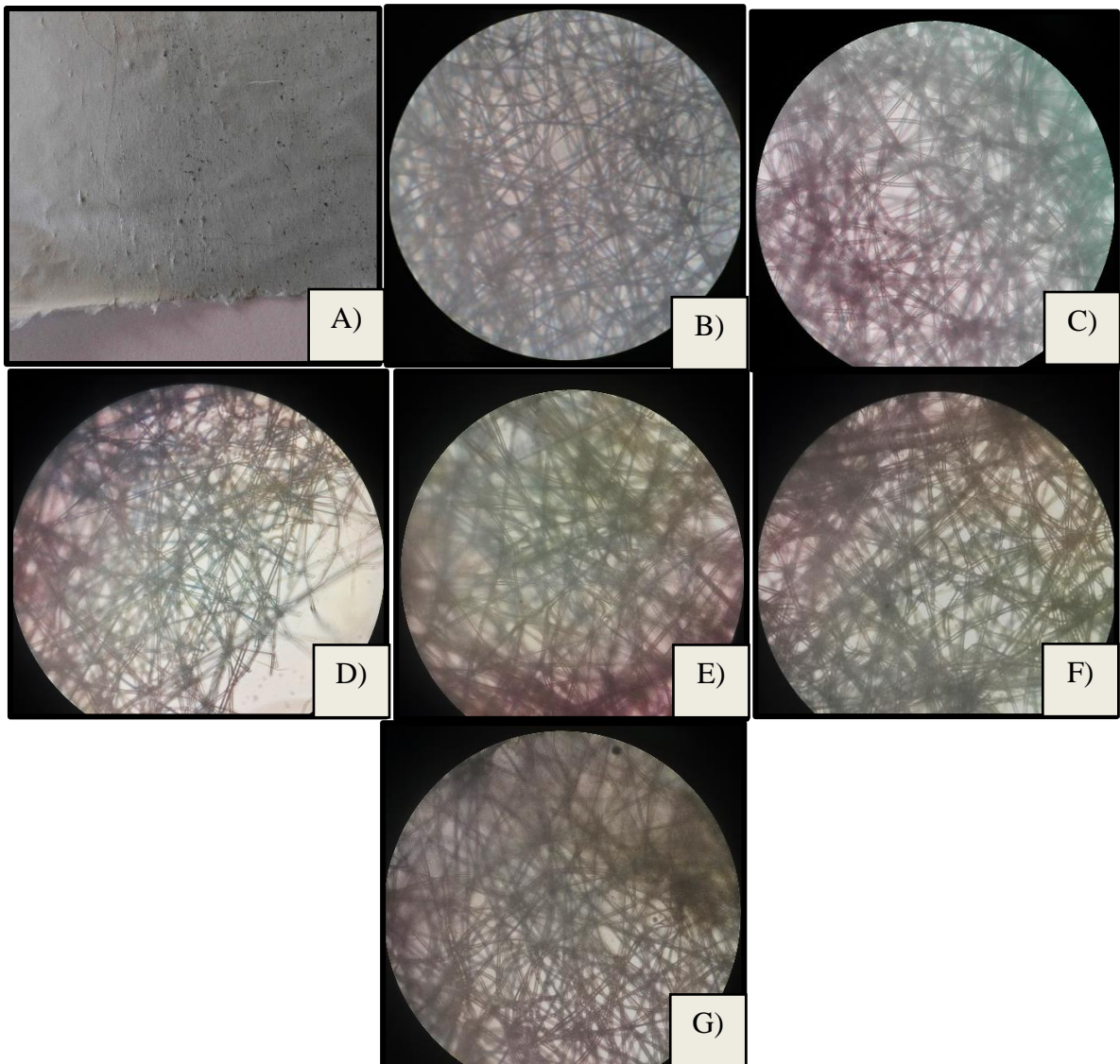

Figure 36 – Photographs of genipin crosslinked fibers. **A)** Bluish fibrous mats of G5_O; images from B) to G) were taken by OM at 1000X magnification: **B)** G2.5_O. **C)** G5_O. **D)** G5_24. **E)** G5_OM. **F)** G7.5_O. **G)** G10_O.
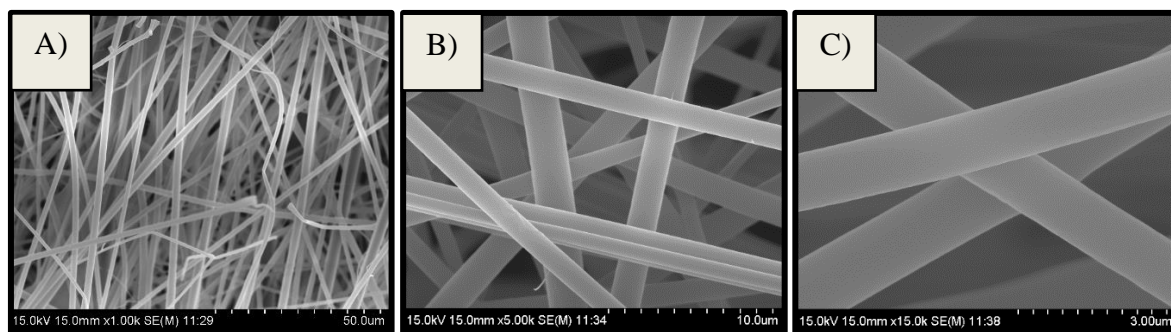
Figure 37 – Micrographs of G5_O fibers. **A)** SEM at 1000X magnification. **B)** SEM at 5000X magnification. **C)** SEM at 15000X magnification.
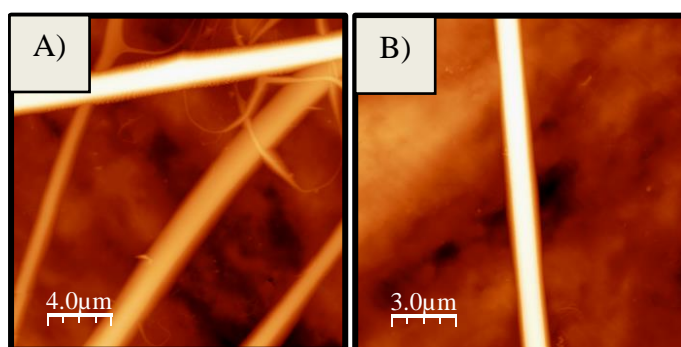
Figure 38 – Topography AFM image of G5_O fibers.

The genipin crosslinked fibers were also subjected to a heat post-treatment at 120ºC. The main objective was to obtain an enhanced combination, equally achieved in other crosslinking methods, such as citric acid, hexamethylene-1,6-diaminocarboxysulphonate or GLU [130,171,198]. A posterior examination showed that fibrous mats turned from blueish to brownish, a change that was more pronounced as the concentration of genipin increased. In addition, the visible larger irregular fibers, and solution drops on the mats, also became darker brown, perceptible in Figure 39 F). Because of thermal treatment, mats detached more easily from the aluminum foil, which facilitated further handling. Fiber morphology remained similar to those crosslinked by genipin but not subjected to the thermal treatment (Figure 39 A) and E)).
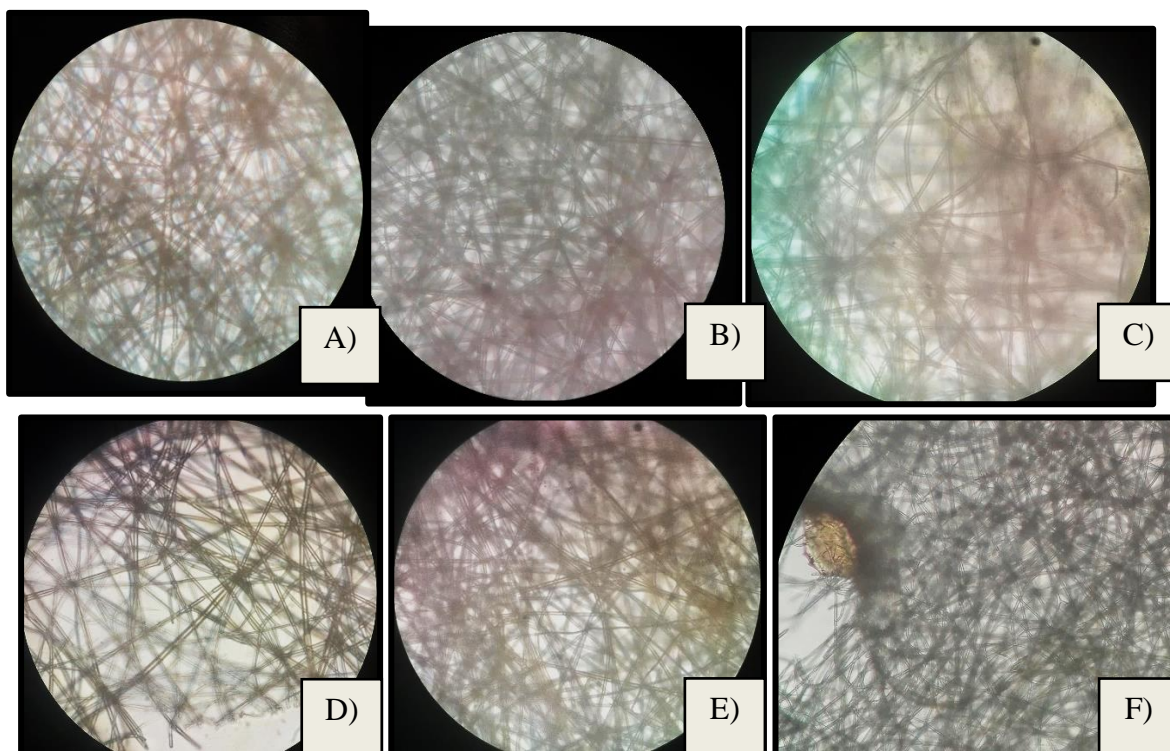
Figure 39 – Photographs of genipin and heat crosslinked fibers, from OM observations. **A)** G2.5_O120, at 1000X magnification. **B)** G5_O120, at 1000X magnification. **C)** G5_OM120, at 1000X magnification. **D)** G7.5_O120, at 1000X magnification. **E)** G10_O120, at 1000X magnification. **F)** Close-up image of G5_O, at 400X magnification. Brown solution drop noticeable.

Glutaraldehyde vapor-rich atmosphere impacted differently on gliadin fibers, depending on the treatment duration time [161,210]. At room temperature, fibers shrunk and showed a yellowish coloration, with the increase of reaction time. Furthermore, with increasing reaction time they became less flexible and maneuverable, until they turned entirely hard and stiff. A treatment for 4 h was defined as the most suitable for achieving manageable fibrous mats, without losing too much flexibility, although a significant shrinkage could not be avoided, comparing for example with the 2 h treatment. For a 24 h treatment, fibrous samples compacted and fused, developing a less fibrous structure, as can be observed by comparing Figure 40 A), B) and C). The presence of water vapor inside the sealed glass container may have contributed to these morphological changes [161, 172]. Nevertheless contradictory results exist regarding the effect of time and GLU concentration on the morphology of electrospun fibers, which seems to be also dependent on polymer type: for GLU-treated fish gelatin fibers, morphological changes were more evident after a short treatment time of 2 h than 5 h; for PVA/gluten fibers, morphology did not significantly changed after a 6 h crosslinking period;

other reports showed a fiber width decrease of 3.8% for spun silk fibers, but of 13.6 % for collagen fibers, after a 48 h treatment, and an increase of fiber stiffness [123,161,209].

Detailed SEM images for the GLU4 sample (Figure 41) showed an heterogenous fibrous network, composed by fine fibers with an average diameter of 596±230 nm (Figure 41 A). Elementary analysis spectrum of GLU4 fibers, on Figure 42, revealed similar fiber element composition as previous tested samples.
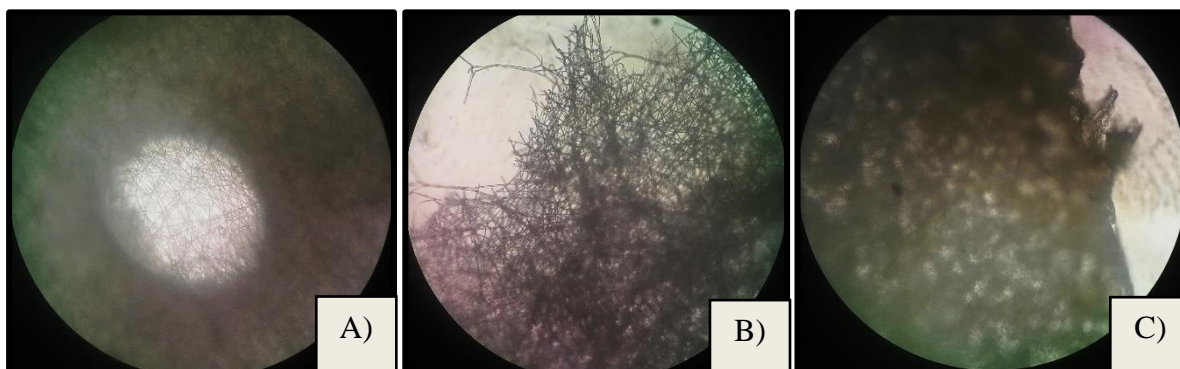

Figure 40– Photographs of glutaraldehyde crosslinked fibers, from OM observations, at 400X magnification. **A)** GLU2. **B)** GLU4**. C)** GLU24.
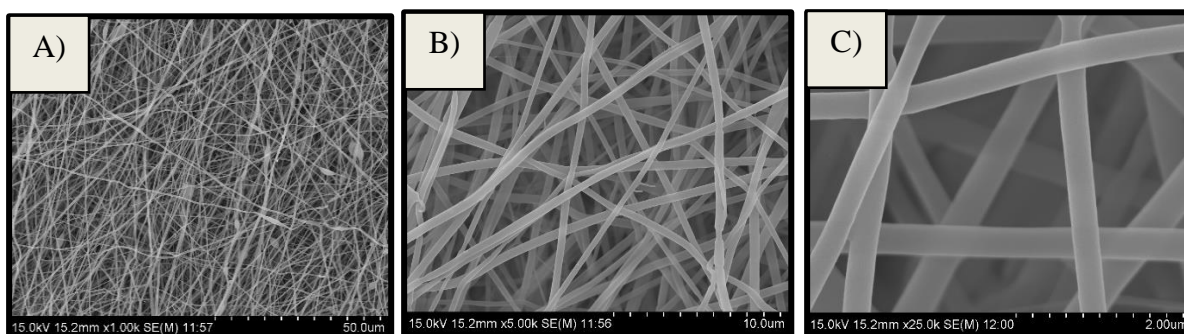
Figure 41– SEM Micrographs of GLU4 fibers. **A)** At 1000X magnification. **B)** At 5000X magnification. **C)** At 25000X magnification.
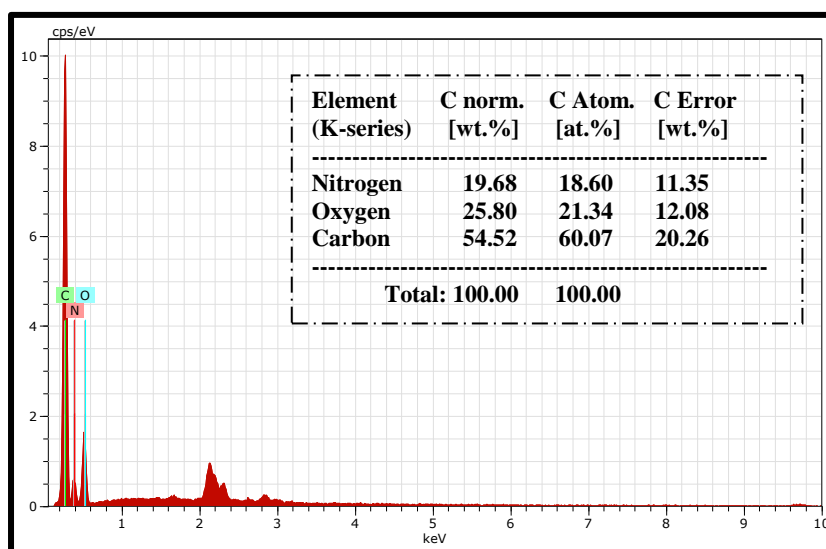
Figure 42 – Elementary analysis spectrum of GLU4 fibers by SEM-EDS.

Citric acid crosslinking was carried out using an alternative preparation of the gliadin spinning solution, based on previous reports for zein and collagen [171,172]. The addition of the crosslinking agent, which drops the solution pH, is then rebalanced by the addition of NaOH to obtain a final pH of 4.9, which was shown to be a adequate pH for the crosslinking reaction to occur [172,174]. All whitish spinning solutions had an electrospinning process slightly unstable, with frequent accumulation of solution at the tip of the needle. The collected fibrous matrix had a homogeneous slightly yellowish aspect, where grains were visible in the surface, as seen on Figure 43 A). We suggest that those grains might have resulted from salt precipitation, with the crystals being projected during the jet phase and incorporated in the fibrous matrix. It was possible to notice, during morphology examination, the existence of a heterogeneous fibrous matrix, consisting in branched and regular fibers of diverse diameters (Figure 43). Detailed SEM images of CA13 samples (Figure 44) complemented the previous findings, showing an average fiber diameter of 1892 ± 758 nm, besides it was observed some roughness on the fibers surface. These diameters were much larger than those previous reported for crosslinked zein fibers with 13% CA [170]. Elementary analysis spectrum of CA13 sample (Figure 45) revealed a similar elementary composition of the fibers, as before, and identified a new element, Sodium (Na), in accordance to what expected. Sodium element (or sodium salts) seem to be located preferably in the branched zones, as can be seen in the colorimetric mapping of the distribution of the elements, on Figure 46.
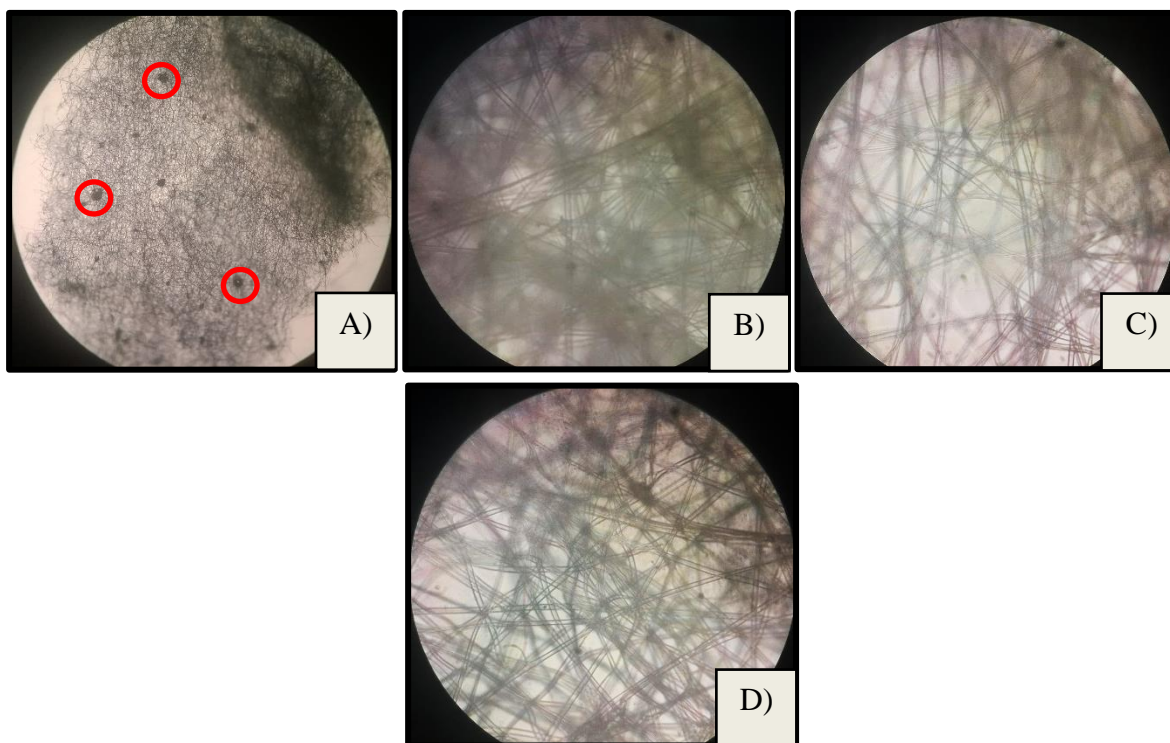
Figure 43 – Photographs of citric acid crosslinked fibers from OM observations. **A)** CA9, at 50X magnification. Visible grains (red circle). **B)** CA5, at 1000X magnification. **C)** CA9, at 1000X magnification. **D)** CA13, at 1000X magnification.
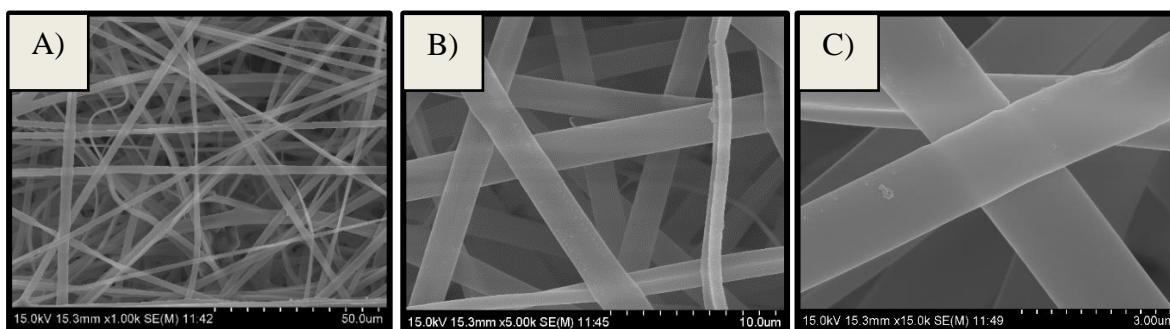

Figure 44 – SEM Micrographs of CA13 fibers. **A)** At 1000X magnification. **B)** At 5000X magnification. **C)** At 15000X magnification.
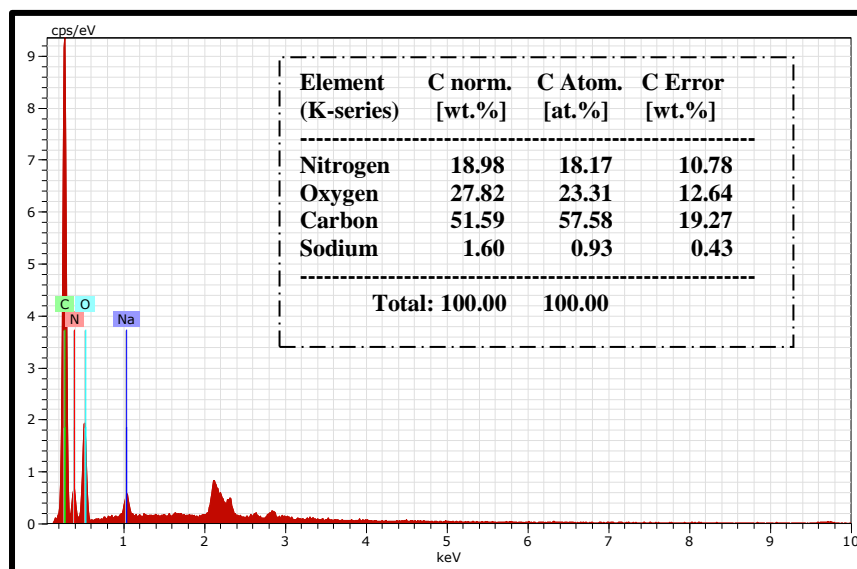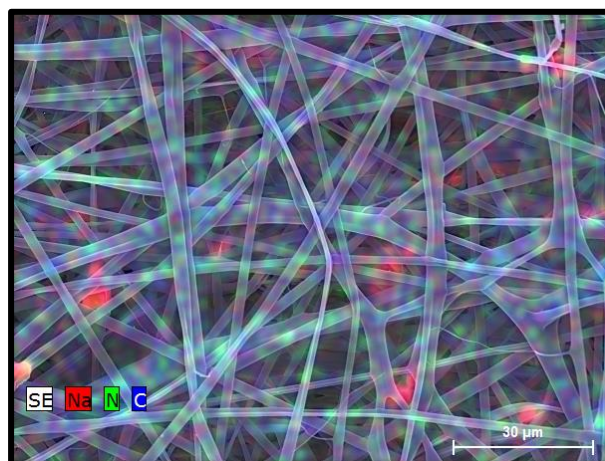
Figure 45 – Elementary analysis spectrum of CA13 fibers by SEM-EDS.

Figure 46 - Colorimetric mapping of Carbon (C), Sodium (Na) and Nitrogen (N) elements in the CA13 crosslinked sample.
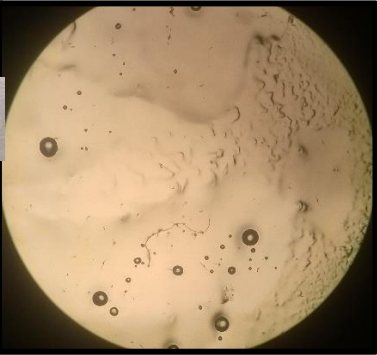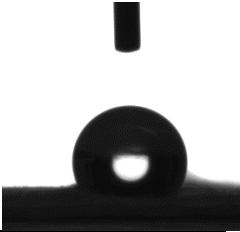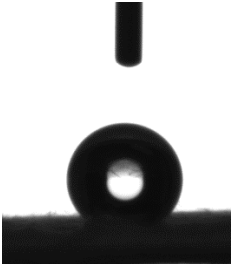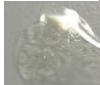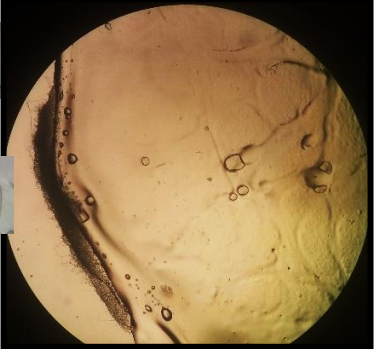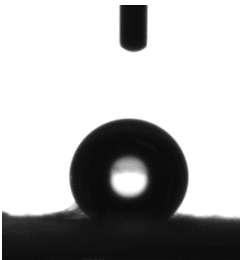
3.2.2 Aqueous behavior: Stability, swelling degree and contact angle

All fiber samples were investigated for their behavior in aqueous environment, by evaluating the degradability in water, swelling behavior, changes in fiber morphology and fiber interactions and their organization within the mat when in contact with water, and surface hydrophilicity by measuring the water contact angle.

Tables below resume the experimental results achieved, for each crosslinking treatment.

Uncrosslinked gliadin fibrous mats, whose surface presents a hydrophobic behavior due to the presence of hydrophobic amino acids, and heat-induced crosslinked gliadin mats demonstrated no resistance to water. Even though that dissolution of the uncrosslinked protein fibers was expected and it is in accordance with previous data [107,158], it could be expected a different behavior for the heat-treated fiber mats [136,211]. Upon contact with water, these fibrous matrices rapidly swelled and disintegrated, losing their fibrous structure and shape, becoming, after drying, a non-porous and non-fibrous film with reduced surfaced area, as seen in Table 6. Above certain temperatures, it is anticipated the formation of heat-stable noncovalent hydrogen-bonds, related with the high content in glutamine, but even more important the covalent crosslinking reaction of intermolecular disulfide bonds, due to the high levels of cysteine [114, 211-214]. From the increase in disulfide bonds between gliadin residues, where a continuous polymerization reaction can be achieved through sulfhydryl-disulfide interchange, from the increase in free sulfhydryl groups and dehydroalanines from the available cysteines, due to the heat-induced protein unfolding, improved mechanical properties, reduced water uptake and an increased water insolubility, while retaining the material structure, could be expected [136,140,214,215]. 120ºC-treated fibers revealed an increased hydrophobic behavior on the surface of the mat and a certain resistance to initial dissolution (in Table 5, for the T120_O sample, it is possible to observe some remained fibrous areas). However, from what was stated above, through the heat treatment especially at 120ºC, gliadin fibers should have shown better water performance. Besides the temperature values, other factors may have affected the crosslinking reaction, such as the treatment time, the sample thickness or moisture conditions [136, 214, 216].

Table 5 – Aqueous behavior of uncrosslinked sample G30 and heat-treated samples.
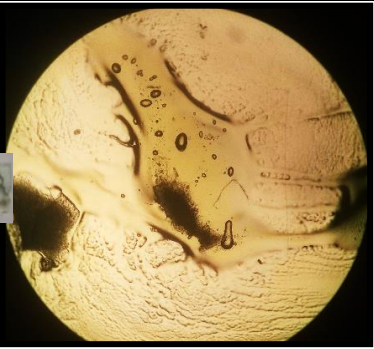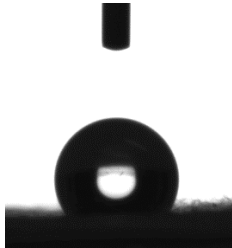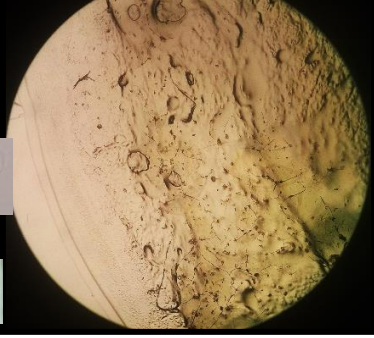
Samples	Stability Test		Swelling Degree (%)	Contact Angle	
	Test Image	OM Image		(º)	Image
Glia30	Control Wet Dried		----	132±5	
T60_O	Control Wet Dried		----	148±11	
T120_O	Control Wet Dried		----	148±9	
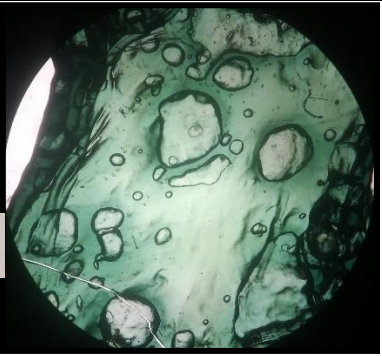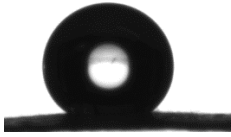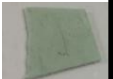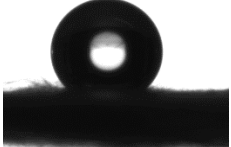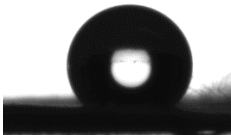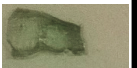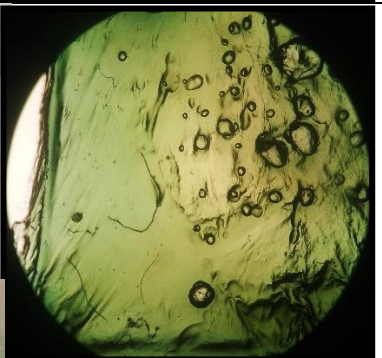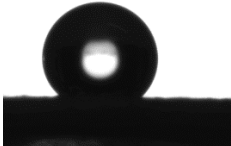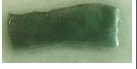
Note: OM photographs of samples were taken at 50X magnification.

For the genipin crosslinking treatment, as shown in Table 6, samples G2.5_O and G5_O in contact with water still lost the fibrous structure, by dissolution, maintaining only some structural insoluble blue residues. Similar non-water-stable scaffolds were obtained from 2% GEN (w/w) crosslinked gelatin fibers [161]. Both samples showed a decrease in surface hydrophobicity when compared to the non-treated samples, but they lost mass in contact with water, making not accurate the attempt to determine the degree of swelling. With the increase of genipin amounts, the water stability improved, as already demonstrated from gelatin fibers [162], but the fiber mats still showed a significant general shrinkage, induced by water, and they lost the fibrous and porous structure, resu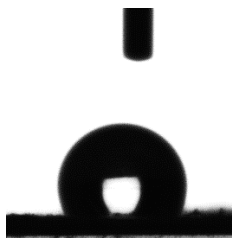lting in a swollen, compact and transparent bluish sample, with no fibrous or porous structure. Time appears to have a double positive impact on water tolerance in genipin mats. On one side, increasing the crosslinking time before the

electrospinning process, samples G5_O and G5_24, resulted in an improved deep blue water-resistant mat, although also exhibiting significant shrinkage, with higher surface hydrophobicity. Similar results regarding membrane enhancement over time were obtained for GEN post-treatment under GEN/ethanol solution immersion and through GEN vapor-rich atmosphere in a dissector [158,159]. On the other side, producing genipin fibers and storing them for a certain period of time, in this case a month and a half, made the mats insoluble in water, they only shrunk slightly, and displayed a lower swelling degree than G5_24, but similar contact angles. This can be attribute to the fact that crosslinking reaction continues slowly over time within the fibers, between genipin unreacted molecules and amine residues of protein fibers. For higher GEN content, the results obtained were similar to the G5_24 and G5_OM samples, in terms of keeping an aqueous stable, yet no fibrous matrix and of wettability performance (no significant differences were obtained for the water contact angles).

Table 6 – Aqueous behavior of GEN crosslinked samples.

Samples	Stability Test		Swelling Degree (%)	Contact Angle	
	Test Image	OM Image		(º)	Image
G2.5_O	Control / Wet / Dried		---	130±14	
G5_O	Control / Wet / Dried		84.7	124±10	
G5_24	Control		69.1	145±3	

	Wet				
	Dried				
G5_OM	Control				
	Wet		61.3	146±5	
	Dried				
G7.5_O	Control				
	Wet		40.7	140±8	
	Dried				
G10_O	Control				
	Wet		89.9	144±9	
	Dried				
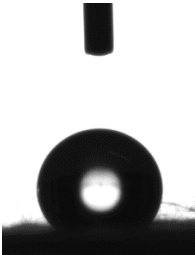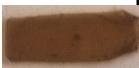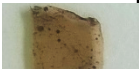
Note: OM photographs of samples were taken at 50X magnification.

After GEN samples have been submitted to heat-induced method, with temperatures of 120ºC overnight, they produced enhanced brownish insoluble mats, that can be compared on Table 7. While it may be easy to associate the employment of a high temperature treatment, at 120 ºC, in dry conditions, on a protein based matrix with consequent formation of insoluble

colored compounds, as Maillard reaction products, in fact, it might be not the case [217,218]. Although gliadin is extracted from a commercial wheat gluten, whose total protein content is according to the supplier information and our laboratorial results >80% and 84.4%, respectively, it is reasonable to indicate that residual starch might represent 8 to 15% [218]. Being so, in that case electrospun fibers produced from that polymer source and subjected to a 120 °C heat treatment, could certainly evidence signs of Maillard reactions, due to interaction between amino groups of amino acids and aldehyde groups of carbohydrates [218,219]. However, because the gliadin polymer exhibits a total protein content of almost 100%, the residual trace amounts of reducing carbohydrates, if they exist, are not responsible for the brownish reaction nor for the observed structural changes, or else it would be already detected, when gliadin fibers where submitted to heat-induced treatments. So, besides the mentioned covalent crosslinking disulfide bonds, due to the accessible cysteine amino acids of gliadin, we suggest that other important crosslinking reactions might take place within the protein fibers, namely the heat-induced isopeptide bond formation, as already been reported for wheat gluten, in a 24 h treatment at 130°C [216, 219]. Thus, this crosslinking reaction involves the bond formation of certain amino acids peptides, such as glutamine and lysine and occurs with or without the presence of cysteine or cystine. As so, this crosslinking reaction, that increases with the heating time, produces large and unextractable molecules [219]. Those generated brownish mats, containing darker spots due to solution drops as discussed, exhibited similar performance while interacting with water, maintaining their structure without considerable loss of size, which means no considerable shrinking. The referred improved insolubility appears to be independent of the genipin amount, considering the tested genipin concentrations. Furthermore, despite the superior overall swelling degree of mats, compared to the GEN crosslinked samples of Table 6, this heat post-treatment guaranteed that they all could kept partially, in some case more than others, their fibrous and porous structure, as seen on the auxiliary images of Figure 47. Even though they all swelled, higher GEN content led to a reduction of swelling [162]. Regarding this, for GEN content above 2.5% (w/w), there was a slightly improvement of the fibrous matrix structure under water interaction, that partially avoided fibers fusion, accompanied by a significant swelling and a slight increase in surface hydrophobicity. For the highest tested GEN concentration there was already a decrease in swelling, suggesting that only higher concentrations of GEN, probably impracticable from a technological or even cost point of view, would lead to significant improvements that would be closer to the objectives of this work in terms of fibers' strength and integrity in aqueous environment. The heat post-treatment tended to induce a much higher swelling degree than

the treatment with GEN alone, but the storage time after production had a positive effect on the swelling (G5_OM120), reducing it by half compared to non-stored mat G5_O120; proper control of the storage of the treated fibers could be an important factor to be explored in the future.

Table 7 – Aqueous behavior of GEN with heat crosslinked samples.

Samples	Stability test		Swelling Degree (%)	Contact Angle	
	Test Image	OM Image		(º)	Image
G2.5_O120	Control / Wet / Dried		205.0	138±7	
G5_O120	Control / Wet / Dried		238.9	141±9	
G5_OM120	Control / Wet / Dried		106.7	148±5	

G7.5_O120	Control			236.9	150±5	
	Wet					
	Dried					
G10_O120	Control			183.6	145±6	
	Wet					
	Dried					

Note: OM photographs were taken at 100X magnification.
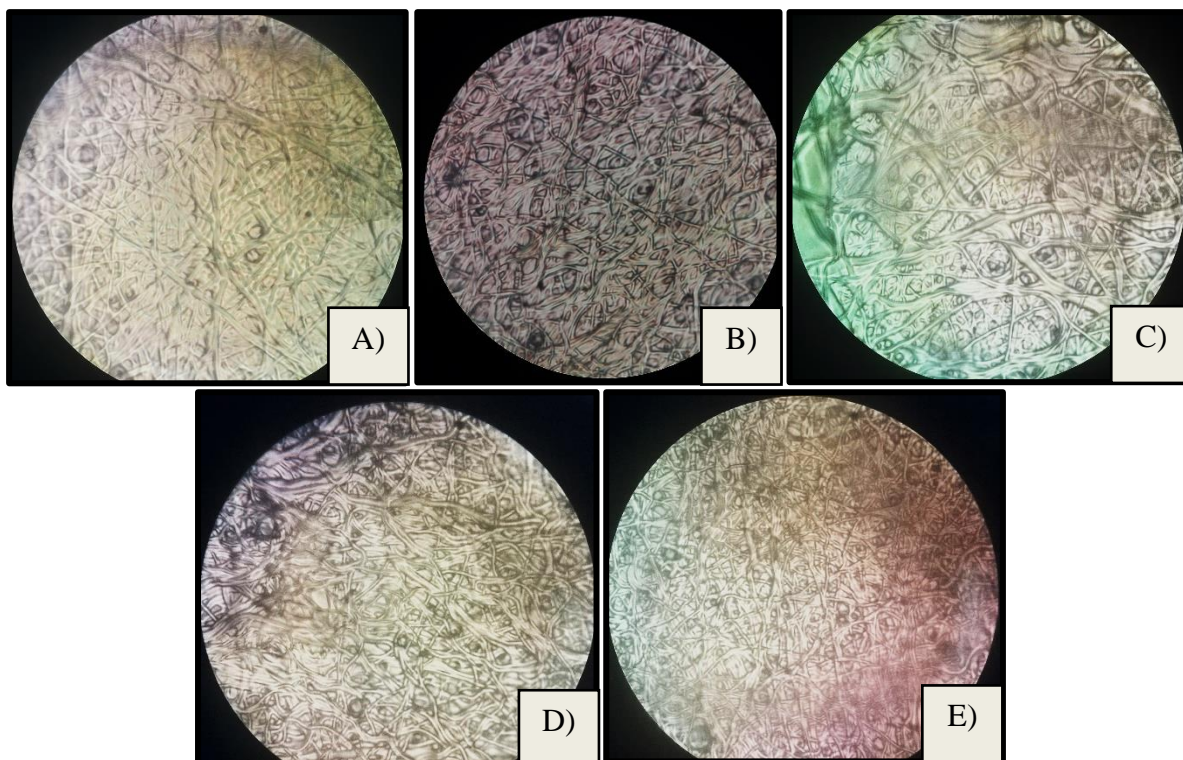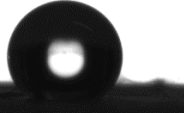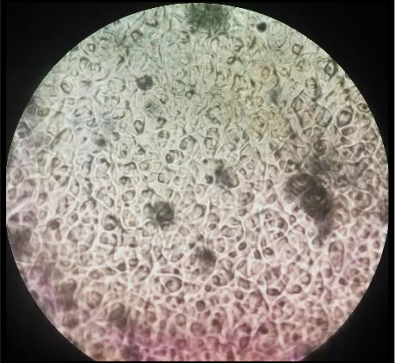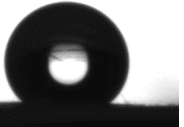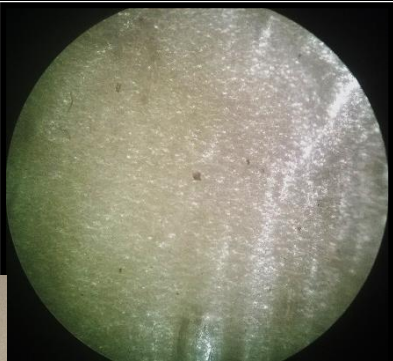
Figure 47 – Photographs of genipin and heat crosslinked fibers, from OM observations at 1000x magnification. **A)** G2.5_O120. **B)** G5_O120. **C)** G5_OM120. **D)** G7.5_O120. **E)** G10_O120.

GLU treated-fibers displayed differences between them, according their reaction time, after having been in contact with water, as seen on Table 8. Visually, GLU2, the sample with the shortest treatment time, demonstrated a non-fibrous shrunk transparent appearance, but still it had the lowest swelling degree. As for the others with increasing crosslinking time, they appeared to better preserve their morphology as well as they retained their original shape, after the water immersion, despite the increase of the swelling degree. GLU4 revealed the existence of a semi-porous structure; regarding GLU24 it was not possible to examine in detail due to low maneuverability of the sample, even after water contact. The water contact angles indicated high hydrophobicity on the surface of the GLU-treated fibers, for both that had similar values, reflecting that higher treatment times could not influence the surface hydrophobicity, being these generally higher than all other crosslinking methods. Thus, increasing the treatment time in a GLU vapor-rich environment seems to improve the water performance, as already reported [210].

Table 8 – Aqueous behavior of GLU crosslinked samples.
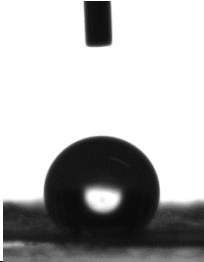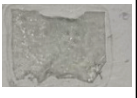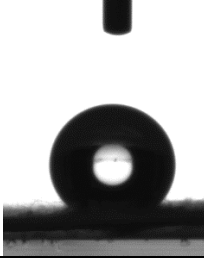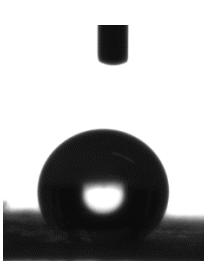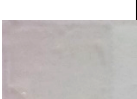
| Samples | Stability test | | Swelling Degree (%) | Contact Angle | |
	Test Image	OM Image		(°)	Image
GLU2	Control / Wet / Dried		91.5	151±5	
GLU4	Control / Wet / Dried		124	153 ±18	

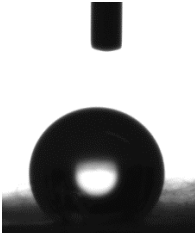|				288.8	----	----
GLU24	Control					
	Wet					
	Dried					

Note: OM photographs of GLU2 were taken at 50X magnification, GLU24 at 100X magnification and GLU4 at 1000X magnification.

Regarding the results obtained for the crosslinked fibers with citric acid, all the samples exhibited an identical morphology, after water immersion, as seen on Table 9, becoming a non-fibrous and non-porous shrunk transparent structure. This loss of fibrous structure was not expected, given that these results differ from those obtained for collagen and zein mats, which when crosslinked by citric acid under similar conditions could retain mostly or totally their fibrous and porous structure after water immersion [170,171]. Nevertheless, the crosslinker increase slightly decreased the swelling degree, 88.5% in CA5 sample and 82.8% in CA13 sample, similar correspondence was verified for higher CA content in zein fibers [171]. In addition, CA mats exhibited similar contact angle values, slightly higher for CA13, showing lower wettability than those membranes crosslinked with less CA concentration.

Table 9 – Aqueous behavior of CA crosslinked samples.

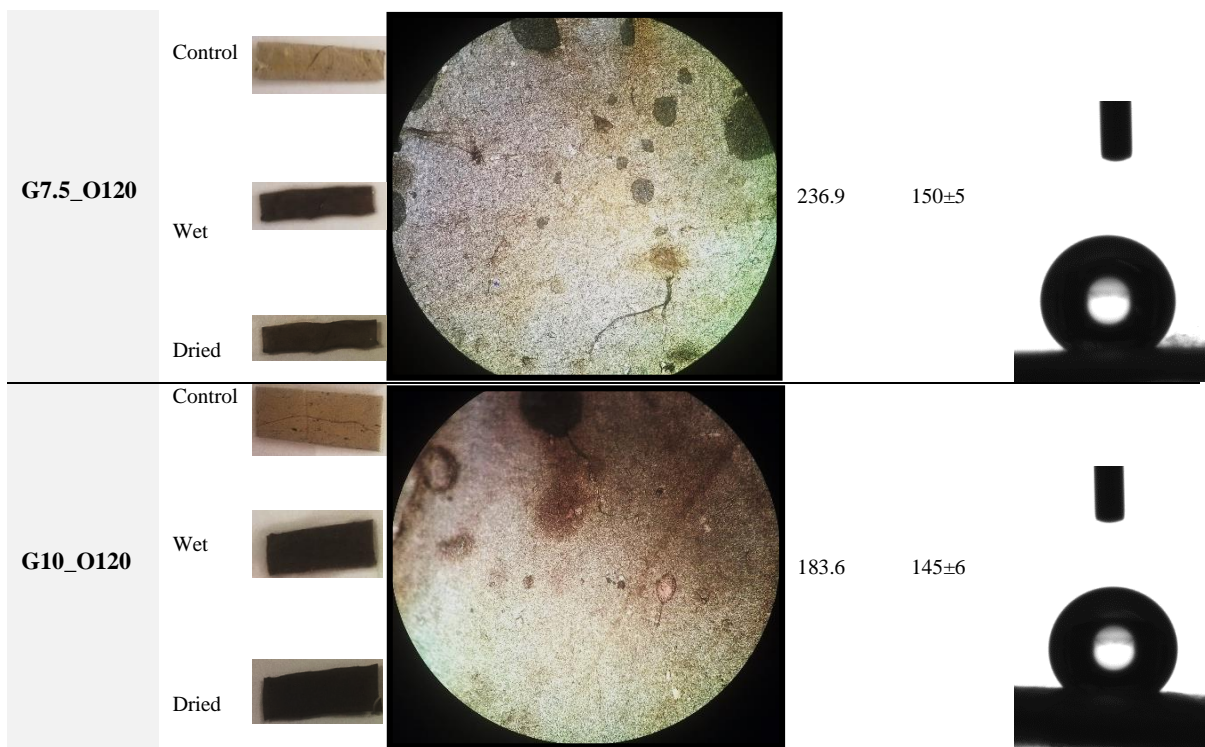| Samples	Stability Test		Swelling Degree (%)	Contact Angle	
	Test Image	OM Image		(°)	Image
CA5	Control / Wet / Dried		88.5	146±6	
CA9	Control / Wet / Dried		86.8	147±3	
CA13	Control / Wet / Dried		82.8	151±5	

Note: OM photographs of samples were taken at 100X magnification.

Therefore, heat treatment alone in the gliadin fibers didn't serve as an improving method to maintain the structural integrity of the electrospun fibrous mats when in contact with water. In its turn, genipin brought observable changes, not only regarding the general aqueous stability but also the fiber swelling behavior, revealing that time, in terms of spinning solution reaction and post-electrospinning fibers storage, acted positively to guarantee an increased crosslinking reaction, in order to keep the mats from losing structure; increasing the GEN content guaranteed a better effect. It became obvious that better results could be obtained by combining the use of GEN with a heat post-treatment. Besides assuring the non-dissolution of the matrix, the heat treatment also could slightly keep the structural integrity of the crosslinked matrix, regarding porosity and individualized fibers, under penalty of increased swelling. This

issue seems to be overcame with storage time of the fibers. The performance of GLU crosslinked mats was time-dependent, however decreasing the treatment time could mean less water stability, but higher time in the vapor-rich atmosphere could led to the production of non-maneuverable, shrunk, stiff mats, nevertheless with good water tolerance. CA crosslinked fibers could reproduce similar results obtained for higher GEN content, however the obtained mats were completely non-fibrous and non-porous, after submerged in water, different from those obtained by the combined use of GEN and heat treatment at 120ºC.

3.2.3 Mechanical properties

The mechanical properties of the fibrous mats were studied by uniaxial tensile tests. Young's modulus, elongation at break and tensile strength were determined from the obtained stress–strain curves. Results obtained for tensile strength, defined as the maximum nominal stress at the breaking point, are shown in Figure 48. Figure 49 shows the results obtained for Young's modulus, considered as the ratio between stress and strain in the initial linear zone of the curve, before the breaking point, and Figure 50 shows the results obtained for the percentage elongation at break, defined as strain at break point.

Similar tensile strength values, below 0.4 MPa, were obtained for the gliadin uncrosslinked mats and those gliadin mats treated at 60 ºC and 120ºC, which means that no tensile advantages were acquired with the heat treatment. Gliadin uncrosslinked mats results didn't match those generated from an identical study, where the tensile strength obtained was of 3.54±0.16 MPa, comparably higher than zein and hordein tensile properties. It was suggested that those superior mechanical properties of gliadin fibrous membranes were correlated with the protein conformational change during the electrospinning, in which gliadin could maintain their secondary structure and stabilization in the fibers [114].
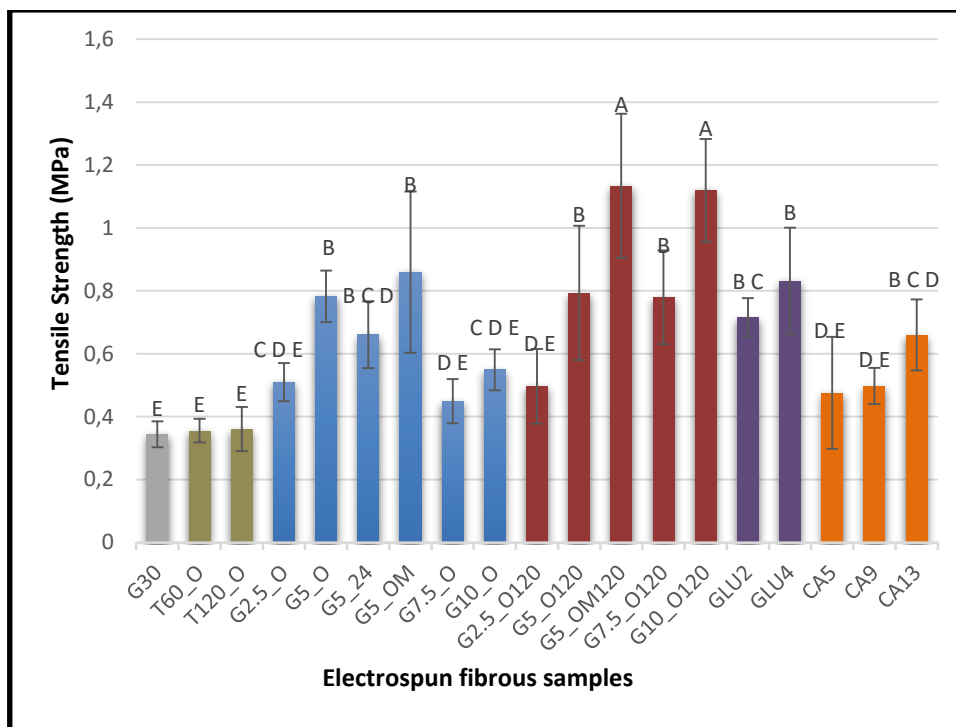
Figure 48 – Tensile strength (MPa) of crosslinked and uncrosslinked gliadin fibers. Full bars represent mean and respective tracing bars represent the standard error of the mean of 10 samples. Results data labeled with different letters exhibit statistical differences, considering *p*-values<0.05.
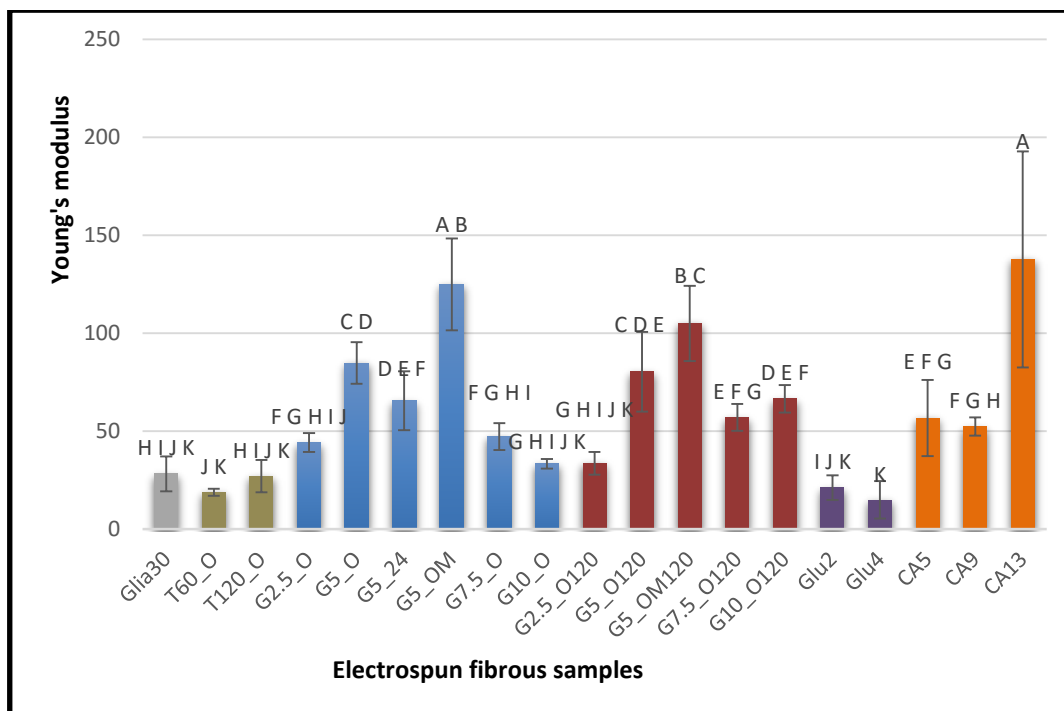
Figure 49 – Young's modulus (MPa) of crosslinked and uncrosslinked gliadin fibers. Full bars represent mean and respective tracing bars represent the standard error of the mean of 10 samples. Results data labeled with different letters exhibit statistical differences, considering *p*-values<0.05.
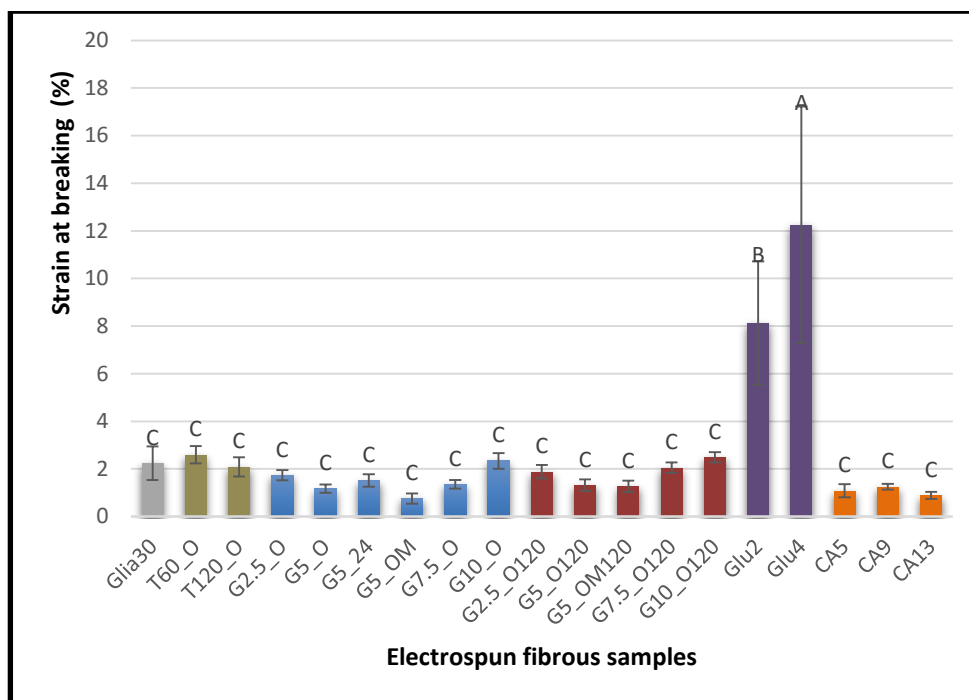
Figure 50 – Comparison of strain (%) at breaking of crosslinked and uncrosslinked gliadin fibers. Full bars represent mean and respective tracing bars represent the standard error of the mean of 10 samples. Results data labeled with different letters exhibit statistical differences, considering *p*-values<0.05.

Once again, the thermal treatment did not show any positive effect on the fibers mechanical properties, contrarily to what was reported for other biopolymer fibers, such as chitosan electrospun fibers heat-treat at 120ºC [198] and wheat gluten/gliadin films [212, 215], in both cases showing a clear positively correlation between the increase of the temperature and better mechanical properties, in terms of mechanical strength and elongation at break. Once more, this mechanical improvement has been related to the increase of covalent crosslinking between the protein chains induced by heat, also with an important role of hydrogen bonding [217]. Even so, other factors could be involved in the improvements of mechanical properties, besides crosslinking, namely enhanced molecular entanglements and changes in molecular protein conformations [222].

The remaining crosslinking methods showed general improvements. Among GEN sample group, gliadin mats crosslinked with 5% GEN had the highest tensile strength as well as Young's modulus (Figure 49), particularly those whose spinning solution reacted overnight, G5_O and G5_OM. Thus, mats tensile properties were enhanced with incrementation of GEN concentration, until they reached a maximum at GEN 5%, and with further GEN increase tensile results were reduced to similar values as those obtained for uncrosslinked gliadin mats.

Similar GEN concentration effects were also verified for electrospun collagen scaffolds, where a maximum in the improvement of mehcanical properties was reached at 5% GEN, and also a similar initial incrementation, for low GEN concentration values, observed for gelatin mats, although; both crosslinking methods were done as post-treatments [221,222]. Considering the effects of reaction time within the spinning solution and of storing time of the produced mats on the mechanical properties, G5_24 and G5_OM, respectively, no significant changes on the tensile strength or Young's modulus were observed. Opposite results were obtained while varying the crosslinking reaction time, from 12 to 72h, while immersing silk fibroin/hydroxybutyl chitosan scaffolds on a genipin solution, in which higher tensile strength values were obtained by increasing the reaction time [158].

The combining of GEN crosslinking with thermal treatment, at 120ºC, registered a general mechanical properties improvement, probably associated to the described heat-induced crosslinking reaction via intramolecular disulfide interharges, and even hydrogen bonding, and the suggested isopeptide bond formation [212,215,219]. Only G2.5_O120 and G5_O120 demonstrated similar tensile values as G2.5_O and G5_O, respectively. The increase GEN amount, of 7.5% and 10% (w/w), benefice from the heat treatment, hence displaying higher tensile results, than those only crosslinked with GEN. Furthermore, a month and a half of storing time, G5_OM120, confirms the storage positive effect even for this combined method, hence obtaining the best result together with G10_O120, which could mean that increasing the GEN content to 10% has a similar tensile strength effect as storing a treated sample with half the GEN amount for a period of time. Even so, G5_OM120 showed higher Young's modulus than G10_O120 or the rest of the crosslinked sample group.

As expected, GLU-treated samples had good tensile strength performance, equally to some GEN and GEN with heat-induced samples, such as G5_O or G5_O120, however the increase of reaction time didn't bring any additional improvement. It is important to refer, that in terms of strain (%), only GLU-treated samples displayed remarkably higher elongation properties, contrary to Young's modulus presenting the lowest values, as seen on Figure 50 and Figure 49, respectively.

The use of citric acid as crosslinker agent demonstrated similar tensile properties among the tested samples, nevertheless CA13 was the only sample which had a comparable better performance, than G30, which also showed a significantly higher Young's modulus. A previous reported also indicated a similar tensile values profile, meaning that for the CA concentration of 5.5 and 7.7% had no significant impact, but increasing CA content had an enhanced effect on the mechanical properties [171].

4. Conclusions

The present work intended to develop, characterize and demonstrated the potentialities of using wheat gliadin biopolymer to design and create innovative materials, with crosslinked improved properties, through an ecological chain of procedures, including electrospinning, optimization of gliadin fibrous mats and the use of various crosslinking methods to improve their properties and potential applications.

First gliadin proteins, extracted from wheat gluten, were successfully electrospun. A solvent-system less dependent on acetic acid was designed and consisted in 85% acetic acid and 15% ethanol, which proved to be suitable for the protein dissolution and further electrospinning into homogeneous gliadin fibrous mats, containing defined and regular beads-free fibers, with smooth surface, with an average diameter of 665 nm.

Unfortunately most of the crosslinking methods tested did not lead to satisfactory results, at least in accordance with the objectives of this work, namely the production of protein nanofibrous membranes that, in addition to the improvement of their mechanical properties, could maintain their nanofibrous structure and porosity when in contact with aqueous environments.

Heat induced treatments, at 60 and 120ºC, demonstrated no significant changes compared to uncrosslinked fibers, even though at higher temperatures crosslinking disulfide bonds reaction should have allowed for enhanced insolubility and tensile performance. Regarding the genipin crosslinking method, fibers exhibited a characteristic blue coloration with higher diameters, and the treated mats when in contact with water lost their fibrous structure and porosity, despite displaying a higher water tolerance. The increase in reaction time, between genipin and the protein before electrospinning, or the increase in storage time after fiber preparation, had a positive impact, reducing the swelling degree and showing a better tensile performance, at least for 5% GEN samples. Post-thermal treatment of these GEN crosslinked fibers revealed improvements in the produced brownish gliadin matrix morphology, after water immersion, with equally good results regarding the mechanical properties, despite the higher swelling degree. The conventional GLU treatment influenced negatively fibers handling, especially with the increase of reaction time, since the fibrous mats became shrunk and stiff and differently changed fiber morphology, even though, as expected, the GLU treated mats presented higher water resistance and enhanced mechanical characteristics. The results obtained from the crosslinking attempts with citric acid also did not show to be promising, at least for the conditions tested: stability in water increased, as well

the mechanical properties were enhanced, for the higher CA concentration tested, but the electrospun fibrous mats lost their structural integrity and porosity when in contact with water.

5. Future Objectives

In order to better understand and characterize the developed gliadin electrospun fibers as well as to develop appropriated methods for their crosslinking and improved final properties in aqueous media, future work will be necessary so that these kinds of bio-based materials could find useful applications in a wider range of fields.

Firstly, it would be relevant to study other important parameters, such as the influence of higher temperatures, higher treatment times, that seem to be involved in the crosslinking process and thus interfere in the aqueous stability and mechanical properties.

Furthermore, it would be important to better comprehend the chemical interactions existing within the gliadin crosslinked fibers, not only to confirm but also enlighten the different interchanges caused by the crosslinkers.

Finally, it would be of great importance to study the crosslinked fibers biocompatibility, for a potential application as a biomaterial, to determine and evaluate cellular viability and proliferation, through *in vitro* cytotoxicity assays.

6. Bibliographic References

1. Wendorff, J. H., Agarwal, S., and Greiner, A. (2012). Electrospinning - Materials, Processing, and Applications. Wiley-VCH Verlag GmbH & Co: Weinheim.

2. Senthil, T., George, G., and Srinivasan, A. (2017). Electrospinning: From Fundamentals to Applications. In: A. Srinivasan and S. Bandyopadhyay (Eds), Advances in Polymer Materials and Technology. CRC Press: Boca Raton.

3. Park, S.-J. (2015). Carbon Fibers. Springer: London.

4. Tucker, N., Stanger, J. J., Staiger, M. P., Razzaq, H., and Hofman, K. (2012). The History of the Science and Technology of Electrospinning from 1600 to 1995. Journal of Engineered Fibers and Fabrics, (SPECIAL ISSUE-July-FIBERS), 63–73.

5. Taylor, G. (1964). Disintegration of Water Drops in an Electric Field. Proceedings of the Royal Society A, 280, 383-397.

6. Taylor, G. (1966). The Force Exerted by an Electric Field on a Long Cylindrical Conductor. Proceedings of the Royal Society A, 291, 145-158.

7. Taylor, G. (1969). Electrically Driven Jets. Proceedings of the Royal Society A, 313, 453-475.

8. Baumgarten, P. K. (1971). Electrostatic Spinning of Acrylic Microfibers. Journal of Colloid and Interface Science, 36, 1, 71-79.

9. Larrondo, L., and Manley, R. St. J. (1981). Electrostatic Fiber Spinning from Polymer Melts. I. Experimental Observations on Fiber Formation and Properties. Journal of Polymer Science: Polymer Physics Edition, 19,909-920.

10. Larrondo, L., and Manley, R. St. J. (1981). Electrostatic Fiber Spinning from Polymer Melts. II. Examination of the Flow Field in an Electrically Driven Jet. Journal of Polymer Science: Polymer Physics Edition, 19,921-932.

11. Larrondo, L., and Manley, R. St. J. (1981). Electrostatic Fiber Spinning from Polymer Melts. III. Electrostatic Deformation of a Pendant Drop of Polymer Melt. Journal of Polymer Science: Polymer Physics Edition, 19,933-940.

12. Hayati, I., Bailey, A. I., and Tadros, T. F. (1986). Mechanism of Stable Jet Formation in Electrohydrodynamic Atomization, Nature, 319, 41–43.

13. Hayati, I., Bailey, A. I., and Tadros, T. F. (1987). Investigations into the Mechanisms of Electrohydrodynamic Spraying of Liquids – I. Effect of Electric Field and the Environment on Pendant Drops and Factors Affecting the Formation of Stable Jets and Atomization. Journal of Colloid and Interface Science, 117, 1, 205-221.

14. Hayati, I., Bailey, A. I., and Tadros, T. F. (1987). Investigations into the Mechanisms of Electrohydrodynamic Spraying of Liquids – II. Mechanism of Stable Jet Formation and Electrical Forces Acting on a Liquid Gone. Journal of Colloid and Interface Science, 117, 1, 222-230.

15. Doshi, J., and Reneker, D. H. (1995). Electrospinning Process and Applications of Electrospun Fibers. Journal of Electrostatics, 35,151-160.

16. Srinivasan, G., and Reneker, D. H. (1995). Structure and Morphology of Small Diameter Electrospun Aramid Fibers. Polymer International, 36,195-201.

17. Jaeger, R., Schönherr, H., and Vancso, G. J. (1996). Chain Packing in Electro-Spun Poly(ethylene oxide) Visualized by Atomic Force Microscopy Electrospun Aramid Fibers. Macromolecules, 29, 7634-7636.

18. Reneker, D. H., and Chun, I. (1996). Nanometre diameter fibres of polymer, produced by electrospinning, Nanotechnology, 7, 216–223.

19. Jaeger, R., Bershoef, M. M., Batlle, C. M., Schönherr, H., and Vancso, G. J. (1998). Electrospinning Of Ultra-Thin Polymer Fibers. Macromolecular Symposia, 127,141-150.

20. Fong, H., Reneker, D. H., and Chun, I. (1999). Beaded nanofibers formed during electrospinning. Polymer, 40, 4585–4592.

21. Scoopus – Analyze Search Results: TITLE-ABS-KEY (electrospinning) AND PUBYEAR > 1966 AND PUBYEAR < 2017 AND (LIMIT-TO (DOCTYPE , "ar")). Available:<https://www.scopus.com/term/analyzer.uri?sid=473150514EBCCF6C55277219F7B0E1AD.wsnAw8kcdt7IPYLO0V48gA%3a210&origin=resultslist&src=s&s=TITLE-ABS-KEY%28electrospinning%29+AND+PUBYEAR+%3e+1966+AND+PUBYEAR+%3c+2017&sort=plf-f&sdt=cl&sot=b&sl=68&count=17289&analyzeResults=Analyze+results&cluster=scosubtype%2c%22ar%22%2ct&txGid=473150514EBCCF6C55277219F7B0E1AD.wsnAw8kcdt7IPYLO0V48gA%3a26> Visited: 21/12/2016

22. Haider, A., Haider, S., and Kang, I.-K. (2015). A comprehensive review summarizing the effect of electrospinning parameters and potential applications of nanofibers in biomedical and biotechnology. Arabian Journal of Chemistry, 1-24.

23. Kalia, S. (2016). Biodegradable green composites. John Wiley & Sons, Inc: New Jersey.

24. Haghi, K. (2012). Electrospinning of Nanofibers in Textiles. CRC Pres: Boca Raton.

25. Dan, L., and Xia, Y. (2004). Electrospinning of Nanofibers Reinventing the Wheel?. Advanced Materials, 16, 14, 1151-1170.

26. Agarwal, S., Greiner, A., and Wendorff, J. (2013). Functional materials by electrospinning of polymers. Progress in Polymer Science, 38, 963– 991.

27. Reneker, D. H., and Yarin, A. L. (2008). Electrospinning jets and polymer nanofibers. Polymer, 49, 2387-2425.

28. Thompson, C. J., Chase, G. G., Yarin, A. L., and Reneker, D. H. (2007). Effects of parameters on nanofiber diameter determined from electrospinning model. Polymer, 48, 6913-6922.

29. Yarin, A. L., Koombhongse, S., and Reneker, D. H. (2001). Taylor cone and jetting from liquid droplets in Electrospinning of nanofibers. Journal of Applied Physics, 90, 9, 4836- 4846.

30. Shin, Y. M., Hohman, M. M., Brenner, M. P., and Rutledge G. C. (2001). Experimental characterization of electrospinning the electrically forced jet and instabilities. Polymer, 42, 9955-9967.

31. Yarin, A. L., Koombhongse, S., and Reneker, D. H. (2001). Bending instability in electrospinning of nanofibers. Journal of Applied Physics, 89, 5, 318-326.

32. Reneker, D. H., Yarin, A. L., Fong, H. and Koombhongse, S. (2000). Bending instability of electrically charged liquid jets of polymer solutions in electrospinning. Journal of Applied Physics, 87,9, 4531-4547.

33. Yarin, A. L., Kataphinan, W. and Reneker, D. H. (2000). Branching in electrospinning of nanofibers. Journal of Applied Physics, 98, 064501-1064512.

34. Mitchell, G. R. (2015). Electrospinning - Principles, Practice and Possibilities. The Royal Society of Chemistry: Cambridge.

35. Wang, Y., Serrano, S., and Santiago-Avilés, J. J. (2003). Raman characterization of carbon nanofibers prepared using Electrospinning. Synthetic Metals, 138, 423–427.

36. Yu, D.-G., Lu, P., Branford-White, C., Yang, J.-H. and Wang, X. (2011). Polyacrylonitrile nanofibers prepared using coaxial electrospinning with LiCl solution as sheath fluid. Nanotechnology, 22, 435301- 435307.

37. Yu, D.-G., Yang, C., Jin, M., Williams, G. R., Zou, H., Wang, X., and Bligh, S.W. A. (2011). Medicated Janus fibers fabricated using a Teflon-coated side-by-side spinneret. Colloids and Surfaces B: Biointerfaces, 138, 110–116.

38. Srivastava,Y., Marquez, M., and Thorsen, T. (2007). Multijet electrospinning of conducting nanofibers from microfluidic manifolds. Journal of Applied Polymer Science, 106, 3171–3178.

39. Veleirinho, B., and Lopes-da-Silva, J. A. (2007). Application of electrospun poly(ethylene terephthalate) nanofiber

mat to apple juice clarification. Process Biochemistry, 44, 353–356.

40. Wang, Y., Serrano, S., and Santiago-Avilés, J. J. (2002). Conductivity measurement of electrospun PAN-based carbon nanofiber. Journal of Material Science Letters, 21, 1055–1057.

41. Li, Z. and Wang, C. (2013). One-Dimensional Nanostructures Electrospinning Technique and Unique Nanofibers. Springer: London.

42. Veleirinho, B., Frei, M. F., and Lopes-da-Silva, J. A. (2008). Solvent and concentration effects on the properties of electrospun poly(ethylene terephthalate) nanofiber mats. Journal of Polymer Science: Part B: Polymer Physics, 46, 460-471.

43. Gomes, D. S., da Silva, A. N. R., Morimoto N. I., Mendes, L. T. F., Furlan, R., and Ramos, I., (2007). Characterization of an electrospinning process using different PAN/DMF concentrations. Polímeros: Ciência e Tecnologia, 17, 3, 206-211.

44. Yang, Q., Li, Z., Hong, Y., Zhao, Y., Qiu, S., Wang, C. and Wei, Y. (2004). Influence of solvents on the formation of ultrathin uniform poly(vinyl pyrrolidone) nanofibers with electrospinning. Journal of Polymer Science: Part B: Polymer Physics, 42, 3721–3726.

45. Jung, B., Yoon, J. K., Kima, B., Rhee, and H.-W. (2004). Effect of molecular weight of polymeric additives on formation, permeation properties and hypochlorite treatment of asymmetric polyacrylonitrile membranes. Journal of Membrane Science, 243, 45–57.

46. Chuangchote, S., Sagawa, T. and Yoshikawa, S. (2009). Electrospinning of Poly(vinyl pyrrolidone) effects of solvents on electrospinnability for the fabrication of poly(p-phenylene vinylene) and TiO2 nanofibers. Journal of Applied Polymer Science, 114, 2777–2791.

47. Nasouri, K., Shoushtari, A. M., and Kaflou, A. (2012). Investigation of polyacrylonitrile electrospun nanofibres morphology as a function of polymer concentration, viscosity and Berry number. IET Micro & Nano Letters, 7, 5, 423–426.

48. He, J.-H., Wan, Y.-Q., and Yu, J.-Y. (2008). Effect of concentration on electrospun polyacrylonitrile (PAN) nanofibers. Fibers and Polymers, 9, 2, 140-142.

49. Fallahi, D., Rafizadeh, M., Mohammadi, N., and Vahidi, B. (2013). Effects of feed rate and solution conductivity on jet current and fiber diameter in electrospinning of polyacrylonitrile solutions. e-Polymers, 9, 1, 1250-1257.

50. Heikkilä, P., and Harlin, A. (2009). Electrospinning of polyacrylonitrile (PAN) solution: effect of conductive additive and filler on the process. eXPRESS Polymer Letters, 3, 7, 437–445.

51. Jalili, R., Hosseini, S. A., and Morshed M. (2005). The effects of operating parameters on the morphology of electrospun polyacrilonitrile nanofibers. Iranian Polymer Journal, 12,1074-1081.

52. Fallahi, D., Rafizadeh, M., Mohammadi, N., and Vahidi, B. (2008). Effect of applied voltage on jet electric current and flow rate in electrospinning of polyacrylonitrile solutions. Polymer International, 57, 1363–1368.

53. Basu, S., Agrawal, A. K., and Jassal, M. (2011). Concept of minimum electrospinning voltage in electrospinning of polyacrylonitrile N,N-Dimethylformamide system. Journal of Applied Polymer Science, 122, 856–866.

54. Saiyasombat, C., and Maensiri, S. (2008). Fabrication, morphology, and structure of electrospun pan-based carbon nanofibers. Journal of Polymer Engineering, 28,1-2, 5-18.

55. Cengiz F., Krucińska I, Gliścińska E., Chrzanowski M, and Göktepe F. (2009). Comparative analysis of various electrospinning methods of nanofibre formation. Fibres & Textiles in Eastern Europe, 17, 1(72), 13-19.

56. Fennessey, S. F., and Farris, R. J. (2004). Fabrication of aligned and molecularly oriented electrospun polyacrylonitrile nanofibers and the mechanical behavior of their twisted yarns. Polymer, 45, 4217–4225.

57. Megelski, S., Stephens, J. S., Chase, D. B., and Rabolt, J. F. (2002). Micro- and nanostructured surface morphology on electrospun polymer fibers. Macromolecules, 35, 8456-8466.

58. Chaudhary, A. R., and Ahuja, B. B. (2014). Characterization and Optimization of Electrospun Polyacrylonitrile (PAN) and Polyvinylidene Fluoride (PVDF) Nanofibers. 5th International & 26th All India Manufacturing

Technology, Design and Research Conference (AIMTDR 2014), IIT Guwahati, Assam, India, December 12th–14th, 2014.

59. Shahabadi, S. M. S., Kheradmand, A., Montazeri, V., and Ziaee, H. (2015). Effects of process and ambient parameters on diameter and morphology of electrospun polyacrylonitrile nanofibers. Polymer Science Series A, 57, 2, 155–167.

60. Tong, H.-W., and Wang, M. (2010). Electrospinning of fibrous polymer scaffolds using positive voltage or negative voltage: A comparative study. Biomedical Materials, 5, 054110-054115.

61. Mit-uppatham, C., Nithitanakul, M., and Supaphol, P. (2004). Ultrafine electrospun polyamide-6 fibers effect of solution conditions on morphology and average fiber diameter. Macromolecular Chemistry and Physics, 205, 2327–2338.

62. Vrieze, S. De, Van Camp, T., Nelvig, A., Hagström, B., Westbroek P., and Clerck, K. De (2009). The effect of temperature and humidity on electrospinning. Journal of Materials Science, 44, 1357–1362.

63. Pelipenko, J., Kristl, J., Janković, B., Baumgartner, S., and Kocbek, P. (2013). The impact of relative humidity during electrospinning on the morphology and mechanical properties of nanofibers. International Journal of Pharmaceutics, 456, 125– 134.

64. Tikekar, N. M. and Lannutti, J. J. (2012). Effects of humidity on titania-based polyvinylpyrolidone (PVP) electrospun fibers. Ceramics International, 38, 4057–4064.

65. Casper, C. L., Stephens, J. S., Tassy, N. G., Chase, D. B., and Rabolt, J. F. (2004). Controlling surface morphology of electrospun polystyrene fibers: effect of humidity and molecular weight in the electrospinning process. Macromolecules, 37, 573-578.

66. Ding, B., and Yu, J. (2014). Electrospun Nanofibers for Energy and Environmental Applications. Springer-Verlag: Berlin.

67. J.A. Lopes da Silva, Functional nanofibers in food processing, in: Q. Wei (Ed.) (2012). Functional Nanofibers and Their Applications. Woodhead Publishing Limited, London, UK, pp. 262–304.

68. Kai, D., Liowa, S. L., and Loh, X. J. (2014). Biodegradable polymers for electrospinning: Towards biomedical applications. Materials Science and Engineering C, 45, 659–670.

69. Electronic Code of Federal Regulations – Polyvinylpolypyrrolidone. Available: < http://www.ecfr.gov/cgi-bin/retrieveECFR?gp=1&SID=3b266d0a5a30f4d25695f8a1692c0a25&ty=HTML&h=L&mc=true&r=SECTION&n=se21.3.173_150> Visited: 01/01/2017

70. Electronic Code of Federal Regulations – Polyvinyl alcohol films. Available: < https://www.accessdata.fda.gov/scripts/cdrh/cfdocs/cfcfr/CFRSearch.cfm?fr=177.1670> Visited: 01/01/2017

71. Electronic Code of Federal Regulations – Polyvinyl alcohol films. Available: <http://www.ecfr.gov/cgi-bin/retrieveECFR?gp=1&SID=3b266d0a5a30f4d25695f8a1692c0a25&ty=HTML&h=L&mc=true&r=SECTION&n=se21.3.172_1770> Visited: 01/01/2017

72. Gunn, J., and Zhang, M. (2010). Polyblend nanofibers for biomedical applications: perspectives and challenges. Trends in Biotechnology, 28, 4, 189-197.

73. Wang, H. B., Mullins, M. E., Cregg, J. M., Hurtado, A., Oudega, M., Trombley, M. T., and Gilbert, R. J. (2009). Creation of highly aligned electrospun poly-L-lactic acid fibers for nerve regeneration applications. Journal of Neural Engineering, 6, 016001-016015.

74. Kumbar, S. G., Nukavarapu, S. P., James, R., Nair, L. S., and Laurencin, C. T. (2008). Electrospun poly(lactic acid-co-glycolic acid) scaffolds for skin tissue engineering. Biomaterials, 29, 4100–4107.

75. Yin, Z., Chen, X., Chen, J. L., Shen, W. L., Nguyen, T. M. H., Gao, L., and Ouyang, H. W. (2010). The regulation of tendon stem cell differentiation by the alignment of nanofibers. Biomaterials, 31, 2163–2175.

76. Pinto, S. C., Rodrigues, A. R., Saraiva, J. A., and Lopes-da-Silva, J. A. (2015). Catalytic activity of trypsin entrapped in electrospun poly(ε-caprolactone) nanofibers. Enzyme and Microbial Technology, 79–80, 8–18.

77. Martins, A. J., Bourbon, A. I., Vincente, A. A., Pinto, S. C., Lopes-da-Silva, J. A., and Rocha, C. M. R. (2015). Physical and mass transfer properties of electrospun ε-polycaprolactone nanofiber membranes. Process Biochemistry, 50, 885–892.

78. Leung, W., W.-F., Hung, C.-H., and Yuen, P.-T. (2010). Effect of face velocity, nanofiber packing density and thickness on filtration performance of filters with nanofibers coated on a substrate. Separation and Purification Technology, 71, 30–37.

79. Wang, C., Yan, P., Wang, S., Bai, X., and Yuan, J. (2011). Novel preparation of Ag2S nanoparticles embedded in photoluminescent polymer nanofibers. Pigment & Resin Technology, 40, 1, 17–23.

80. Jung, J. H., Hyun, Y. H., Park, S. Y. and Lee, Y. P. (2011). Giant superparamagnetic nanocomposites using ferritin. Journal of the Korean Physical Society, 58, 4, 797-800.

81. Park, S.-H., Choi1, H.-J., Lee, S.-B., Lee, S.-M., Cho, S.-E., Kim, K.-H., Kim, Y.-K., Kim, M.-R., and Lee, J.-K. (2011). Fabrications and photovoltaic properties of dye-sensitized solar cells with electrospun poly(vinyl alcohol) nanofibers. Macromolecular Research, 19, 2, 142-146.

82. Sóti, P. L., Weiser, D., Vigh, T., Nagy, Z. K., Poppe, L., and Marosi, G. (2016). Electrospun polylactic acid and polyvinyl alcohol fibers as efficient and stable nanomaterials for immobilization of lipases. Bioprocess and Biosystems Engineering, 39, 449–459.

83. Salalha, W., Kuhn, J., Dror, Y., and Zussman, E. (2006). Encapsulation of bacteria and viruses in electrospun nanofibers. Nanotechnology, 17, 4675–4681.

84. Shankhwar, N., Kumar, M., Mandal, B. B., Robi, P. S., and Srinivasan, A. (2016). Electrospun polyvinyl alcohol-polyvinyl pyrrolidone nanofibrous membranesfor interactive wound dressing application. Journal of Biomaterials Science, Polymer Edition, 27, 3, 247-262.

85. Givehchi, R., Li, Q., and Tan, Z. (2016). Quality factors of PVA nanofibrous filters for airborne particles in the size range of 10–125 nm. Fuel, 181, 1273–1280.

86. Kobayashi, S. and Müllen, K. (2015). Encyclopedia of Polymeric Nanomaterials. Springer: London.

87. Zhang,Y., Shi, R., Yang, P., Song, X., Zhu, Y., and Ma, Q. (2016). Fabrication of electronspun porous CeO2 nanofibers with large surface area for pollutants removal. Ceramics International, 42, 14028–1403.

88. Sutjarittangtham, K., Tragoolpua, Y., Tunkasiri, T., Chantawannakul, P., Intatha, U., and Eitssayeam, S. (2015). The preparation of electrospun fiber mats containing propolis extract/CL-CMS for wound dressing and cytotoxicity, antimicrobial, anti-herpes simplex virus. Journal of Computational and Theoretical Nanoscience, 12, 804–808.

89. Jia, Y., Huang, G., Dong, F., Liu, Q., and Nie, Q. (2016). Preparation and characterization of electrospun poly(ε-caprolactone)/poly(vinyl pyrrolidone) nanofiber composites containing silver particles. Polymer Composite, 37, 9, 2847-2854.

90. Quirós, J., Borges, J. P., Boltes, K., Rodea-Palomares, I., Rosal, R., (2015). Antimicrobial electrospun silver-, copper- and zinc-doped polyvinylpyrrolidone nanofibers. Journal of Hazardous Materials, 299, 298–305.

91. Mendes, A. C., Stephansen, K., and Chronakis, I. S. (2017). Electrospinning of food proteins and polysaccharides. Food Hydrocolloids, 68, 53-68.

92. Stijnman, A. C., Bodnar, I., Tromp, R. H. (2016). Electrospinning of food-grade polysaccharides. Food Hydrocolloids, 25,1393-1398.

93. Ohkawa, K., Minato, K.-I., Kumagai, G., Hayashi, S., and Yamamoto, H. (2006). Chitosan Nanofiber. Biomacromolecules, 7, 3291-329.

94. Sedghi, R., Shaabani, A., Mohammadi, Z., Samadi, F. Y., and Isaeic, E. (2017). Biocompatible electrospinning chitosan nanofibers: A novel delivery system with superior local cancer therapy. Carbohydrate Polymers, 159, 1–10.

95. Semnani, D., Naghashzargar, E., Hadjianfar, M., Manshadi, F. D., Mohammadi, S., Karbasi, S., and Effaty, E. (2017). Evaluation of PCL/chitosan electrospun nanofibers for liver tissue engineering. International Journal of

Polymeric Materials and Polymeric Biomaterials, 66, 3, 149-157.

96. Oh, G.-W., Ko, S.-C., Je, J.-Y., Kim, Y.-M., Oh, J.H., and J., W.-K. (2016). Fabrication, characterization and determination of biological activities of poly(caprolactone)chitosan-caffeic acid composite fibrous mat for wound dressing application. International Journal of Biological Macromolecules, 93,201, 1549–1558.

97. Atila, D., Keskin, D., and Tezcaner, A. (2016). Crosslinked pullulancellulose acetate fibrous scaffolds for bone tissue engineering. Materials Science and Engineering C, 69, 1103–1115.

98. Chitpong, N., and Husson, S. M. (2017). Polyacid functionalized cellulose nanofiber membranes for removal of heavy metals from impaired waters. Journal of Membrane Science, 523, 418–429.

99. Wang, S., Zhang, X., Luo, T., Zhu, J., and Su, S. (2017). Preparation of native cellulose-AgCl fiber with antimicrobial activity through one-step electrospinning. Journal of Biomaterials Science, Polymer Edition, 28, 3, 284-292.

100. Ritcharoen, W., Thaiying, Y., Saejeng, Y., Jangchud, I., Rangkupan, R., Meechaisue, C., and Supaphol, P. (2008). Electrospun dextran fibrous membranes. Cellulose, 15, 435–444.

101. Kumara, Y. S., Unnithan,A. R., Sen, D., Kim, C. S., and Lee, Y. S. (2015). Microgravity biosynthesized penicillin loaded electrospunpolyurethane–dextran nanofibrous mats for biomedical applications. Colloids and Surfaces A: Physicochemical and Engineering Aspects, 477, 77–83.

102. Liao, N., Unnithan, A. R., Joshi, M. K., Tiwari, A. P., Hong, S. T., Park, C.-H., and Kim, C. S. (2015). Electrospun bioactive poly (ε-caprolactone)–celluloseacetate–dextran antibacterial composite mats for wound dressingapplications. Colloids and Surfaces A: Physicochemical and Engineering Aspects, 469, 194–201.

103. Gupta, P., and Nayak, K. K. (2015). Characteristics of protein-based biopolymer and its application. Polymer Engineering and Science, 55, 3, 485–498.

104. Miyoshi, T., Toyohara, K., and Minematsu, H. (2005). Preparation of ultrafine fibrous zein membranes via electrospinning. Polymer International, 54, 1187–1190.

105. Wang, Y., and Chen, L. (2012). Fabrication and characterization of novel assembled prolamin protein nanofabrics with improved stability, mechanical property and release profiles. Journal of Materials Chemistry 22, 21592- 21601.

106. Han, Y., and Chen, H. (2013). Enhancement of nanofiber elasticity by using wheat glutenin as an addition. Polymer Science, Series A, 55, 5, 320–326.

107. Xiao, J., Shi, C., Zheng, H., Shi, Z., Jiang, D., Li, Y., and Huang, Q. (2016). Kafirin protein based electrospun fibers with tunable mechanical property, wettability, and release profile. Journal of Agricultural and Food Chemistry, 64, 3226−3233.

108. Arendt, E. K., and Zannini E. (2013) Cereal Grains for the Food and Beverage Industries. Woodhead Publishing Limited: Cambridge.

109. Taylor, J. R. N., Schussler, L., and van der Walt, W. H (1984). Fractionation of proteins from low-tannin sorghum grain. Journal of Agricultural and Food Chemistry, 32, 149-154.

110. Corradini, E., Curti, P. S., Meniqueti, A. B, Martins, A. F., Rubira, A. F., and Muniz, E. C. (2014). Recent advances in food-packing, pharmaceutical and biomedical applications of zein and zein-based materials. International Journal of Molecular Sciences, 15, 22438-22470.

111. Lin, J., Li, C., Zhao, C., Hu, J., and Zhang L.-M. (2012). Co-electrospun nanofibrous membranes of collagen and zein for wound healing. ACS Applied Materials & Interfaces, 4, 1050−1057.

112. Unnithan, A. F., Gnanasekaran, G., Sathishkumar, Y., Lee, Y. S., and Kim, C. S. (2014). Electrospun antibacterial polyurethane–cellulose acetate–zein composite mats for wound dressing. Carbohydrate Polymers, 102, 884–892.

113. Brahatheeswaran, D., Mathew, A., Aswathy, R. G., Nagaoka, Y., Venugopal, K., Yoshida, Y., Maekawa, T., and Sakthikumar, D. (2013). Hybrid fluorescent curcumin loaded zein electrospun nanofibrous scaffold for biomedical applications. Biomedical Materials, 7, 045001-045016.

114. Wang, Y., and Chen, L. (2012). Electrospinning of prolamin proteins in acetic acid: the effects of protein

conformation and aggregation in solution. Macromolecular Materials and Engineering, 297, 9, 902–913.

115. Shi, X., Chen, E.-X., Zhang, J., Zeng, H., and Chen, L. (2016). Fabrication of ultrathin conductive protein-based fibrous films and their thermal sensing properties. Journal of Materials Chemistry A, 4, 4711-4717.

116. Wang, Y., Yang, J., and Chen, L. (2016). Convenient fabrication of electrospun prolamin protein delivery system with three-dimensional shapeability and resistance to fouling. ACS Applied Materials and Interfaces, 7, 24, 13422-13430.

117. Wang, Y., and Chen, L. (2016). Cellulose nanowhiskers and fiber alignment greatly improved mechanical properties of electrospun prolamin protein fibers. ACS Applied Materials and Interfaces, 6, 1709−1718.

118. Barak, S., Mudgil D., and Khatkar, B. S. (2014). Influence of gliadin and glutenin fractions on rheological, pasting, and textural properties of dough. International Journal of Food Properties, 17, 7, 1428-1438.

119. Woerdeman, D. L., Ye, P., Shenoy, S., Parnas, R. S., Wnek, G. E., and Trofimova, O. (2005). Electrospun fibers from wheat protein investigation of the interplay between molecular structure and the fluid dynamics of the Electrospinning Process. Biomacromolecules, 6, 707-71.

120. Woerdeman, D. L., Shenoy, S., and Breger, D. (2007) Role of chain entanglements in the electrospinning of wheat protein-poly(vinyl alcohol) blends. The Journal of Adhesion, 83, 8, 785-798.

121. Dong, J., Asandei, A. D., and Parnas R. S. (2010). Aqueous electrospinning of wheat gluten fibers with thiolated additives. Polymer, 51, 3164-3172.

122. Castro-Enríquez, D. D., Rodríguez-Félix, F., Ramírez-Wong, B., Torres-Chávez, P. I., Castillo-Ortega, M. M., Rodríguez-Félix, D. E., Armenta-Villegas, L., and Ledesma-Osuna, A. I. (2012). Preparation, characterization and release of urea from wheat gluten electrospun membranes. Materials, 5, 2903-2916.

123. Dhandayuthapani, B., Mallampati, R., Sriramulu, D., Dsouza, R. F., and Valiyaveettil, S. (2014). PVA/Gluten hybrid nanofibers for removal of nanoparticles from water. ACS Sustainable Chemistry and Engineering, 2, 4, 1014–1021.

124. Wang, H., She, Y., Chu, C., Liu, H., Jiang, S., Sun, M., and Jiang, S. (2015). Preparation, antimicrobial and release behaviors of nisin-poly(vinyl alcohol)/wheat gluten/ZrO2 nanofibrous membranes. Journal of Materials Science, 50, 5068–5078.

125. Han, Y., and Chen, H. (2013). Enhancement of nanofiber elasticity by using wheat glutenin. Polymer Science Series A, 55, 5, 320–326.

126. Xua, H., Caib, S., Sellersc, A., and Yanga, Y. (2014). Electrospun ultrafine fibrous wheat glutenin scaffolds with three-dimensionally random organization and water for tissue engineering. Journal of Biotechnology, 184,179–186.

127. Barak, S., Mudgil, D., and Khatkar, B. S. (2015). Biochemical and functional properties of wheat gliadins: a review. Critical Reviews in Food Science and Nutrition, 55, 3, 357-368.

128. Soaresa, R. M. D., Patzera, V. L., Derschc, R., Wendorffc, J., da Silveira, N. P., and Prankeb, P. (2011). A novel globular protein electrospun fiber mat with the addition of polysilsesquioxane. International Journal of Biological Macromolecules, 49, 480– 486.

129. Reddy, N., Reddy, R., and Jiang, Q. (2015). Crosslinking biopolymers for biomedical applications. Trends in Biotechnology, 33, 6, 362-369.

130. Selling, G. W., Woods, K. K., Sessa, D., and Biswas, A. (2008). Electrospun zein fibers using glutaraldehyde as the crosslinking reagent: effect of time and temperature. Macromolecular Chemistry Physics, 209, 1003–1011.

131. Aceituno-Medina, M., Mendoza, S., Rodríguez, B. A., Lagaron, J. M., and López-Rubio, A. (2015). Improved antioxidant capacity of quercetin and ferulic acid during in-vitro digestion through encapsulation within food-grade electrospun fibers. Journal of Functional Foods, 12, 332–341.

132. Salas, C., Ago, M., Lucia, L. A., and Rojas, O. J. (2015). Synthesis of soy protein–lignin nanofibers by solution electrospinning. Reactive & Functional Polymers, 85, 221–227.

133. Nagiah, N., Johnson, R., Anderson, R., Elliott, and Tan, W. (2015). Highly compliant vascular grafts with gelatin-

sheathed coaxially structured nanofibers. Langmuir, 31, 12993−13002.

134. Kluger, R., and Alagic, A. (2004). Chemical cross-linking and protein–protein interactions—a review with illustrative protocols. Bioorganic Chemistry, 32, 451–472.

135. Shankar, A., M. Seyam, A.-F. M., and Hudson, S. M. (2011). Electrospinning of soy protein fibers and their compatibility with synthetic polymers. Journal of Textile and Apparel Technology and Mangement, 8, 1, 1-14.

136. Sullivan, S. T., Tang, C., Kennedy, A., Talwar, S., and Khan, S A. (2014). Electrospinning and heat treatment of whey protein nanofibers. Food Hydrocolloids, 35, 36-50.

137. Yao, C., Li, X., and Song, T. (2007). Electrospinning and crosslinking of zein nanofiber mats. Journal of Applied Polymer Science, 103, 380–385.

138. McManus, M. C., Boland, E. D., Koo, H. P., Barnes, C. P., Pawlowski, K. J., Wnek, G. E., Simpson, D. G, and Bowlin, G. L. (2006. Mechanical properties of electrospun fibrinogen structures. Acta Biomaterialia, 2, 19–28.

139. Ramji, K., and Shah, R. N. (2014). Electrospun soy protein nanofiber scaffolds for tissue regeneration. Journal of Biomaterials Applications, 29, 3, 411-422.

140. Lagrain, B., Goderis, B., Brijs, K., and Delcour, J. A. (2010). Molecular basis of processing wheat gluten toward biobased materials. Biomacromolecules, 11, 533–541.

141. Rabiatul, A. R., Lokanathan, Y., Rohaina, C. M., Chowdhury, S. R., Aminuddin, B. S., and Ruszymah, B. H. I. (2015). Surface modification of electrospun poly(methyl methacrylate) (PMMA) nanofibers for the development of in vitro respiratory epithelium model. Journal of Biomaterials Science, Polymer Edition, 26,17, 1297-1311.

142. de Góes-Favoni, S. P., and Bueno, F. R. (2014) Microbial transglutaminase: general characteristics and performance in food processing technology. Food Biotechnology, 28,1, 1-24.

143. Cecoltan, S., Serafim, A., Dragusin, D. M., Lungu, A., Lagazzo, A., Barberis, F., and Stancu, I., C. (2016). The potential of NDPs-loaded fish gelatin fibers as reinforcing agent for fish gelatin hydrogels. Key Engineering Materials, 695, 278-283.

144. Migneault, I., Dartiguenave, C., Bertrand, M. J., and Waldron, K. C. (2004). Glutaraldehyde: behavior in aqueous solution, reaction with proteins, and application to enzyme crosslinking. BioTechniques, 37,5,790-802.

145. Lam, P.-L., Wong, W.-Y., Bian, Z., Chui C.-H., and Gambari, R. (2017). Recent advances in green nanoparticulate systems for drug delivery: efficient delivery and safety concern. Nanomedicine, 12, 4, 357-385.

146. Barbosa, O., Ortiz, C., Berenguer-Murcia, A., Torres, R., Rodrigues, R. C., and Fernandez-Lafuente, R. (2014). Glutaraldehyde in bio-catalysts design: a useful crosslinker and a versatile tool in enzyme immobilization. RSC Advances, 4, 1583-1600.

147. Skotak, M., Noriega, S., Larsen, G., and Subramanian, A. (2010). Electrospun cross-linked gelatin fibers with controlled diameter: the effect of matrix stiffness on proliferative and biosynthetic activity of chondrocytes cultured in vitro. Journal of Biomedical Materials Research A, 95A, 3, 828-836.

148. Sisson, K., Zhang, C., Farach-Carson, M. C., Chase, D. B, and Rabolt, J. F. (2009). Evaluation of cross-linking methods for electrospun gelatin on cell growth and viability. Biomacromolecules, 10, 7, 1675-1680.

149. Chen, Z., Wang, L., and Jiang, H. (2012). The effect of procyanidine crosslinking on the properties of the electrospun gelatin membranes. Biofabrication, 4, 3, 035007.

150. Torres-Giner, S., Gimeno-Alcañiz, J. V., Ocio, M. J., and Lagaron, J. M. (2009). Comparative performance of electrospun collagen nanofibers cross-linked by means of different methods. ACS Applied Materials & Interfaces, 1, 1, 218–223.

151. Taylor, B. L., Limaye, A., Yarborough, J., and Freeman, J. W (2016). Investigating processing techniques for bovine gelatin electrospun scaffolds for bone tissue regeneration. Journal of Biomedical Materials Research B: Applied Biomaterials, 105, 5, 1131-1140.

152. Ramos-de-la- Peña, A. M., Renard, C. M. G. C., Montañez, J., Reyes-Vega, M. de la L., and Contreras-Esquivel, J. C. (2016). A review through recovery, purification and identification of genipin. Phytochemicals Reviews, 1, 37–

49.

153. Xiao, W., Li, S., Wang, S., and Ho, C.-T. (2017). Chemistry and bioactivity of Gardenia jasminoides. Journal of Food and Drug Analysis, 25, 43-61.

154. Sung, H. W., Huang, R. N., Huang, L. L., Tsai, C. C., and Chiu, C. T. (2018). Feasibility study of a natural crosslinking reagent for biological tissue fixation. Journal of Biomedical Materials Research, 42, 560–567.

155. Wang, C., Lau, T. T., Loh, W. L., Su, K., and Wang, D.-A. (2011). Cytocompatibility study of a natural biomaterial crosslinker—genipin with therapeutic model cells. Journal of Biomedical Materials Reaserch B: Applied Biomaterials, 87B, 1 58-65.

156. Sell, S. A., Francis, M. P., Garg, K., McClure, M. J. Simpson, D. G. and Bowlin, G. L. (2008). Cross-linking methods of electrospun fibrinogen scaffolds for tissue engineering applications. Biomedical Materials, 3,4, 045001.

157. Li, Q., Wang, X., Lou, X., Yuan, H., Tu, H., Li, B., and Zhang, Y. (2015). Genipin-crosslinked electrospun chitosan nanofibers: Determination of crosslinking conditions and evaluation of cytocompatibility. Carbohydrate Polymers, 130, 166–174.

158. Zhang, K., Qian, Y., Wang, H., Fan, L., Huang, C., Yin, A., and Mo, X. (2010). Genipin-crosslinked silk fibroin/hydroxybutyl chitosan nanofibrous. Journal of Biomaterials Materials Research A, 95A, 3, 870-881.

159. Panzavolta, S., Gioffrè, M., Focarete, M. L., Gualandi, C., Foroni, L., and Bigi, A. (2011). Electrospun gelatin nanofibers: optimization of genipin cross-linking to preserve fiber morphology after exposure to water. Acta Biomaterialia, 7, 1702–1709.

160. Baiguera, S., Del Gaudio, C, Lucatelli, E., Kuevda, E., Boieri, M., Mazzanti, B., Bianco, A., and Macchiarini, P. (2014). Electrospun gelatin scaffolds incorporating rat decellularized brain extracellular matrix for neural tissue engineering. Biomaterials, 35, 1205-1214.

161. Gomes, S. R., Rodrigues, G., Martins, G. G., Henriques, C. M. R., and Silva, J. C. (2013). In vitro evaluation of crosslinked electrospun fish gelatin scaffolds. Materials Science and Engineering C, 33, 1219–1227.

162. Ko, J. K., Yin, H.Y., An, J., and Chung, D. J. (2010). Characterization of cross-linked gelatin nanofibers through electrospinning. Macromolecular Research, 18, 2, 137-143.

163. Ciriminna, R., Meneguzzo, F., Delisi, R., and Pagliaro, M. (2017). Citric acid: emerging applications of key biotechnology industrial product. Chemistry Central Journal, 11, 22-31.

164. PubChem: Citric Acid. Available: < https://pubchem.ncbi.nlm.nih.gov/compound/citric_acid#section=Top> . Visited: 19/10/2017.

165. Tran, R. T., Yang, J., and Ameer, G. A. (2016). Citrate-based biomaterials and their applications in regenerative engineering. Annual Review of Materials Research, 45, 277-310.

166. Ertas, Y., and Uyar, T. (2017). Fabrication of cellulose acetate/polybenzoxazine cross-linked electrospun nanofibrous membrane for water treatment. Carbohydrate Polymers, 177, 378-387.

167. Fu, Q., Wang, X., Yang, L., Yu, L., and Ding, B. (2016). Scalable fabrication of electrospun nanofibrous membranes functionalized with citric acid for high performance protein adsorption. ACS Applied Materials Interfaces, 8, 18, 11819–11829.

168. Çay, A., Akçakoca Kumbasar, E. P., Keskin, Z., Akduman, Ç., and Ürkmez, A. S. (2017). Crosslinking of poly(vinyl alcohol) nanofibers with polycarboxylic acids: biocompatibility with human skin keratinocyte cells. Journal of Materials Science, 52, 20, 12098–12108.

169. Xu, W., Karst, D., Ynag, W., and Yiang Yiqi (2008). Novel zein-based electrospun fibers with the water stability and strength necessary for various applications. Polymer International, 57, 10, 1110–1117.

170. Jiang, Q., Reddy, N., and Yang, Y. (2010). Cytocompatible cross-linking of electrospun zein fibers for the development of water-stable tissue engineering scaffolds. Acta Biomaterialia, 6, 10, 4042-4051.

171. Jiang, Q., and Yang, Y. (2011). Water-stable electrospun zein fibers for potential drug delivery. Journal of Biomaterials Science, Polymer Edition, 22, 10, 1393-1408.

172. Jiang, Q., Reddy, N., Zhang, S., Roscioli, N. and Yang, Y. (2013). Water-stable electrospun collagen fibers from a non-toxic solvent and crosslinking system. Journal of Biomedical Materials Research Part A, 101, 5, 1237-47.

173. Esparza, Y., Ullah, A., Boluk, Y., and Wu, J. (2017). Preparation and characterization of thermally crosslinked poly(vinyl alcohol)/feather keratin nanofiber scaffolds. Materials & Design, 133, 1-9.

174. Reddy, N.,Li, Y., and Yang, Y. (2009). Alkali-catalyzed low temperature wet crosslinking of plant proteins using carboxylic acids. Biotechnology Progress, 25, 1,139-1346.

175. Reddy, N.,Li, Y., and Yang, Y. (2009). Wet cross-linking gliadin fibers with citric acid and a quantitative relationship between cross-linking conditions and mechanical properties. Journal of Agricultural and Food Chemistry, 57, 90–98.

176. Shen, L., Helan, X., and Yang, Y., (2015). Quantitative correlation between cross-linking degrees and mechanical properties of protein films modified with polycarboxylic acids. Macromolecular Materials & Engineering, 300, 1133–1140.

177. Figoli, A., Marino, T., Simone, S., Di Nicolò, E., Li, X.-M., He, T., Tornaghi S., and Drioli, E. (2014). Towards non-toxic solvents for membrane preparation: a review. Green Chemistry, 16, 4034–4059.

178. Byrne, F. P., Jin, S., Paggiola, G., Petchey, T. H. M., Clark, J. H., Farmer, T. J., Hunt, A. J., Robert McElroy, C., and Sherwood, J. (2016). Tools and techniques for solvent selection: green solvent selection guides. Sustainable Chemical Process, 4, 7, 1-24.

179. Lohokare, H., Bhole, Y., Taralkar, S., and Kharul, U. (2011). Poly(acrylonitrile) based ultrafiltration membranes Optimization of preparation parameters. Desalination, 282, 46–53.

180. Jabbarnia, A., Khan, W. S., Ghazinezami, A., and Asmatulu R. (2016). Investigating the thermal, mechanical, and electrochemical properties of PVdF/PVP nanofibrous membranes for supercapacitor applications. Journal of Applied Polymer Science, 133, 30, 1-10.

181. Hou, T., Li, X., Lu, Y., and Yang, B. (2017). Highly porous fibers prepared by centrifugal spinning. Materials & Design, 114, 303–311.

182. Freire, M. G., Teles, A. R. R., Ferreira, R. A. S., Carlos, L.D., Lopes-da-Silva, J. A. and Coutinho, J. A. P. (2011). Electrospun nanosized cellulose fibers using ionic liquids at room temperature. Green Chemistry, 13, 3173-2180.

183. Nguyen, H. D., Ko, J. M., Kim, H. J., Kim, S. K., Cho, S. H., Nam, J. D., and Lee, J. Y. (2008). Electrochemical properties of poly(3,4-ethylenedioxythiophene) nanofiber non-woven web formed by electrospinning. Journal of Nanoscience and Nanotechnology, 8, 4718–4721.

184. Binulal, N. S., Natarajan, A., Menon, D., Bhaskaran, V. K., Mony, U., and Nair, S. V. (2014). PCL–gelatin composite nanofibers electrospun using diluted acetic acid–ethyl acetate solvent system for stem cell-based bone tissue engineering. Journal of Biomaterials Science, Polymer Edition, 25, 4, 325-340.

185. Puniya, A. K. (2015). Fermented Milk and Dairy Products. Boca Raton: CRC Press.

186. Eurostat - Milk and milk product statistics. Available: <http://ec.europa.eu/eurostat/statistics-explained/index.php/Milk_and_milk_product_statistics> . Visited: 04/08/2017.

187. Simpson, B. K. (2012). Food Biochemistry and Food Processing, 2nd Edition. Wiley-Blackwell: Oxford.

188. Park, K.-H. (2008). Carbohydrate-active Enzymes - Structure, Function and Applications. CRC Press: Boca Raton.

189. Prazeres, A. R., Carvalho, F., and Rivas, J. (2012). Cheese whey management: A review. Journal of Environmental Management, 110, 48-68.

190. Chen, X. Y., and Gänzle, M. G., (2017). Lactose and lactose-derived oligosaccharides: more than prebiotics?. International Dairy Journal, 67,61-72.

191. Cabral, J. M. S., Aires-Barros, M. R., and Gama, M. (2003). Engenharia Enzimática. Lidel, Edições Técnicas: Lisboa.

192. Kriegel, C., Arrechi, A., Kit, K., McClements, D. J., and Weiss, J. (2008). Fabrication, functionalization, and

application of electrospun biopolymer nanofibers, Critical Reviews in Food Science and Nutrition, 48, 775–797.

193. Wang, Z.-G., Wan, L.-G., Liu, Z.-M., Huang, X.-J., and Xu, Z.-K. (2009). Enzyme immobilization on electrospun polymer nanofibers: An overview. Journal of Molecular Catalysis B: Enzymatic, 56, 189–195.

194. El-Aassar, M. R., Al-Deyab, S. S., and Kenawy, E.-R. (2013). Covalent Immobilization of β -galactosidase onto Electrospun Nanofibers of Poly (AN-co-MMA) Copolymer. Journal of Applied Polymer Science, 127, 35, 1873-1884.

195. Wong, D. E., Dai, M., Talbert, J. N., Nugen, S. R., and Goddard, J. M. (2014) Biocatalytic polymer nanofibers for stabilization and delivery of enzymes, Journal of Molecular Catalysis B: Enzymatic. 110, 16–22.

196. Blomfeldt, T, Kuktaite, R, Plivelic, T, Rasheed, F, Johansson, E., and Hedenqvist, M. S. (2012). Novel freeze-dried foams from glutenin- and gliadin-rich fractions. RSC Advances, 2, 6617–6627.

197. Reddy, N., Jiang, Q., and Yang, Y. (2011). Novel wheat protein films as substrates for tissue engineering. Journal of Biomaterials Science, 22, 2063–2077.

198. Donius, A. E., Kiechel, M. A., Schauer, C. L., and Wegst, U. G. K. (2013). New crosslinkers for electrospun chitosan fibre mats. Part II: mechanical properties. Journal of the Royal Society Interface, 10, 81, 20120946-20120956.

199. Scharlab: Acetic Acid. Available: <http://scharlab.com/catalogo-productos-detalle-articulo.php?c=40&sc=244&p=6914&ra=AC034425007 > . Visited: 15/11/2017.

200. PubChem: Acetic Acid. Available: <https://pubchem.ncbi.nlm.nih.gov/compound/acetic_acid> . Visited: 15/11/2017.

201. Physicochemical Properties Of Popular Liquids. Available: <http://www.trimen.pl/witek/ciecze/liquids.html> . Visited: 15/11/2017.

202. Scharlab: Ethanol. Available: <http://scharlab.com/catalogo-productos-detalle-articulo.php?c=40&sc=245&p=7270> . Visited: 15/11/2017.

203. PubChem: Ethanol. Available: <https://pubchem.ncbi.nlm.nih.gov/compound/ethanol>. Visited: 15/11/2017.

204. PubChem: Water. Available: <https://pubchem.ncbi.nlm.nih.gov/compound/water#section=Top> . Visited: 15/11/2017.

205. Selling, G. W, Biswas, A., Patel, A., Walls, D. J., Dunlap, C., and Wei, Y. (2007). Impact of solvent on electrospinning of zein and analysis of resulting fibers. Macromolecular Chemistry and Physics, 208, 1002–1010.

206. Xiao, J., Li, Y., Li, J., Gonzalez, A. P., Xia, Q., Huang, Q. (2015). Structure, morphology, and assembly behavior of kafirin. Journal of Agricultural and Food Chemistry, 63, 216−224.

207. Mekhail, M., Wong, K. K. H, Padavan, D. T., Wu, Y., O'Gorman, D. B., and Wan, W. (2011). Genipin-cross-linked electrospun collagen fibers. Journal of Biomaterials Science, Polymer Edition, 22,17, 2241-2259.

208. Liu, T. and Wang, Z. (2013). Collagen crosslinking of porcine sclera using genipin. Acta Ophthalmologica, 91,4, e253–e257.

209. Torricelli, P., Gioffrè, M., Fiorani, A., Panzavolta, S., Gualandi, C., Fini, M., Focarete, M. L. and Bigi A (2014). Co-electrospun gelatin-poly(L-lactic acid) scaffolds: modulation of mechanical properties and chondrocyte response as a function of composition. Materials Science and Engineering C, 36,130–138.

210. Zhu,B., Li, W., Chi, N., Lewis, R. V., Osamor, J., and Wang, R. (2017). Optimization of Glutaraldehyde Vapor Treatment for Electrospun Collagen/Silk Tissue Engineering Scaffolds. ACS Omega, 2 ,6, 2439-2450.

211. Delcour, J. A., Joye, I. J., Pareyt, B., Wilderjans, E., Brijs, K., and Lagrain, B. (2012) Wheat gluten functionality as a quality determinant in cereal-based food products. Annual Review of Food Science and Technology, 3, 469-492.

212. Mangavel, C., Barbot, J., Popineau, Y., and Guéguen, J. (2001). Evolution of Wheat Gliadins Conformation during Film Formation: A Fourier Transform Infrared Study. Journal of Agricultural and Food Chemistry, 49, 867-872.

213. Secundo, F., and Guerrieri, N. (2005). ATR-FT/IR Study on the Interactions between Gliadins and Dextrin and

Their Effects on Protein Secondary Structure. Journal of Agricultural and Food Chemistry, 53, 1757-1764.

214. Lagrain, B., Rombouts I., Brijs K., and Delcour J. A. (2011). Kinetics of heat-induced polymerization of gliadin. Journal of Agricultural and Food Chemistry, 59, 5, 2034-2039.

215. Balaguer-Grimaldo, M. D. L. P., Gomez-Estaca, J., Cerisuelo-Ferriols, J. P., Gavara Clemente, R., Hernández-Muñoz, P. (2014). Effect of thermo-pressing temperature on the functional properties of bioplastics made from a renewable wheat gliadin resin. Food Science and Technology, 56,1, 161-167.

216. Jansens, K. J. A., Lagrain, B., Rombouts, I., Brijs, K., Smet, M. and Delcour, J. A. (2011). Effect of temperature, time and wheat gluten moisture content on wheat gluten network formation during thermomolding. Journal of Cereal Science, 54, 3, 434-441.

217. Fogliano, V., Monti, S. M., Musella, T., Randazzo, G., and Ritieni, A. (1999). Formation of coloured Maillard reaction products in a gluten-glucose model system. Food Chemistry, 66,3,293–299.

218. Pommet, M., Red, A., Guilbert, S., and Morel, M. H. (2005). Impact of protein size distribution on gluten thermal reactivity and functional properties. Journal of Agricultural and Food Chemistry, 18, 53, 10, 3943-3949.

219. Rombouts, I., Lagrain, B., Brunnbauer, M., Koehler, P., Brijs, K., and Delcour, J.A. (2011). Identification of isopeptide bonds in heat-treated wheat gluten peptides. Journal of Cereal Science, 59,4, 1236-1243.

220. Jansens, K. J. A., Bruyninckx, K., Redant, L., Lagrain, B., Brijs K., Goderis B., Smet, M., and Delcour, J. A. (2015). Importance of crosslinking and disulfide bridge reduction for the mechanical properties of rigid wheat gluten bioplastics compression molded with thiol and/or disulfide functionalized additives. Journal of Applied Polymer Science, 131, 23, 41160- 41169.

221. Huang, G. P., Shanmugasundaram, S., Masih, P., Pandya, D., Amara, S., Collins, G., and Arinzeh, T. L. (2015). An investigation of common crosslinking agents on the stability of electrospun collagen scaffolds. Journal of Biomedical Materials Research Part A, 103,2, 762-771.

222. Del Gaudio, C., Baiguera, S., Boieri, M., Mazzanti, B., Ribatti, D., Bianco, A. and Macchiarini, P. (2013). Induction of angiogenesis using VEGF releasing genipin-crosslinked electrospun gelatin mats. Biomaterials, 34, 31, 7754–7765.